Coordination Chemistry Reviews 254 (2010) 2933–2958

Contents lists available at ScienceDirect

Coordination Chemistry Reviews

journal homepage: www.elsevier.com/locate/ccr

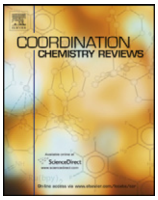

Review

Structural and magnetic studies on copper(II) azido complexes

Chandan Adhikary[a,b], Subratanath Koner[a,*]

[a] Department of Chemistry, Jadavpur University, Kolkata 700032, India
[b] Government College of Education Burdwan, Kazirhat, Burdwan 713102, India

Contents

Abbreviations: L^{1}, 1-(N-salicylideneimino)-2-(N,N-diethyl)-aminoethane; HL^{2}, 4-chloro-2-[(2-piperidin-1-ylethylimino)methyl]phenol; HL^{3}, N-(1H-pyrrol-2-ylmethylene)-2-pyridineethanamine; HL^{4}, 1-(N-salicylideneamino)-2-aminoethane; HL^{5}, 1-(N-ortho-hydroxyacetophenimine)-2-aminoethane; HL^{6}, N-(3aminopropyl) salicylaldimine; L^{7}, 7-amino-4-methyl-5-azahept-3en-2-one; HL^{8}, 7-(ethyl-amino)-4-methyl-5-azahept-3en-2-one; HL^{9}, N-[2-(ethylamino)ethyl] salicylaldimine; HL^{10}, 7-amino-4-methyl-5-azaoct-3en-2-one; HL^{11}, 2-[(3-methylaminopropylimino)methyl]phenol; L^{12}, 1-(N-pyridylimino)-3-aminopropane; HL^{13}, 1-(N-ortho-hydroxyacetophenimine)-2,2-diethyl-aminoethane; L^{14}, N,N-bis-(2-methylpyridyl)(3,5-dimethyl-2-hydroxy-benzyl)amine; L^{15}, 1-(imidazol-4-yl)-2-[pyridylmethylene-amino]-ethane; L^{16}, 8-amino-4-methyl-5-azaoct-3en-2-one; L^{17}, 7-amino-4-methyl-5-aza-3 hepten-2-onato (-1); H$_2$L^{18}, dimethyl-5,6,7,8,15,16-hexahydro-15-methyl-6,7-dioxodibenzo-[1,4,8,11]-tetraazacyclotetradecine-13,18-dicarboxylate; L^{19}, N-(2-pyridylmethyl)-N′,N′-dimethyl-ethylenediamine; L^{20}, Schiff base derived from condensation of Py-2-carbaldehyde and 2,2-dimethyl-propylene-diamine; L^{21}, 2,6-(3,5-dimethylpyrazol-1-ylmethyl)pyridine; L^{22}, (E)-4-(2-(dimethylamino)ethyl-imino-1,1,1-trifluropenten-2-one); HL^{23}, (1,1,1-trifluoro-7-(dimethylamino)-4-methyl-5-aza-3-hepten-2-onate); L^{24}, hydridotris (3,5-dimethylpyrazolyl)borate; L^{25}, tridentate Schiff base derived from condensation of pyridine-2-aldehyde with 1-(2-aminoethyl)-piperidine; L^{26}, tridentate Schiff base derived from condensation of pyridine-2-aldehyde with N,N,2,2-tetramethylpropane-1,3-diamine; L^{27}, tridentate Schiff base derived from condensation of pyridine-2-aldehyde with 1-dimethylamino-2-propylamine; L^{28}, Schiff bases obtained by the condensation of pyridine-2-carbaldehyde with N,N-dimethylethane-1,2-diamine; L^{29}, Schiff bases obtained by the condensation of pyridine-2-carbaldehyde with N,N-diethylethane-1,2-diamine; L^{30}, Schiff bases obtained by the condensation of pyridine-2-carbaldehyde with 4-(2-aminoethyl)morpholine; L^{31}, N-(2-pyridylmethyl)-N′,N′-diethylethylenediamine; *R*-L^{32} or *S*-L^{32}, *R* or *S*-pyridine-2-carbaldehyde-imine; L^{33}, 4-(dimethylamino)pyridine; L^{34}, the dinucleating macrocyclic ligand bis-p-xylyl-BISDIEN; L^{35}, Schiff base derived from condensation of salicylaldehyde and N,N-dimethyl-ethylenediamine; L^{36}, dinucleating macrocyclic ligand bis-p-xylyl-BISDIEN; L^{37}, 2-(pyrazol-1-ylmethyl)pyridine; Me-L^{37}, 2-(3-methylpyrazol-1-ylmethyl)pyridine; L^{38}, Schiff base of 2-pyridylaldehyde with aniline; L^{39}, Schiff base of 2-pyridylaldehyde with p-chloroaniline; L^{40}, (1*R*)-6,6-dimethyl-5,7-methano-2-(2-pyridinyl)-4,5,6,7-tetrahydroquinoline; L^{41}, 2-bromo-4-chloro-6-[(2-dimethylaminoethylimino)methyl]phenol; L^{42}, 5-methylpyrimidin-2-amine; HL^{43}, 1-(N-ortho-hydroxyacetophenimino)-2,2-dimethyl-aminoethane; L^{44}, 2-(dimethylamino)-ethylamine; HL^{45}, 1-(N-5-methoxy-ortho-hydroxyacetophenimino)-2,2-dimethyl-aminoethane; *R*-L^{46}, *R*-2-(N-(2-hydroxybutyl)carbaldimino) pyridine; H$_3$L^{47}, 2,6-bis[[(2-hydroxyethyl)imino]methyl]-4-methylphenol; L^{48}, 4-terpyridone; bpm, bis (pyrazol-1-yl)methane; bmdp, dinucleating ligand based on 1,3-diamino-propan-2-ol and three N-methyl-benzimidazole groups; 4,4′-dmbpy, 4,4′-dimethyl-2,2′-bipyridine; 14ane, 1,4,8,11-tetraazacyclothetradecane; dpyam, di-2-pyridylamine; H$_2$salen, Schiff base derived from condensation of salicylaldehyde and ethylenediamine; bpds, 4,4′-bipyridyl sulfide; ampym, 2-aminopyrimidine; bpt-H, 3,5-bis(pyridin-2-yl)-1,2,4-triazolate; nic, nicotinate; trz, 1,2,4-triazolate; pbpd, N,N′-(bis(pyridine-2-yl)benzylidene)propane-1,3-diamine; pfbd, N,N′-(bis(pyridine-2-yl)formylidene)butane-1,4 diamine; 1,3-tpbd, 1,3-bis-((2-pyridylmethyl)amino-benzene); pmp, 2,6-(pyrazol-1-ylmethyl)pyridine; β-collidine, 3-ethyl-4-methyl pyridine; pmap, bis[2-(2-pyridylethyl)]-(2-pyridylmethyl)amine; H$_2$bdea, N-butyldiethanolamine; 4-Etpy, 4-ethylpyridine; 3-ampy, 3-aminopyridine; 4-Hpya, 4-pyridylacrylic acid; *t*-Bupy, *p-tert*-butylpyridine; Dur, 1,2,4,5-tetrakis(1,4,7-triazacyclonon-1-ylmethyl)benzene; DMPTD, 2-(3,5-dimethyl pyrazol-1-ylmethyl)pyridine; [24] ane-N$_2$O$_6$, 1,13-dioxa-4,7,10,16,19,23-hexaazacyclotetracosane; Phprpy, 4-(3-phenylpropyl)pyridine; tbz, bis-(2-benzimidazolyl)propane; tacn, 1,4,7-triazacyclononane; Him2-py, 2-(2′-pyridyl)-4,4,5,5-tetramethylimidazoline-1-hydroxy); Hdipn, (4-[(3-aminopentylimino)-methyl]-benzene-1,3-diol; dpt, dipropylenetriamine; aepi, 1-(2-aminoethyl)piperidine; Medien, methyldiethylene-triamine; DMP, 2-(3,5-dimethyl pyrazol-1-ylmethyl)pyridine; [Bu$_4$N]$^+$, tetrabutyl-amonium cation; PAP, 1-phenyl-2-(2-pyridyl)-1-azapropylene; dmterpy, 5,5′-dimethyl-2,2′,2″-terpyridine; Hz, Tridentate hydrazone ligand obtained by the condensation of benzhydrazide and 2-acetylpyridine; Medpt, methyl-dipropylenetriamine; Et$_5$dien, 1,1,4,7,7-pentaethyl-diethylene-triamine; Me$_5$dien, 1,1,4,7,7-pentamethyl-diethyl-triamine; tmen, N,N,N′,N′-tetramethylene-diamine; Et$_3$dien, triethyldiethylene-triamine; Meinic, methylisonicotinate; dien, diethylene-triamine; msalen, Schiff base derived from condensation of Salicylaldehyde and N,N dimethyl-ethylenediamine; [Pr$_4$N]$^+$, tetrapropyl-amonium cation; atrz, 4-amino-1,2,4-triazole; bpym, 2,2′-bipyrimidine; H$_2$oxen, N,N′-bis(2-aminoethyl)oxamide; dpa, di-2-pyridylamine; Me$_2$Eten, N,N-dimethyl-N′-ethyl-ethylenediamine; deen, N,N-diethyletane-1,2-diamine; H$_2$oxen, N,N′-bis(2-aminoethyl)oxamide; [NMe$_4$]$^+$, tetramethylamonium cation; hppz, homopiperazine; bben, 1,2-bis-(benzylamino)-ethane; NITmPy, 2-(3′-pyridyl)-4,4,5,5-tetramethylimidazoline-1-oxyl-3-oxide; chea, 1-cyclohexylethylamine; pn, 1,3-diaminopropane; Hhpt, hydrogen phthalate; atrz, 4-amino-1,2,4-triazole; N-Eten, N-ethylethylenediamine; 4-abpt, 4-amino-3,5-bis(4-pyridyl)-1,2,4-triazole; 4-abpt, 4-amino-3,5-bis(4-pyridyl)-1,2,4-triazole; bzp, 2-benzoylpyridyl; N-Ipren, N-isopropylethylenediamine; pymca, pyrimidine-2; dpyam, di-2-pyridylamine; hnta, 6-hydroxynicotinate.

* Corresponding author. Tel.: +91 33 2414 6666x2505; fax: +91 33 2414 6584.
E-mail address: snkoner@chemistry.jdvu.ac.in (S. Koner).

doi:10.1016/j.ccr.2010.06.001

ARTICLE INFO

Article history:
Received 7 November 2009
Accepted 4 June 2010
Available online 22 June 2010

Keywords:
Copper(II)
Azido complexes
X-ray structure
Magnetic study
Magneto-structural correlations

ABSTRACT

The azide ligand has been receiving intense attention in the rapid growth of literature in the field of molecular magnetism. Primarily, azide ion functions as a bridging ligand and magnetic coupler of paramagnetic metal ions. This review is centered on the study of diverse structural and magnetic properties of copper(II) azido complexes. Some of the trends identified could serve as a privileged starting point for the further development of this promising area.

1. Introduction

An important branch of the molecular magnetism deals with molecular systems with bulk physical properties such as long-range magnetic ordering. The first molecular compounds with spontaneous magnetization below a critical temperature were reported during eighties [1,2]. The pioneering reports encouraged many research groups in organic, inorganic, or organometallic chemistry to initiate activity in this subject, and many new molecule-based magnets have been designed and characterized [3]. Amongst the metal-based systems, several families such as oxalato ($C_2O_4{}^{2-}$) [4,5], cyano (CN^-) [5–7], oximato [8], azido ($N_3{}^-$) [9] and dicyanomido ($N(CN)_2{}^-$) [10] bridged compounds play important roles in the understanding of basics of molecular magnetism. Pseudohalide anions act as excellent bridging ligands for obtaining dinuclear, trinuclear, and tetranuclear, one-dimensional, two-dimensional or three-dimensional systems [11–16]. Amongst them azido ligand has been extensively used as it affords an efficient super exchange pathway between paramagnetic centers such as Cu(II), Ni(II), Mn(II), Mn(III), Fe(III), etc. [17–23].

The flexidentate azide ligand shows its versatility and efficiency either as terminal monodentate (Fig. 1a), or as bridging-bi, -tri and -tetradentate linker in complexes (Fig. 1b–i) [18,24,25].

As bridging bidentate ligand azide binds the metal *via* EO (end-on) (Fig. 1b–c) and EE (end-to-end) (Fig. 1d–e) mode. The EO coordination modes are of two types: (i) $\mu_{1,1}$-N_3 (namely single EO) (Fig. 1b) and (ii) di-$\mu_{1,1}$-N_3 (double EO) (Fig. 1c). The EE coordination modes are also of two types: (i) $\mu_{1,3}$-N_3 (single EE) (Fig. 1d) and (ii) di-$\mu_{1,3}$-N_3 (double end-to-end) (Fig. 1e). The possible tridentate bridging coordination modes of azido ligand are $\mu_{1,1,1}$-N_3 (Fig. 1f) and $\mu_{1,1,3}$-N_3 (Fig. 1g), respectively [24]. A rare variety of coordination mode $\mu_{1,1,1,1}$-N_3 (Fig. 1h) was observed in a few nickel(II) and cobalt(II) complexes [25,26]. Recently, unprecedented azido coordination modes like $\mu_{1,1,3,3}$-N_3 (Fig. 1i) and $\mu_{1,1,1,3,3,3}$ (Fig. 1j) have been reported [18].

The azide group, however, may be monocoordinated or bridging with the degree of coordination depending on the requirements of the complex as a whole. In binuclear complexes, where the azide group may function as a bridging group, the factors influencing the mode of bridging, that is, whether the azide coordinates

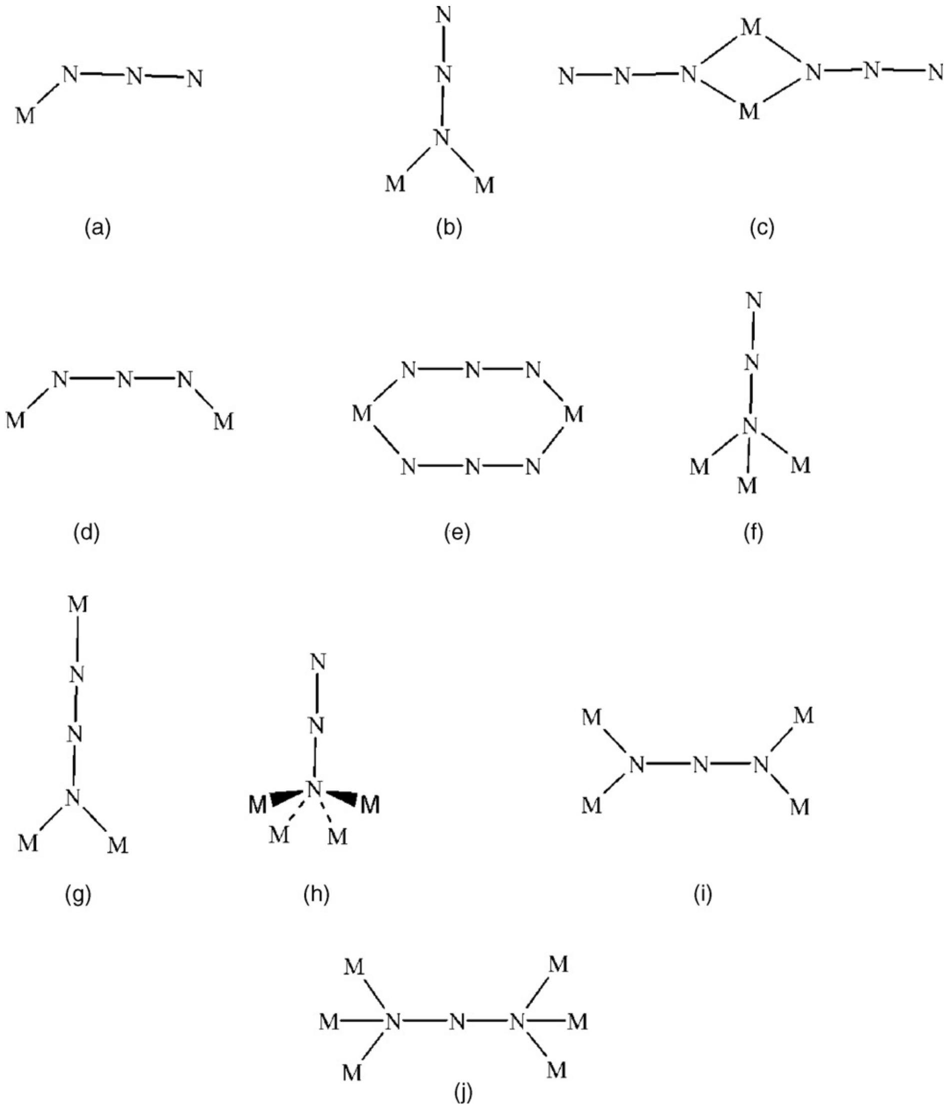

Fig. 1. Different binding modes of azide ($N_3{}^-$) ion.

as an end-on bridge ($\mu_{1,1}$-azido) forming a four-membered ring (Fig. 1c) or as an end-to-end bridge ($\mu_{1,3}$-azido) forming an eight-membered ring (Fig. 1e) are not fully known. However, a structure of four-membered ring with a relatively short M–M distance will be unfavorable in cases where nonbonded repulsions will increase owing to crowding of the coordination sphere.

Thus on steric grounds it seems that a structure of an eight-membered ring (Fig. 1e) is a very usual geometry for the double bridging $\mu_{1,3}$-azido ligand. Two factors which may contribute to this geometry (eight-membered ring) are, first, packing effects which optimize the efficiency of the packing and minimize the non-bonded repulsions and second the allenic nature of the middle nitrogen which together with the trigonal hybridization of the terminal nitrogens oppose the planarity of $M–N_3–M$ bridge. It is safe to say that the coordination mode will depend on the geometry of the complex as a whole, the nature of the other co-ligands present, the central metal atom and its oxidation state.

Besides, azide is also used as a ligand to study the interaction between small molecules and the metal centers of metalloenzymes [27–33]. In many cases it is observed that azide bridges metal centers in multicopper enzymes [27–33]. Spectroscopic studies on the active sites in copper proteins focus on defining the structures of the active sites and their interaction with small molecules (such as azide), substrates, and cofactors related to the molecular mechanism [27–33]. Such azido-bridged copper(II) complexes are of great interest for biologists and bioinorganic chemists investigating the structure and role of active sites in copper proteins. To understand the active sites of met-azido hemocyanins and tyrosinases many efforts have been made to synthesize azido-bridged binuclear copper complexes [27–33]. However, discussion on these topics will not be included in this review.

Generally, the end-on (EO) and end-to-end (EE) coordination modes give ferromagnetic and antiferromagnetic coupling, respectively, albeit these rules do not apply under certain specific circumstances. Only recently, the capability of azide to afford efficient metal–metal bridge is being increasingly exploited in the formation of discrete polynuclear complexes, coinciding with the renewed interest in cluster coordination chemistry caused by the discovery of single-molecule magnets (SMMs = molecular species capable of maintaining the orientation of their magnetization fixed below a certain blocking temperature, T_b) [18]. When the azido bridges are exclusively end-to-end or end-on it does not mean that all bridges are structurally and crystallographically identical. Within the same system (one- or two-dimensional) two or more different structural bridges may present, owing to different distances and/or angles found in the structure. These systems may

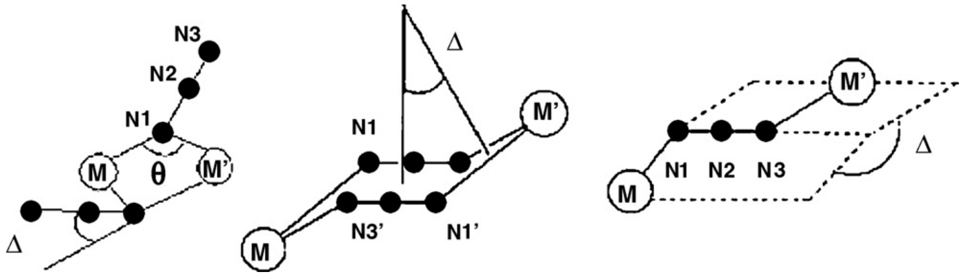

Fig. 2. The structural parameters for EO and EE azido bridges.

be antiferro- or ferromagnetic, belong to the so-called "alternating magnetic systems" (Figs. 29 and 32). This situation necessitates in introducing two or more exchange coupling parameters (J) so as to fit the experimental results in contrast with the "uniform magnetic systems" (Figs. 23 and 26) in which all azido bridges have the same coordination mode and the same structural parameters, hence, they need only one J. Finally, for low-dimensional complexes, highly unusual systems containing simultaneously both kinds of coordination mode (EE or EO) (Figs. 27 and 28) are also of considerable interest in terms of their behavior as alternating ferro-antiferromagnetic (F–AF) coupled systems. With our present state of knowledge, it is impossible to predict which coordination mode will be adopted during synthesis.

Theoretically, just what constitutes the most suitable method for analyzing the superexchange interaction through an azido bridge has been extensively discussed in recent years. Magneto-structural correlations in dinuclear or polynuclear systems are not easily identified because the superexchange mechanism is affected by several structural parameters. The type and the magnitude of the magnetic exchange interaction depends on the bridge identity, the metal–metal separation, the bond angles subtended to the bridging atoms, the dihedral angles between the planes containing the metal ions, the metal bridging ligand bond lengths, and the metal ion stereochemistries (Fig. 2). Furthermore, various factors such as strict and accidental orthogonality of magnetic orbitals, spin polarization, and delocalization of unpaired electrons including charge transfer, have considerable influence in determining the nature of the magnetic coupling between spin centers [11]. The first approach for calculation was undertaken by means of extended Hückel method [34–36]. Kahn and coworkers [35] noted that the spin polarization model would describe the superexchange for the azido ligand more accurately, particularly for the EO coordination mode. More recently, spin density maps in the triplet ground state of $[Cu_2(\text{t-Bupy})_4(\mu\text{-}N_3)_2](ClO_4)_2$ were determined by polarized neutron diffraction [36]. This study suggests that the spin distribution in the triplet ground state in $[Cu_2(\text{t-Bupy})_4(\mu\text{-}N_3)_2](ClO_4)_2$ [36] is dominated by a spin delocalization mechanism, to which is superimposed a spin polarization effect within the π-orbitals of the azido groups. Theoretical studies conducted on coupled dimers [37,38] for EE azido bridges seem to indicate that, at least for this coordination mode, MO extended Hückel calculations are appropriate. Recently, some DFT [39] calculations on these systems have been reported by Ruiz et al. [40,41]. Magneto-structural correlations are also reported by the other group of researchers [9,17–19,42–44]. Long-range ferromagnetic cooperative phenomena were observed in some complexes having low-dimensional (1D or 2D) architectures [9,17–23,45–49]. Usually, exchange interactions between orthogonal magnetic orbitals lead to F coupling. While the coupling occurs in a nonorthogonal magnetic orbital, different cases emerge: (i) the θ angle of M–N_3(EO)–M greatly affects the magnitude or nature of superexchange interactions. For Cu(II) ions, the transition angle is ~104° (theory) or ~108° (experiment) from F to AF coupling. (ii) The longer the bond distances of M–N_3(EO), the weaker the F interactions will be. The exchange coupling switches into AF interaction at Cu–N distances larger than 2.05 Å for a Cu(II) system. (iii) Although the out of plane displacement of an EO azido group has a small effect on exchange coupling from theoretical calculations, experimental data suggest that a good coplanar structure ($\Delta_{1,1}$ close to 0°) leads to strong F coupling (J increases) (Fig. 2). (iv) The AF coupling becomes small as the dihedral angle $\Delta_{1,3}$ increases for double EE azido bridging complexes. That is, the coplanarity would enhance AF interactions ($-J$ increases). (v) The longer the distance of M–N_3(EE), the poorer is the AF coupling. A larger M...M distance would weaken the exchange interaction. (vi) The M–N–N angle and dihedral M–NNN–M angle $\Delta_{1,3}$ are the two main factors to affect the nature of coupling J in a single EE azido system. The large M–N–N angle and distorted M–NNN–M angle may mediate F coupling for d^9 configuration.

In 1996 Thompson and Tandon published a short comments on structural and magnetic behavior of copper(II) and nickel(II) azido complexes [17]. Ribas et al. published a comprehensive review on nickel(II) and manganese(II) azido complexes [9]. Recently two more reviews on magnetic properties of transitional metal clusters are published [18,19]. As regards the magnetochemistry of copper(II) complexes, a wealth of information have been gathered since the comments offered by Thompson and Tandon [17]. This includes well developed theoretical calculations. However, no review article has been published in the last few years focusing on copper(II) compounds. Polynuclear metal complexes have demonstrated many other important properties such as catalysis, clathration, and molecular sieving [50–53], besides their interesting magnetic properties.

In this review we will be discussing the different complexes according to the nuclearity and dimensionality of metal-assembled systems in the following sections.

2. Complexes with terminal (monodentate) azide

Different organic blockers with stereochemical control are used to vary nuclearity through available coordination sites in combination with suitable metal ions and bridges. The coordination mode of the azido ligand depends on the nature and oxidation state of the central metal ion as well as nature of the other coordinating ligands. Complexes containing terminal monodentate azido ligand in mononuclear or polynuclear complexes which exist in different geometries are collated in Table 1.

A representative example of terminal azido coordination is shown in Fig. 3.

In this complex $[Cu(L^1)(N_3)]$ (**1**) [54], the central copper(II) ion assumes a regular square planar arrangement. Out of its four coordination sites three positions are occupied by the tridentate Schiff base through two nitrogen (amino and imino) atoms and while other one is occupied by de-protonated phenoxo group. The remaining fourth coordination site is satisfied by an azido ligand. Here the Cu–N bond lengths are Cu(1)–N(1) = 1.935(2);

Table 1
Complexes with terminal monodentate azido linkage.

Complex	Coordination environment	Ref.
[i]$[Cu(L^1)(N_3)]$ (**1**)	Tridentate (NNO) donor Shiff base and one terminal azide.	[54]
[i]$[Cu(L^2)(N_3)]$ (**2**)	Tridentate (NNO) donor Shiff base and one terminal azide.	[55]
[ii]$[Cu(pbpd)(N_3)]PF_6$ (**3**)	Two pyridine nitrogen, two imine nitrogen, one terminal azide.	[56]
[ii]$[Cu(pfbd)(N_3)]ClO_4$ (**4**)	Two pyridine nitrogen, two imine nitrogen, one terminal azide.	[56]
[iii]$[Cu_2(1,3\text{-tpbd})(N_3)_4]$ (**5**)	Two terminal azide coordinated to each copper (II) ion.	[57]
[iii]$[Cu(N_3)(pyrazinato)(H_2O)]_n$ (**6**)	NNO-tridentate pyrazinato ligand, terminal azide and water molecule.	[58]
[iv]$[Cu(pmp)(N_3)(ClO_4)]_n$ (**7**)	Bridged perchlorate, monodentate azide.	[59]
[v]$[Cu(N_3)_2(sparteine)]$ (**8**)	The chiral alkaloid acts as bidentate NN donor, two terminal azide occupy the remaining coordination.	[60]
[vi]$[Cu(\beta\text{-collidine})_4(N_3)](ClO_4)$ (**9**)	Four β-collidine ligands occupy basal sites with terminal azide at apical position.	[61]
[vii]$[Cu(s\text{-collidine})_2(N_3)_2]$ (**10**)	Terminal azide.	[62]
[ii]$[Cu(3,4\text{-lutidine})(N_3)_2]$ (**11**)	Terminal azide.	[63]
$[Cu(3\text{-Etpy})_2(N_3)_2]_n$ (**12**)	Terminal azide present in both the unit.	[64]
[iii]$[Cu(terpy)(N_3)Cl]$ (**13**)	Three nitrogen atoms of terpyridine ligand and azide comprise the basal plane.	65]
[iii]$[Cu(pmap)(N_3)]ClO_4$ (**14**)	Four N atoms of the pmap and N atom of the terminal azide result the penta coordinated environment.	[66]
[iii]$[Cu_2(\mu\text{-Hbdea})_2(N_3)_2]$ (**15**)	Two monodentate azide ligands.	[67]

[i]Square planar; [ii]distorted TBP; [iii]square pyramidal; [iv]quasi-one-dimensional; [v]distorted tetrahedron; [vi]tetragonal pyramidal; [vii]distorted octahedron/octahedron.

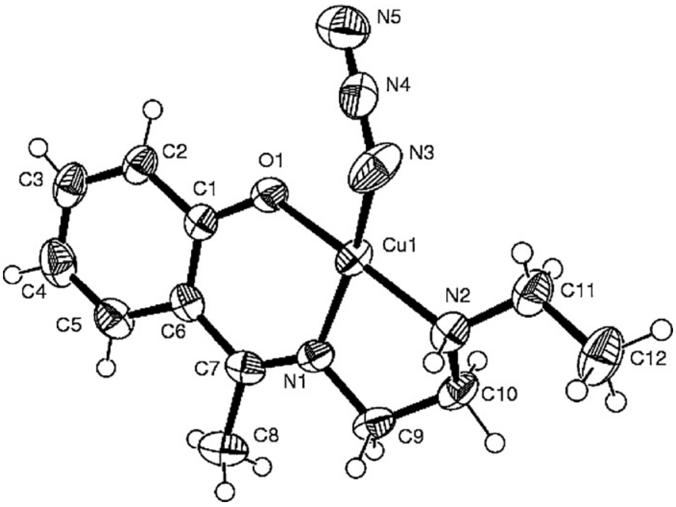

Fig. 3. Ortep diagram of complex $[Cu(L^1)(N_3)]$ (**1**) showing atom numbering scheme with thermal ellipsoids at 30% probability (reprinted with permission from Elsevier© [54]).

Cu(1)–N(2) = 2.063(2); Cu(1)–N(3) = 1.946(2) Å while the Cu(1)–O(1) bond length is 1.888(2) Å. The azide group, which acts as a monodentate ligand is slightly asymmetric [N(3)–N(4) = 1.184(3) and N(4)–N(5) = 1.141(3) Å] and linear within the experimental error [N(5)–N(4)–N(3) = 175.6(2)]. All the above monomeric complexes show usual paramagnetic property due to presence of discrete copper(II) ion.

3. Dinuclear azido-bridged complexes

3.1. *Complexes with double end-on (EO) azido ($\mu_{2\text{-}1,1}$-N_3) bridges*

Double EO azido bridging coordination modes are of two types: (i) symmetric double end-on azido bridges (Fig. 4a) and (ii) asymmetric double end-on azido bridges (Fig. 4b).

3.1.1. *Symmetric double end-on azido ($\mu_{2\text{-}1,1}$-N_3) bridged dimeric complexes*

Table 2 illustrates the magnetic and structural data of some double end-on symmetric azido-bridged dimers. The dinuclear complexes have a $[Cu_2(\mu_{1,1}\text{-}N_3)_2]^{2+}$ core with Cu–N_{azide}–Cu angle close to ≤ 104° and are ferromagnetically coupled. The *J* value varies within a broad range (2.5–230 cm^{-1}). The weakest ferromagnetic coupling is observed in $[Cu_2(\mu\text{-}N_3)_2(tacn)_2](ClO_4)_2{\cdot}CH_3OH$ (**27**) [76] while the strongest ferromagnetic coupling is observed in the complex $[Cu_2(\mu\text{-}N_3)_2(4\text{-Etpy})_4(\mu\text{-}NO_3)_2]$ (**16**) [68].

The eq–eq disposition of the EO azide bridges [68–76] can lead to strong ferromagnetic coupling, unless the Cu–N–Cu angle is large than 108°. Amongst others, three structural parameters may impose significant influences on the magnetic interaction: (i) the Cu–N–Cu angle (θ), (ii) the Cu–N bond distances and (iii) the distortion of the coordination geometry. The Cu–Cu distance is not an independent factor and depends on θ and Cu–N distances (Fig. 2).

As can be seen, the strong ferromagnetic interaction with $J > 200\ cm^{-1}$ in compounds $[Cu_2(N_3)_2(4\text{-Etpy})_4(\mu\text{-}NO_3)_2]$ (**16**) and $[Cu_2(N_3)_2(3\text{-ampy})_4(\mu\text{-}NO_3)_2]{\cdot}EtOH$ (**17**), which have Cu–N distances comparable to $[Cu_2(4\text{-pya})_2(N_3)_2(DMF)_2$ (**18**), can be attributed to the relatively small θ angles (<100°). On the other hand the much lower *J* value for $[Cu_2(N_3)_2(N_3)_2([24]ane\text{-}N_2O_6)]{\cdot}H_2O$ (**22**) is likely due to its relatively large θ angle (av. 103.6°). The comparison clearly suggests the general trend that ferromagnetic interactions decreases with increased θ angle. Compounds $[Cu_2(N_3)_2(O_2CCH_3)_2(dpyam)_2]$ (**23**) and $[Cu_2(N_3)_2(O_2CH)_2(dpyam)_2]$ (**24**) exhibit slightly smaller θ angles and much weaker ferromagnetic interaction than $[Cu_2(4\text{-pya})_2(N_3)_2(DMF)_2$ (**18**). This can be justified by considering by other two factors. Firstly Cu–N distances (and hence the Cu…Cu distances) in $[Cu_2(N_3)_2(O_2CCH_3)_2(dpyam)_2]$ (**23**) and $[Cu_2(N_3)_2(O_2CH)_2(dpyam)_2]$ (**24**) are longer than those in (**16**–**18**, **22**). It is easy to understand that longer Cu–N distance should lead to weaker coupling. Secondly, Cu(II) geometry in (**23**–**24**) is square pyramid with severe distortion towards TBP. This distortion is not conducive to the efficient delocalization of the $d_{x^2-y^2}$ type magnetic orbital towards the equatorial bridging ligands and hence the interaction is reduced.

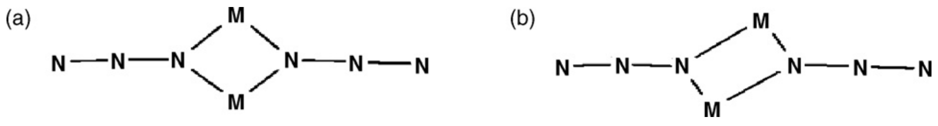

Fig. 4. Symmetric double end-on mode (a) and asymmetric double end-on mode (b).

Table 2
Main structural and magnetic parameters for symmetric double end-on ($\mu_{2\text{-}1,1}$-N_3) azido bridged dimeric complexes.

Compounds	Cu–Cu (Å)	Cu–N (Å)	Cu–N–Cu (°)	J (cm^{-1})	Ref.
$[Cu_2(N_3)_2(\text{4-Etpy})_4(\mu\text{-}NO_3)_2]^{vii}$ (**16**)	3.024	2.004, 1.99	98.2	230.1	[68]
$[Cu_2(N_3)_2(\text{3-ampy})_4(\mu\text{-}NO_3)_2]\cdot EtOH^{ii}$ (**17**)	3.011	2.006, 2.000	97.5	223.2	[68]
$[Cu_2(\text{4-pya})_2(N_3)_2(DMF)_2]^{vii}$ (**18**)	3.123	2.00, 2.01	102.1	145	[69]
$[Cu_2(N_3)_2(\text{t-Bupy})_4](ClO_4)_2{}^{i}$ (**19**)	3.045	1.99, 1.97	100.5	105 ± 20[a] (235)	[36,70]
$[Cu_4(N_3)_4(Dur)](PF_6)_4\cdot 4H_2O\cdot 6CH_3CN$ (**20**)	–	2.030, 1.970 1.993, 2.012	98.1, 96.6	94	[71]
$[Cu_2(DMPTD)_2(\mu\text{-}N_3)_2(N_3)_2]$ (**21**)	3.076	2.043, 1.995 2.022, 1.986	98.3, 101.9	85 ± 1	[72]
$[Cu_2(N_3)_2(N_3)_2([24]\text{ane-}N_2O_6)]\cdot H_2O^{vii}$ (**22**)	3.162	2.043, 1.990 2.035, 1.983	101.7, 105.4	70 ± 20	[34]
$[Cu_2(N_3)_2(O_2CCH_3)_2(dpyam)_2]^{iii}$ (**23**)	3.20	2.00, 2.14	101.2	64	[73]
$[Cu_2(N_3)_2(O_2CH)_2(dpyam)_2]^{iii}$ (**24**)	3.19	2.00, 2.14	101.1	63	[73]
$[Cu_2(N_3)_2(N_3)_2(phprpy)_2]$ (**25**)	–	1.99, 2.14	101.9	25.6	[74]
$[Cu_2(N_3)_2(N_3)_2(tbz)_2]\cdot 2CH_3OH$ (**26**)	–	2.059, 2.037	104.7	23	[75]
$[Cu_2(N_3)_2(tacn)_2](ClO_4)_2\cdot CH_3OH$ (**27**)	–	2.007, 1.997	99.9	2.5	[76]

[a] The J value in the parentheses is calculated with the neutron diffraction data [36].

3.1.2. *Asymmetric double end-on ($\mu_{2\text{-}1,1}$-N_3) azido-bridged dimeric complexes*

Some selected structural and magnetic data for double end-on asymmetric azido bridged (Fig. 4b) transition-metal complexes with antiferromagnetic and ferromagnetic interactions are summarized in Tables 3 and 6, respectively. In most of these Cu(II) complexes, the Cu(II) ion assumes a square pyramidal coordination environment and the azido bridge adopts a basal–apical asymmetric disposition between copper ions. From the structural point of view (Tables 3 and 6) it is evident that Cu–N_{azido}(basal) bond distance is smaller than Cu–N_{azido} (apical) bond distance. The inequality in bond lengths arise due to one azido nitrogen directly related Cu–N_{azido}(basal) to the Cu atom and another Cu–N_{azido}(apical) comes, generally, from the center of inversion related equivalent.

Although the reported M–N_{azido}–M bond angles lie within cut off angle 104° [40] yet the magnetic interaction varies from antiferromagnetic to ferromagnetic; suggesting that the angular dependence proposed for symmetric azido bridges is not valid for asymmetric bridges. In these cases, each coordination geometry implies a different admixture of $d_{x^2-y^2}$ and d_{z^2} orbitals for the resulting magnetic orbitals and consequently a different superexchange interaction and different J coupling constant results. The trigonality index τ [$\tau = (\beta - \alpha)/60$, where β and α are the two largest L–M–L (L = ligand) angles of the coordination sphere] ($\tau = 0$ infers a perfect square pyramid, and a $\tau = 1$ a perfect trigonal bipyramid) [77] plays an important role in determining magnetic interactions in such complexes.

A representative example of asymmetric double end-on azido-bridged Cu(II) dimer $[Cu(L^4)(N_3)]_2$ (**31**) [81] is shown in Fig. 5. The structural and magnetic parameters are listed in Table 3. In this complex the magnetic data were fitted in two steps. First the g value was obtained from the high temperature $\chi_M T$ (Fig. 6) data and then the $\chi_M = f(T)$ in the temperature range 300–3 K were fitted leading to the following parameters: $J = -8.5(5)\,cm^{-1}$, $g = 2.10(2)$, $\rho = 0.012$ and $R = 2 \times 10^{-4}$ (disagreement factor). Though it is well established that end-on double azido-bridged copper(II) dimers are usually ferromagnetic, magnetic measurement of complex (**31**) indicates that the coupling between two copper(II) ions in this complex is antiferromagnetic. This is really unusual for a dimer of this kind. A closer look into the structure, however, reveals the probable cause for this unusual magnetic behavior. The magnetic orbital describing the single electron on Cu and CuA are mainly of an $x^2 - y^2$ type, extended along the basal plane of the copper ions. The azido group connecting Cu and CuA through end-on bridge, for example N3 atom of N3–N4–N5 belongs to the basal plane of Cu but occupying axial coordination position of square-pyramidal geometry of CuA. The situation is the same for another azide group, *viz.* N3A–N4A–N5A in the dimeric molecular entity. Consequently the interaction between the Cu and CuA magnetic orbitals is expected to be very weak leading to a small exchange coupling parameter.

Another similar type of asymmetric double end-on azido-bridged Cu(II) dimer was also reported by our group $[Cu(L^5)(N_3)]_2\cdot CH_3OH\cdot H_2O$ (**32**) [82] in which magneto-structural correlations have been undertaken along with other structurally

Table 3
Main structural and magnetic parameters for asymmetric double end-on ($\mu_{2\text{-}1,1}$-N_3) azido bridged complexes having antiferromagnetic interaction.

Compounds	R	$R^{\#}$	M–N–M (°)	τ	J (cm^{-1})	Ref.
$[Cu(\text{Him2-py})(N_3)]_2$ (**28**)	1.961	2.531	94.3	–	−0.3	[78]
$[Cu(L^3)(N_3)]_2$ (**29**)	–	–	–	0.08	−1.29	[79]
$[Cu_2(dipn)_2(\mu\text{-}N_3)_2]$ (**30**)	2.02	2.617	92.2	0.08	−2.1	[80]
$[Cu(L^4)(N_3)]_2$ (**31**)	1.998	3.181	89.1	0.18	−8.5	[81]
$[Cu(L^5)(N_3)]_2\cdot CH_3OH\cdot H_2O$ (**32**)	1.991	2.569	89.2	0.209, 0.206	−4.2	[82]
$[Cu(L^6)(N_3)]_2$ (**33**)	1.985	2.447	93.0	0.23	−1.8	[83]
$[Cu(L^7)(N_3)]_2$ (**34**)	2.039	2.546	86.8	0.17	−3.1	[83]
$[Cu(L^8)(N_3)]_2$ (**35**)	2.039	2.440	90.5	0.02	−1.8	[84]
$[Cu(L^9)(N_3)]_2$ (**36**)	1.999	2.443	88.3	0.13	−2.6	[84]
$[Cu(L^{10})(N_3)]_2$ (**37**)	2.016	3.273	90.8	0.21	−5.4	[84]
$[Cu(L^{11})(N_3)]_2\cdot CH_3OH$ (**38**)	2.048	2.356	–	–	–	[101]
$[Cu(L^{12})(N_3)]_2(NO_3)_2$ (**39**)	1.927	2.548	85.3	Octahedral	−1.3	[102]
$[Cu(L^{13})(N_3)]_2$ (**40**)	2.012	2.681	99.4	0.275	−146	[103]
$[Cu(terpy)(N_3)(H_2O)]_2(PF_6)_2$ (**41**)	1.927	2.851	95.7	0.06	−2.9	[104]
$[Cu(dpt)(N_3)]_2(ClO_4)_2$ (**42**)	2.022	2.398	101.0 100.7	0.28, 0.49	−2.9	[59]
$[Cu(aepi)(N_3)_2]_2$ (**43**)	2.016	3.35	98.8	0.15	−3.1	[105]
$[Cu(L^{14})(N_3)]_2(ClO_4)_2$ (**44**)	1.972	3.452	98.3	–	−3.2	[106]
$[Cu(Medien)(N_3)]_2(ClO_4)_2$ (**45**)	2.098	3.343	92.5	0.37	−16.8	[107]
$[Cu(DMP)(N_3)_2]_2$ (**46**)	1.996	3.32	103.1	0.64	−27.6	[108]
$[Bu_4N]_2[Cu_2(\mu_{1,1}\text{-}N_3)_2(N_3)_4]$ (**47**)	1.953	3.126	104.3	–	−36.0	[109]

R = M–N_{azido} (basal) Å; $R^{\#}$ = M–N_{azido} (apical) Å; τ = trigonality index.

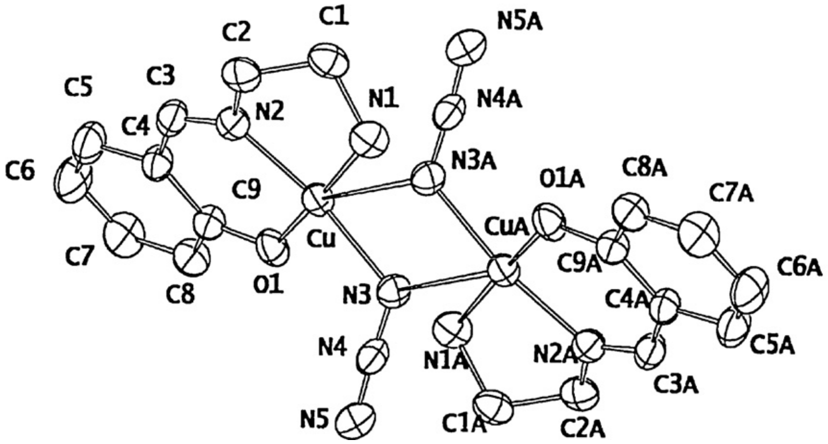

Fig. 5. Ortep diagram of complex $[Cu(L^4)(N_3)]_2$ (**31**) (reprinted with permission from ACS© [81]).

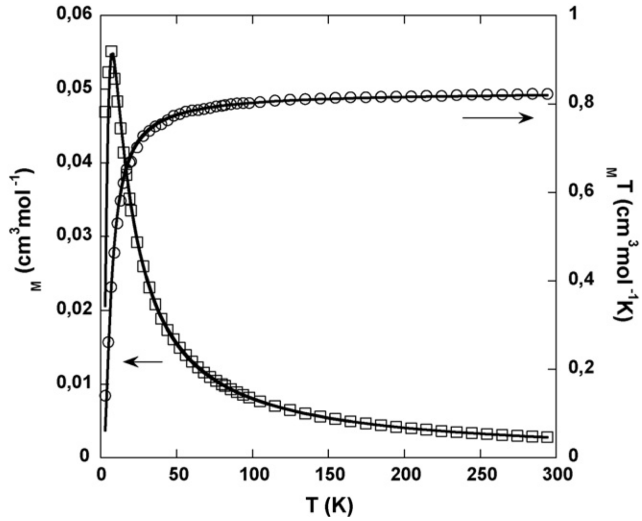

Fig. 6. χ_M*T versus T* (○) plot and χ_M *versus T* (□) under an applied magnetic field of 1.0 T for complex $[Cu(L^4)(N_3)]_2$ (**31**) (reprinted with permission from ACS© [81]).

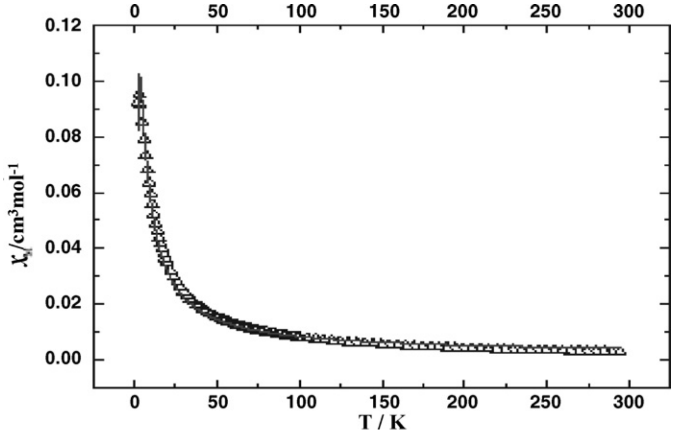

Fig. 8. χ_M*T versus T* (△) plot for complex $[Cu(L^5)(N_3)]_2CH_3OH{\cdot}H_2O$ (**32**) (reprinted with permission from Elsevier© [82]).

related dimers. The Ortep diagram and χ_M*T versus T* plot are given in Figs. 7 and 8, respectively.

The Cu–N(azide)–Cu angles in $[Cu(L^5)(N_3)]_2{\cdot}CH_3OH{\cdot}H_2O$ (**32**) is 90.4° [82]. This is unusually low in comparison to that of the same angle in other end-on azido-bridged binuclear complexes [83–84]. Though a strong ferromagnetic interaction between the metal centers is expected in the complex the coupling has actually been found to be antiferromagnetic ($J = -4.2$ cm^{-1}), instead. To rationalize this paradoxical magnetic behavior, DFT calculation of this and other four complexes with very similar structure have been performed within broken-symmetry (BS) framework. The calculated magnetic

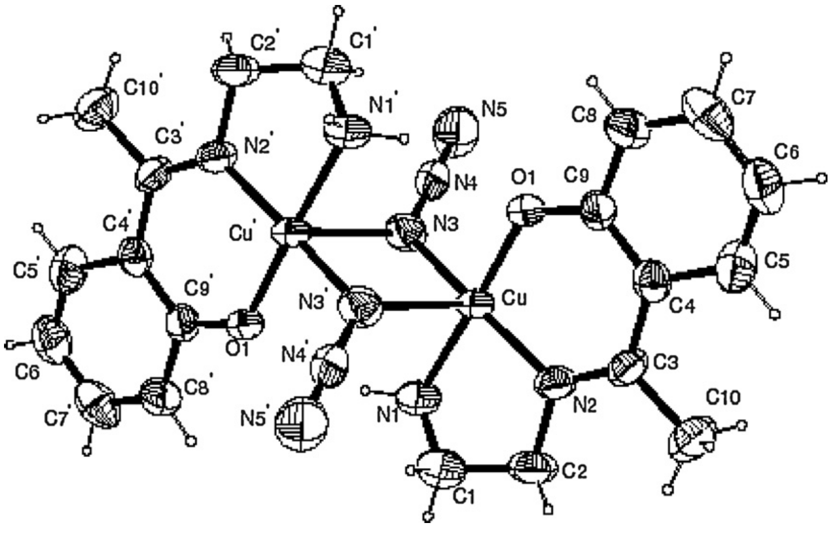

Fig. 7. Ortep diagram of complex $[Cu(L^5)(N_3)]_2CH_3OH{\cdot}H_2O$ (**32**). Solvent molecules are omitted for clarity (reprinted with permission from Elsevier© [82]).

Table 4
Comparison of calculated exchange coupling constants (cm^{-1}) (using spin-projected [Eqs. (2) or (3)] or non-spin projected [Eq. (1)] methods) and experimental results (Expt.). Expectation values of total square spin operators for both broken symmetry (BS) and high spin (HS) states, used for Eq. (3), are shown (reprinted with permission from Elsevier© [82]).

Compounds	$\langle S^2\rangle_{BS}$	$\langle S^2\rangle_{SH}$	Eq. (2)	Eq. (3)	Eq. (1)	Expt.
$[Cu(L^4)(N_3)]_2$ (**31**)	1.0040	2.0039	−9.08	−9.08	−4.54	−8.5
$[Cu(L^5)(N_3)]_2{\cdot}CH_3OH{\cdot}H_2O$ (**32**)	1.0035	2.0036	−6.72	−6.72	−3.36	−4.2
$[Cu(L^6)(N_3)]_2$ (**33**)	1.0036	2.0035	−6.62	−6.62	−3.31	−1.8
$[Cu(L^7)(N_3)]_2$ (**34**)	1.0028	2.0030	−2.56	−2.56	−1.28	−3.1
$[Cu(L^{15})(N_3)]_2$ (**48**)	1.0045	2.0043	8.34	8.34	4.17	2.9

All the compounds have same core structure, $[Cu_2L_2(\mu_{1,1}\text{-}N_3)_2]$.

coupling constants (J) are in excellent agreement, both in sign and in the magnitude of the exchange interaction, with the experimental data, and the spin density map is correctly reproduced.

3.1.3. DFT calculations

The calculations were carried out using the Amsterdam Density Functional (ADF) package version (2004.01) [85,86]. All electron calculations using triple-ζ STO set plus one polarization function (TZP) were done. Both the Local Density Approximation (LDA) and the hybrid (Hyb-GGA) for exchange-correlation functionals were used. The LDA was applied with the Vosko, Wilk, and Nusair functional [87], the hybrid method was applied using the hybrid functional B3LYP for the exact exchange part and Lee–Yang–Par for the correlation part [88]. The implementation in ADF of the calculations of the exact exchange (Hartree–Fock exchange), which is needed for the hybrid method, is based on work published by Watson et al. [89].

The experimentally determined geometries for the complete structures of compounds (**31**–**34**) and complex (**48**) were used for the calculation of the magnetic exchange coupling constants. Neither variation of the geometrical parameters nor the geometry optimization [90] were attempted in these calculations because a small variation in the geometry can have a big effect on the calculated magnetic interaction parameters.

To study the effect of the functional (LDA, GGA, etc.), first step DFT calculations were carried out with non-hybrid DFT functionals [87]. The use of the GGA yields positive values (ferromagnetic interaction) of the calculated exchange magnetic coupling constants for the four complexes. Thus, the magnetic interaction is only well described for the compound $[Cu(L^{15})(N_3)]_2$ (**48**) [83], which shows experimentally a ferromagnetic coupling ($J = 2.9\,cm^{-1}$). The calculated J values for (**48**) using PW91 [91], BLYP [92–95], and BP [92,96] functionals (from Eq. (1)) are found to be 2.7, 2.55 and 3.01 cm^{-1}, respectively. Here, non-hybrid DFT functionals can describe correctly the ferromagnetic interaction for compound (**48**) only, but fails to reproduce experimentally observed magnetic interaction of the compounds showing antiferromagnetic coupling (**31**, **32**, **33**, and **34**). It is well established that the combination of Hartree–Fock (HF) and DFT within the B3LYP hybrid functional allows to get a good description for both broken-symmetry (BS) and high-spin (HS) states and hence yields the singlet–triplet gap (J) that are in good agreement with the experimental values [97–100]. The results of the calculations for compounds (**31**), (**32**), (**33**), (**34**) and (**48**) are given in Table 4. Three approaches are used *via* non-spin-projected (Eq. (1)) and spin-projected functionals (Eqs. (2) and (3)) to estimate the magnetic coupling constant of all the compounds. It is clear from the comparison of results obtained that the two spin-projected techniques give essentially the same results. This is due to the fact that the broken-symmetry (BS) and high-spin (HS) states are well localized, *i.e.* $\langle S^2\rangle_{BS} \approx 1$ and $\langle S^2\rangle_{BS} \approx 2$ in these cases. The results are in excellent agreement, both in sign and in magnitude of the exchange coupling constant, with experimental data. Spin-projected techniques (Eqs. (2) and (3)) give most accurate results for compounds (**31**), (**32**), and (**34**). On the other hand non-spin-projected (Eq. (1)) gives a better agreement for complexes (**33**) and (**48**). However, due to the strong localization of the wave function at the metal centers both computational techniques produce results that are in remarkable agreement with the experimental value. In addition to the magnetic coupling constant, it is interesting to study the spin density distribution in the complexes. Mulliken spin population in atoms/ions present in the coordination sphere of copper(II) including metal ion itself of the complexes (**31**–**34**) and (**48**) were also calculated using the B3LYP method. This type of calculation was successfully implemented in other $\mu_{1,1}$-azido copper(II) dimers earlier to understand the spin polarization mechanism and delocalization of the unpaired electrons of metal centers. Table 5 presents the calculated Mulliken spin densities for the triplet state using B3LYP hybrid method for the dimers (**31**–**34**) and (**48**). Small positive values of spin density on the bridging and terminal nitrogen atoms (N1 and N3) of the azido groups as well as on the other coordinated atoms (N4, N5 and O1), and weakly negative on the central nitrogen atoms (N2) of the N_3^- bridge were observed in these calculations. This is in agreement with the other reports available in the literature [36,40]. The sign alternation of the spin density at the N2 and N3 atoms of the azido-bridge is consistent with spin polarization by the bridging nitrogen atoms (Table 6).

A full molecule calculation using hybrid B3LYP functional to reproduce singlet-triplet energy gap of $\mu_{21,1}$-azido copper(II) complexes is not only successful in correctly describing the magnetic behavior of the complexes in this study but also yielded a J value that is in excellent agreement with the experimental value. Pure DFT functional fails to afford satisfactory analysis of magnetic behavior of these complexes. The magneto-structural correlations including DFT calculation derived results of $\mu_{21,1}$-azido copper(II) complexes which have metal–metal azido bridge through basal–basal coordination linkage could not be applied as

Table 5
Calculated Mulliken spin populations in the triplet state of the complexes (**31**, **32**, **33**, **34** and **48**) using B3LYP (reprinted with permission from Elsevier© [82]).

	$[Cu(L^4)(N_3)]_2$ (**31**)	$[Cu(L^5)(N_3)]_2{\cdot}CH_3OH{\cdot}H_2O$ (**32**)	$[Cu(L^6)(N_3)]_2$ (**33**)	$[Cu(L^7)(N_3)]_2$ (**34**)	$[Cu(L^{15})(N_3)]_2$ (**48**)
Cu1	+0.52	+0.52	+0.52	+0.53	+0.52
N1	+0.074	+0.08	+0.076	+0.069	+0.081
N2	−0.001	−0.007	−0.008	−0.005	−0.009
N3	+0.11	+0.1	+0.098	+0.081	+0.11
N4	+0.09	+0.08	+0.098	+0.01	+0.09
N5	+0.09	+0.09	+0.1	+0.1	+0.08
O1	+0.13	+0.13	+0.11	+0.12	+0.13

Table 6
Structural and magnetic parameters for asymmetric double end-on ($\mu_{2\text{-}1,1}$-N_3) azido bridged transition metal complexes having ferromagnetic interaction.

Compounds	M–N–M (°)	R	$R^{\#}$	J (cm^{-1})	Ref.
$[Cu(L^{15})(N_3)]_2$ (**48**)	93.6	2.06	2.48	2.9	[83]
$[Cu(L^{16})(N_3)]_2(ClO_4)_2$ (**49**)	96.7	–	2.54	WF	[110]
$[Cu(L^{17})(N_3)]_2$ (**50**)	86.9	–	2.55	24	[111]
$[Cu(PAP)(N_3)_2]_2$ (**51**)	92.0	1.99	2.50	35	[108]
$Cu_2(NiL^{18})_2(N_3)_4$[a] (**52**)	–	1.98	2.00	20.3	[112]
$Cu_2(dmterpy)_2(N_3)]_2(N_3)_2(NO_3)(H_2O)_2$[b] (**53**)	117.4	1.99	2.31	2.9	[113]
$[Cu(Hz)(N_3)]_2$ (**54**)	89.9	1.95	2.02	0.75	[114]

R = M–N$_{azido}$(basal) Å; $R^{\#}$ = M–N$_{azido}$(apical) Å; [M = Cu(II)]; WF = weak ferromagnetic.

[a] First example of end-on azido bridged dicopper(II) complex incorporating a macrocyclic complex (NiL^{18}) as ancillary ligand.

[b] Single EO azido bridged dimer.

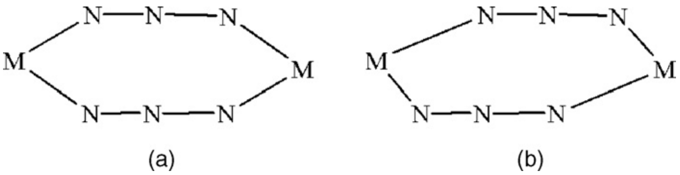

Fig. 9. Symmetric double end-to-end mode (a); asymmetric double end-to-end mode (b).

such to the complexes those are possessing basal–apical linkage to explain the experimentally observed magnetic data of the latter class of complexes. Nonetheless full molecule DFT based calculations based on X-ray structural data could be successfully used to rationalize the magnetic behavior of this class of complexes:

$$J = E_{BS} - E_T \qquad (1)$$

$$J = 2(E_{BS} - E_{HS}) \qquad (2)$$

$$J = \frac{2(E_{BS} - E_{HS})}{\langle S^2\rangle_{HS} - \langle S^2\rangle_{BS}} \qquad (3)$$

3.2. *Complexes with double end-to-end (EE) azido ($\mu_{2\text{-}1,3}$-N_3) bridges*

Two types of $\mu_{2\text{-}1,3}$-azido-bridged binuclear transition-metal complexes are found in the literature: (i) having four M–N$_{(azide)}$ short distances (≤2.10 Å) [symmetrical double $\mu_{1,3}$-azido bridges] (Fig. 9a) which are strongly antiferromagnetically coupled [34,115,116] and ii) having two M–N$_{(azide)}$ short (≤2.10 Å) and two M–N$_{(azide)}$ long distances (≥2.20 Å) [asymmetrical $\mu_{2\text{-}1,3}$ azido bridges] (Fig. 9b) which are weakly antiferro/or ferromagnetically coupled [107,117–124].

3.2.1. *Asymmetric double end-to-end (EE) azido ($\mu_{1,3}$-N_3) bridged dimeric complexes*

In Tables 7 and 8, the J coupling constants together with the τ and Δ (Δ = M–N–N–N–M torsion angle) (Fig. 2) parameters of the asymmetrical double-bridged ($\mu_{1,3}$-N_3) compounds are summarized. From Table 7 it is evident that complex $[Cu(Medpt)(\mu_{1,3}\text{-}N_3)]_2(ClO_4)_2$ (**55**) [107] has the same τ value of 0.23 as for $[Cu(Me_5dien)(\mu_{1,3}\text{-}N_3)]_2(ClO_4)_2$ (**57**) [118] but J values are quite different; *viz.* −150 and −7.5 cm^{-1} for complexes (**55**) and (**57**), respectively. Complex $[Cu(Medpt)(\mu_{1,3}N_3)]_2(ClO_4)_2$ (**55**) [107] has a Δ (M–N$_3$–M torsion angle) value of 11.3° and R [M–N$_{azido}$(basal) Å] value of 2.31 Å; the same parameters for $[Cu(Me_5dien)(\mu\text{-}N_3)]_2(ClO_4)_2$ (**57**) [118] were 15.7° and 2.33 Å, respectively. Thus, smaller R and Δ values clearly enhancing the antiferromagnetic coupling.

Table 7
Selected structural and magnetic interaction parameters for asymmetrical double bridging ($\mu_{1,3}$-N_3) complexes with antiferromagnetic coupling.

Compounds	R	τ	J (cm^{-1})	Δ	Ref.
$[Cu(Medpt)(\mu\text{-}N_3)]_2(ClO_4)_2$ (**55**)	2.10	0.23	−105	11.3	[107]
$[Cu(Et_5dien)(\mu\text{-}N_3)]_2(ClO_4)_2$ (**56**)	1.98	0.43	−28	15.7	[117]
$[Cu(Me_5dien)(\mu\text{-}N_3)]_2(BPh_4)_2$ (**57**)	1.99	0.29	−13	–	[118]
$[Cu(Me_5dien)(\mu\text{-}N_3)]_2(ClO_4)_2$ (**58**)	1.20	0.23	−7.5	15.7	[117]
$[Cu(L^{19})(\mu\text{-}N_3)]_2(ClO_4)_2$ (**59**)	1.96	0.16	−3.4	–	[120]

R = M–N$_{azido}$(basal) Å.

Table 8
Selected structural and magnetic interaction parameters for asymmetric double bridging ($\mu_{1,3}$-N_3) azido copper(II) complexes with ferromagnetic coupling.

Compounds	τ	J (cm^{-1})	Δ	Ref.
$[Cu(N_3)(tmen)(\mu\text{-}N_3)]_2$ (**60**)	0.20	≈0	–	[120]
$[Cu(L^{20})(\mu\text{-}N_3)]_2(ClO_4)_2$ (**61**)	–	2.4	38.1	[121]
$[Cu(Et_3dien)(\mu\text{-}N_3)]_2(ClO_4)_2$ (**62**)	0.20	9	35.8	[107]
$[Cu(L^{21})(\mu\text{-}N_3)]_2(ClO_4)_2$ (**63**)	0.08	90.7, 185.6	–	[59]
$[Cu(L^{22})(\mu\text{-}N_3)]_2$ (**64**)	–	13.6	–	[122]
$[\{Cu(phen)(N_3)_2\}(4,4'bpy)](ClO_4)_2$ (**65**)	–	5.52	–	[123]
$[CuL^{23}(\mu\text{-}N_3)]_2$ (**66**)	0.18	7.96	29.0	[124]

It can be seen that antiferromagnetic interactions through the double EE azide ligands are observed for the complex with torsion angles Δ less than 30.5°, and ferromagnetic interactions are observed for the complex with torsion angle greater than 32° (Table 8). However, it can be concluded from the above discussion that, in addition to the trigonality index parameter τ [77], Δ (Fig. 2) is another dominant factor that governs the magnetic coupling; probably contributes to the ferromagnetic interaction through the end-to-end azido ligands.

4. Trinuclear systems with azido bridge

Only a few complexes under this category are reported in the literature (Fig. 10).

Notably $\{[Pr_4N]_2[Cu_3(\mu_{1,1}\text{-}N_3)_4(N_3)_4]\}_n$ (**67**) [109] with interconnected symmetry related trinuclear $[Cu_3(N_3)_8]^{2-}$ moieties forms unprecedented infinite zigzag chains parallel to the

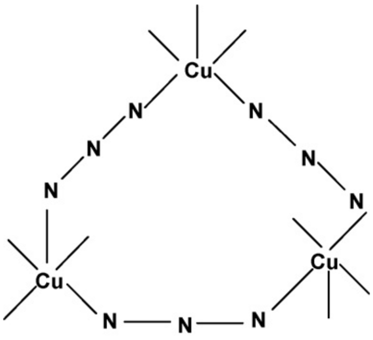

Fig. 10. Model diagram of trinuclear copper azido complex.

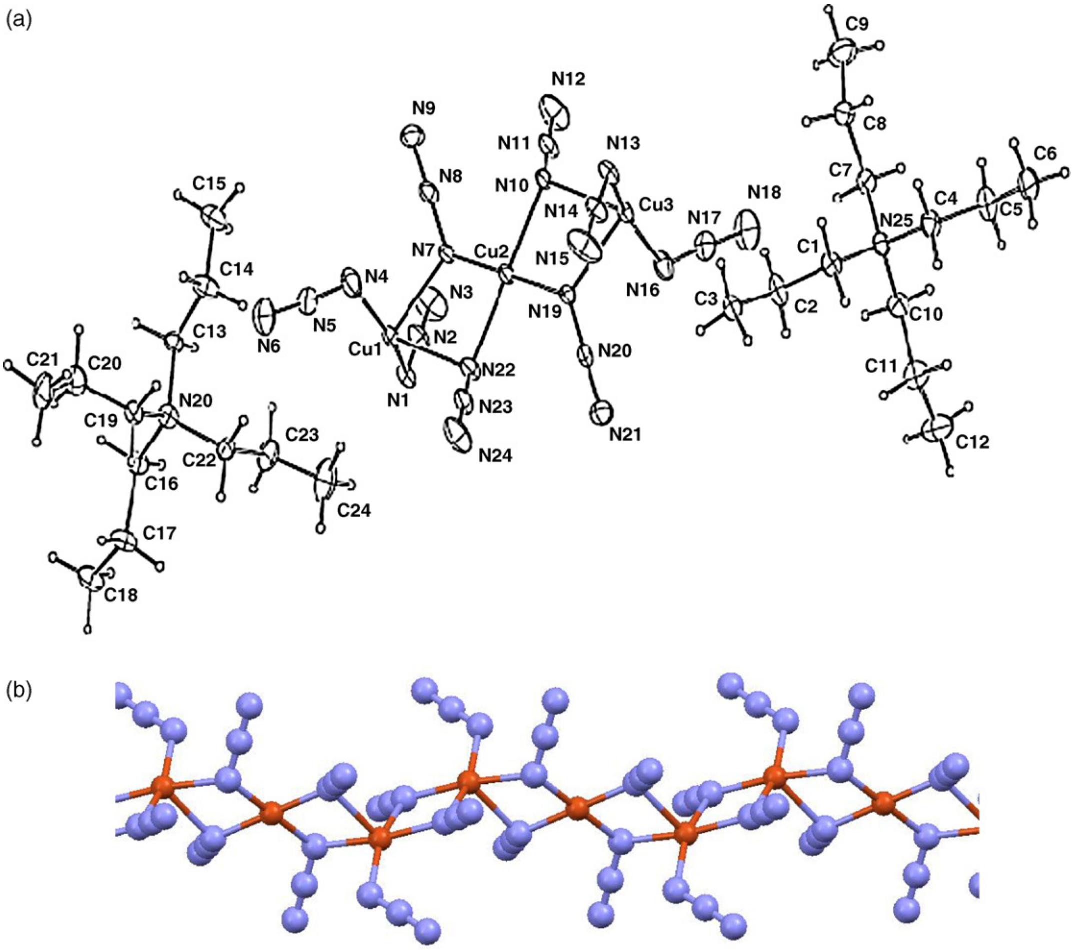

Fig. 11. (a) Ortep view of the complex $\{[Pr_4N]_2[Cu_3(\mu_{1,1}\text{-}N_3)_4(N_3)_4]\}_n$ (**67**) (reprinted with permission from ACS© [109]). (b) A zigzag 1D chain of the complex $\{[Pr_4N]_2[Cu_3(\mu_{1,1}\text{-}N_3)_4(N_3)_4]\}_n$ (**67**) (reprinted with permission from ACS© [109]).

crystallographic *a*-axis mediating ferromagnetic interactions (Figs. 11a and b, and 12).

Complex $[Cu_3(\mu_{1,1}\text{-}N_3)_4(N_3)_2(\text{Meinic})_2(\text{DMF})_2]$ (**68**) [68] has the $[Cu(\mu_{1,1}\text{-}N_3)_2Cu]$ core and showed a bulk ferromagnetic coupling. While a neutral trinuclear $\mu_{1,1}$-azido-bridged copper(II) complex $[L^{24}Cu(\mu_{1,1}\text{-}N_3)_2Cu(\mu\text{-}N_3)_2CuL^{24}]$ (**69**) [125] contains a square-planar central copper(II) and two distorted square-pyramidal terminal copper(II) atoms with centro-symmetric environment. Copper ions are antiferromagnetically coupled in complex (**69**). In a centro-symmetric complex $[Cu_3(\text{dien})_2(N_3)_6]$ (**70**) [126] the central copper(II) ion is coordinated by two monodentate azide anions and link copper atoms by double end-on azide bridges to give a linear trinuclear unit. The complex showed weak antiferromagnetic exchange between copper(II) ions ($J = -2.09\,\text{cm}^{-1}$) through the double end-on azide bridges. $Cu_3(\text{msalen})_2(N_3)_4(\text{DMF})_2$ (**71**) [127] has a trinuclear unit in which Cu(II) ions are bridged by single end-on azido ligands. Copper(II) ions are ferromagnetically coupled in complex (**71**). Further example of trinuclear copper(II) complex is $[Cu_3(\text{ampym})_2(\mu_{1,1}\text{-}N_3)_4(\mu_{1,3}\text{-}N_3)_2(\text{dmf})_2]_n$ (**72**) [128]. In complex (**72**) the trinuclear units (each of them contains two double end-on azido bridges) are linked through two azide ions in an end-to-end (EE) fashion, to yield the polymer chain. Interestingly complex $[Cu_3(\text{ampym})_2(\mu_{1,1}\text{-}N_3)_4(\mu_{1,3}\text{-}N_3)_2(\text{dmf})_2]_n$ (**72**) exhibits a ferromagnetic interaction above 30 K and weak antiferromagnetic interaction prevails in the range of 30–2 K. Addition of tetrakis-(2-pyridyl)cyclobutane (2,2′-tpcb) in a Cu^{II}/N_3 – solution afforded the 1D coordination polymer $[Cu_3(N_3)_6(2,2''\text{-tpcb})(\text{DMF})_2]_n$ (**73**) [129]. The ligand 2,2′-tpcb serves as a tetradentate bis-chelating ligand by linking linear $[(\text{DMF})Cu(\mu_{1,1}\text{-}N_3)_2Cu(N_3)_2(\mu_{1,1}\text{-}N_3)_2Cu(\text{DMF})]$ trinuclear units to produce a zigzag chain. Within each centro-symmetric trinuclear unit there exist two irregularly asymmetric end-on double azido-bridged $[Cu(\mu_{1,1}\text{-}N_3)_2Cu]^{2+}$ cores. Magnetic susceptibility measurement show bulk ferromagnetic coupling within the magnetically isolated trinuclear units ($J_1 = +70(3)\,\text{cm}^{-1}$, $J_2 = -3(2)\,\text{cm}^{-1}$). Density functional calculations reproduce the *J*

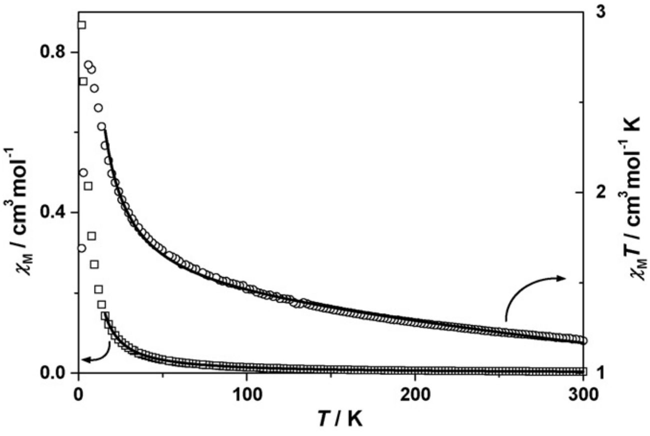

Fig. 12. $\chi_M T$ *versus* T (○) plot and χ_M *versus* T (□) of the complex $\{[Pr_4N]_2[Cu_3(\mu_{1,1}\text{-}N_3)_4(N_3)_4]\}_n$ (**67**) (reprinted with permission from ACS© [109]).

Table 9
Magneto-structural data for trinuclear copper(II) azido complexes.

Compounds	J (cm^{-1})	Ref.
$[Pr_4N]_2[Cu_3(\mu_{1,1}\text{-}N_3)_4(N_3)_4]_n$ (**67**)	7.0	[109]
$[Cu_3(\mu_{1,1}\text{-}N_3)_4(N_3)_2(\text{Meinic})_2(\text{DMF})_2]$ (**68**)	Bulk ferromagnetic	[68]
$[L^{24}Cu(\mu\text{-}N_3)_2Cu(\mu\text{-}N_3)_2CuL^{24}]$ (**69**)	Weak antiferromagnetic	[125]
$[Cu_3(\text{dien})_2(N_3)_6]$ (**70**)	−2.1	[126]
$[Cu_3(\text{msalen})_2(N_3)_4(\text{DMF})_2]$ (**71**)	32.6	[127]

value that agrees well with the corresponding experimental value. Ferromagnetic behavior of this complex is developed mainly due to the topology of the magnetic orbitals and the different coordination spheres of two neighboring Cu(II) atoms that result in small overlap of the orbitals possessing the unpaired electrons.

$[Cu_3(\text{dpyam})_2(\mu_{1,1}\text{-}N_3)_2(\mu\text{-}CH_3COO\text{-}\kappa\text{-}O^1)_2(\mu\text{-}CH3COO\text{-}\kappa\text{-}O^1O^2)_2]\cdot 2H_2O$ (**74**) is a unique azido-acetato bridged Cu(II) compound where trinuclear copper centers are triply bridged [130]. In this centro-symmetric compound, the central Cu atom is linked to two terminal Cu atoms by a double acetato bridge and an azido bridge, thereby providing a linear trinuclear unit. The coordination geometry around each of the terminal Cu(II) ions is distorted square pyramidal, while the geometry of the central Cu(II) ion is elongated octahedral. The magnetic susceptibility measurements revealed a weak antiferromagnetic interaction between the Cu(II) ions with a J value of −10.2 cm^{-1} [130]. Trinuclear azido Cu(II) carboxylate complexes $[Cu_3(\text{hnta})_4(N_3)_2(H_2O)_3]$ (**75**) exhibits long-range ferromagnetic ordering probably due to the short distance between the terminal nitrogen atom of the bridging azido ligand of one entity and the nitrogen atom of the pyridine ring of the neighboring entity [131] (Table 9).

The complex $[Cu_3(\text{atrz})_2(N_3)_6$ (**76**) [132] has a linear trinuclear Cu(II) structure with bridging bond angles Cu–N–N (atrz) 119.3(3) and 123.4(3)°, while Cu–N–Cu angle was 118.7(2)°. The Cu(II) ions are strongly antiferromagnetically coupled (J = −108.8 cm^{-1}) in (**76**).

5. Tetranuclear and other high nuclearity azido-bridged clusters

The tetranuclear moieties exhibit a variety of structural types (Fig. 13) namely cyclic types (metallocrowns), linear arrays, cubanes and defective cubanes of Cu(II) azido systems.

5.1. Cyclic Cu$_4$ azido clusters

Three Cu$_4$ clusters $[Cu_4(\text{pap})_2(N_3)_8(\text{MeOH})_2]$ (**77**) [133], $[Cu_4(\text{papMe})_2(N_3)_4(H_2O)_2(NO_3)_2](NO_3)_2$ (**78**) [134], $[Cu_4(\text{macy2})(N_3)_4]$ (**79**) [135] with cyclic topologies are known. In addition to EO N_3^- ligands, which bridge the Cu pairs, complexes (**77**) and (**78**) also contain dinucleating ligand phthalazine aminopyridyl ligand (pap or papMe). The $[Cu^{II}_2]$ dimers are linked to each other by EE bridging N_3^- ligands. Nevertheless, the difference between the complexes lies in the terminal ligands, which affect the charge of the complex, and $[Cu_4(\text{pap})_2(N_3)_8(\text{MeOH})_2]$ (**77**) [133] has two additional μ-MeOH ligands. The magnetic coupling in complexes (**77**) and (**78**) is antiferromagnetic. The large macrocyclic ligand in complex $[Cu_4(\text{macy2})(N_3)_4]$ (**79**) [135] maintains a tetranuclear cycle by means of four alkoxide bridges, whereas two EE N_3^- bridges support the link between two pairs of Cu(II) ions (Figs. 14 and 15).

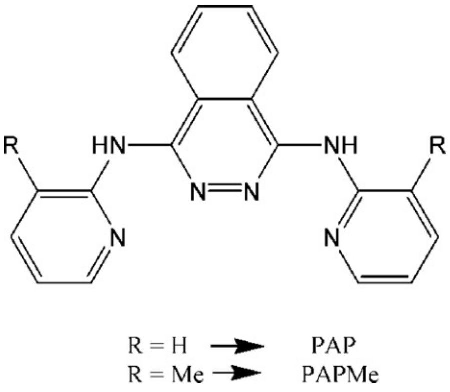

Fig. 14. The structure of the ligand PAP and PAPMe.

5.2. Linear Cu$_4$ azido clusters

Complexes $[Cu_4(\text{msalen})_2(N_3)_2(H_2O)(\text{MeOH})]$ (**80**) [136], $Cu_4(\text{msalen})_2\ (N_3)_2(\text{DMSO})_2]$ (**81**) [137] and $[Cu_4(\text{salen})_2(N_3)_4]$ (**82**) [138] consist of a pair of dimers. Polydentate Schiff-base ligands bridge two Cu(II) ions to yield the dimers which are interconnected linearly through a pair of $\mu_{1,1}$-N_3 groups. The overall structure is a dimer of dimers. The magnetic studies of complexes (**80**) and (**81**) are not reported.

$[Cu_4(\text{salen})_2(N_3)_4]$ (**82**) (Fig. 16) [138] yielded antiferromagnetic coupling (J_1 = −12.8 cm^{-1}; J_2 = −10 cm^{-1}) for both Cu...Cu bridges. This compound was the first to exhibit antiferromagnetic coupling for the Cu–$(\mu_{1,1}\text{-}N_3)_2$–Cu bridging mode (Fig. 17).

Half of the tetranuclear complex $[Cu_4(\text{salen})_2(N_3)_4]$ (**82**) is symmetry related to the other half, and three coupling constants are required to explain its magnetic properties. However, magnetic interactions through next nearest neighbors are expected to be at least one order of magnitude lower than those between nearest neighbors. Therefore, to avoid overparametrization two coupling constants, J_1 between Cu(1) and Cu(2) and symmetry related Cu(1)* and Cu(2)*, and J_2 between Cu(1) and Cu(1)* are considered.

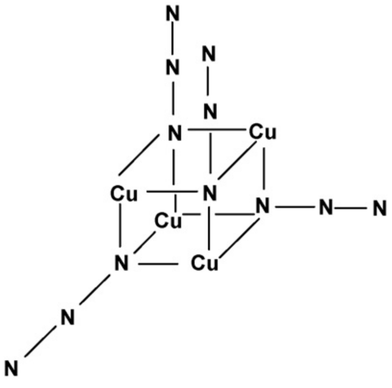

Fig. 13. Diagram representing tetranuclear array of copper azido complexes.

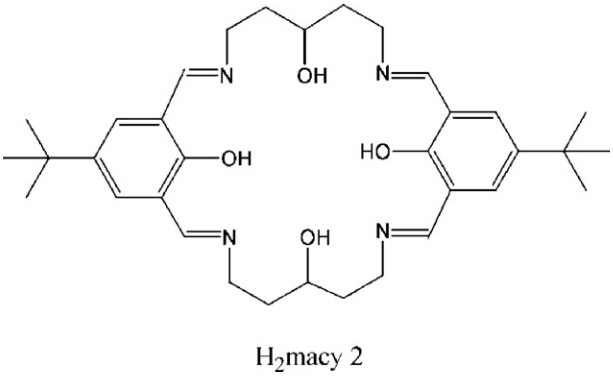

Fig. 15. The structure of the ligand H$_2$macy2.

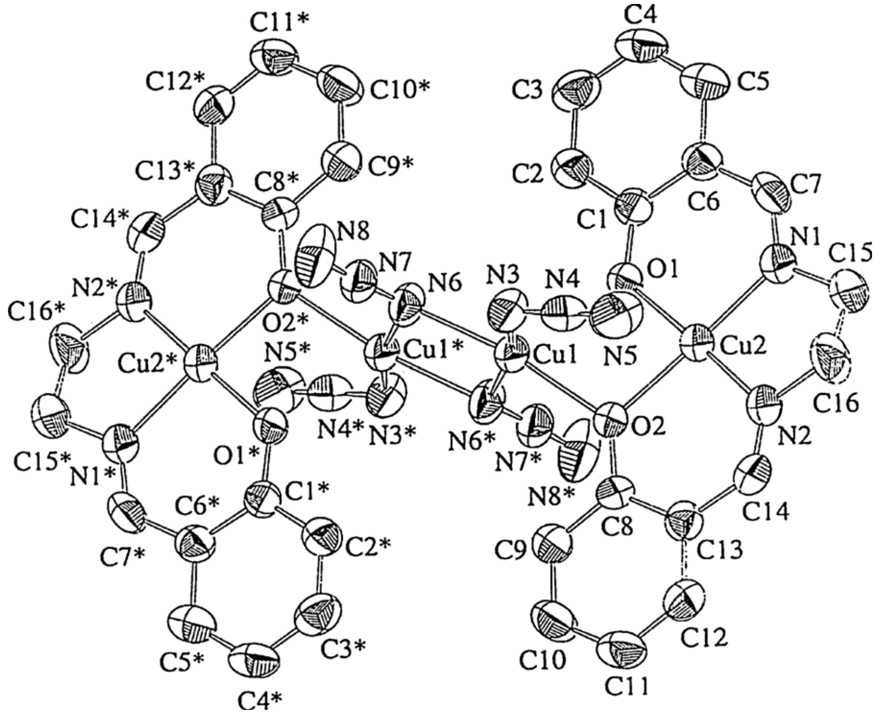

Fig. 16. Ortep diagram for the complex $[Cu_4(salen)_2(N_3)_4]$ (**82**) (reprinted with permission from ACS© [138]).

The spin Hamiltonian $\hat{H} = -2J_1(\hat{S}_1\hat{S}_2 + \hat{S}_3\hat{S}_4) - 2J_2\hat{S}_2\hat{S}_3$ appropriate for this type of tetranuclear copper(II) system has been used to derive the susceptibility expression. In order to calculate the energy levels and magnetic properties, diagonalization of the full matrix has been carried out. The best fit of the magnetic data was obtained with the following set of parameters $J_1 = -12.8\ cm^{-1}$, $J_2 = -10\ cm^{-1}$, $g = 2.171$, 2.1% of paramagnetic component, and negligible temperature independent paramagnetism (5×10^{-8}). Fig. 18 shows the contour plot for J_1 and J_2. The minimum FCN value (corresponding to the best fit) is 0.1; it is in the middle of the 1.0 contour. There is no secondary minimum in this plot, thereby proves the reliability of the values of J_1 and J_2 [138].

Complex $[Cu_4(bpt\text{-}H)_4(N_3)_4]\cdot 4.5H_2O$ (**83**) is a neutral tetranuclear grid-like complex with four Cu^{2+} ions in a tetrahedral arrangement in which the azides act as monodentate ligands [139]. The asymmetric unit of the said complex consists of two metal atoms, two *cis–cis* $(bpt\text{-}H)^-$, two N^{3-} ligands and 2.25 lattice water molecules on general positions. Both Cu^{2+} ions are in elongated [4 + 1] square pyramidal coordination geometries (τ = 0.23 for Cu1 and 0.236 for Cu2) surrounded by one azide on the basal plane. A moderate antiferromagnetic coupling between the Cu^{2+} ions *via* the double N–N bridges of $(bpt\text{-}H)^-$ was observed in the complex [139]. Complexes $[Cu_4(bmdp)_2(OAc)_2(N_3)](ClO_4)_3$ (**84**) [140] ((Fig. 19); OAc = acetate ion) and $[Cu_4(O_2cyclam1)_2(tmen)_2(N_3)](ClO_4)_3$ (**85**) [141] resulted from two dimers of asymmetric dinucleating ligands, each featuring a coordinatively unsaturated Cu(II) that reacts selectively with one azido ligand to form $\mu_{1,3}$-N_3^- linked tetranuclear complexes. Complex $[Cu_4(bmdp)_2(OAc)_2(N_3)](ClO_4)_3$ (**84**) [140] shows weak ferromagnetic coupling. In complex $[Cu_4(O_2cyclam1)_2(tmen)_2(N_3)](ClO_4)_3$ (**85**) [141], the dinucle-

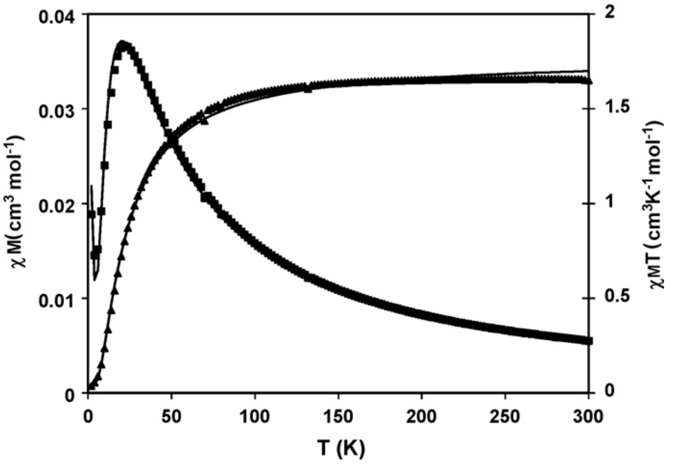

Fig. 17. $\chi_M T$ *versus* *T* (●) plot and χ_M *versus* *T* (■\) of the complex $[Cu_4(salen)_2(N_3)_4]$ (**82**) (reprinted with permission from ACS© [138]).

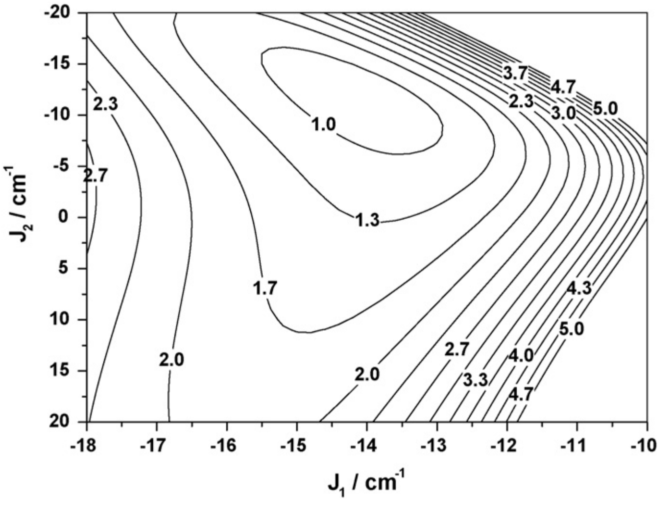

Fig. 18. Counter plot of J_1 and J_2 of the complex $[Cu_4(salen)_2(N_3)_4]$ (**82**). The numerical figures mentioned on the curves are the values of the reliability parameter FCN (reprinted with permission from ACS© [138]).

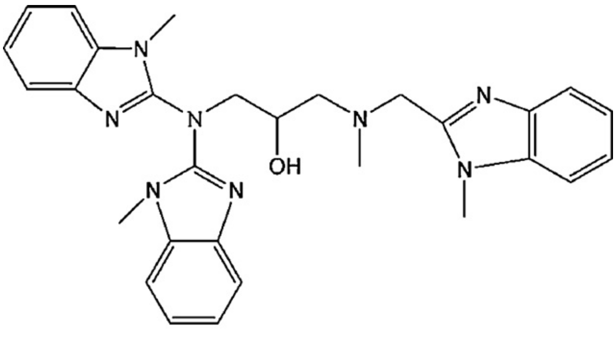

Hb mdp

Fig. 19. The structure of the ligand Hbmdp.

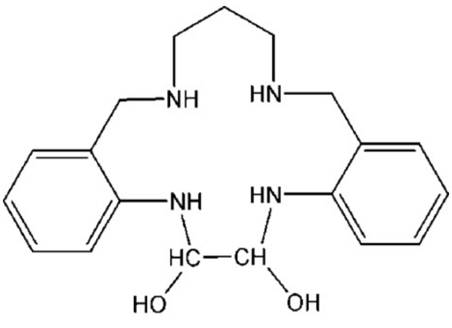

O_2cyclam 1

Fig. 20. The structure of the ligand O_2 cyclam 1.

ating ligand is a cyclic oxamide ligand (Fig. 20). No magnetic study was reported for complex (**85**). The complex $[Cu_4(acac)_2(phen)_4(N_3)_4(ClO_4)_2]$ (**86**) [142] is a genuine linear tetranuclear array exclusively bridged by (single or double) μ-N_3^- ligands; the remaining coordination sites are occupied by chelating ligands, acetylacetonato (acac) and phenanthroline (phen) or perchlorate. Despite the bridge being axial-equatorial type, the magnetic coupling is ferromagnetic with the ground state $S = 2$.

Tetranuclear copper(II) compounds with formulae $[Cu_4(\mu_2\text{-}PhCOO)_2(\mu\text{-bdmap})_2(\mu_{1,3}\text{-}N_3)_2(N_3)_2(H_2O)_2]$ (**87**), and $[Cu_4(\mu_2\text{-}PhCOO)_2\text{-}(\mu\text{-bdmap})_2(\mu_{1,3}\text{-}N_3)_2(PhCOO)_2(CH_3OH)_2]$ (**88**), exhibited bulk antiferromagnetic coupling with J values of -85.4 and $-89.5\,cm^{-1}$ for (**87**) and (**88**), respectively [143].

5.3. M_4 cubanes with azide bridging ligand

The cubic arrangement is one of the most common structural motifs of tetranuclear coordination clusters $[Cu_4O_4]$. In most cases the cube is formed by four symmetrically equivalent metals and four monoatomic donors in a μ_3-bridging mode, which are usually alkoxides, hydroxides or oxides. Because of its coordination versatility the N_3^- group has also been found to act as a core ligand within cubane structures in a few occasions.

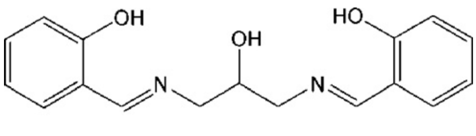

H_3bsi

Fig. 21. The structure of the ligand H_3bsi.

The complex $[Cu_4(bsi)_2(N_3)_2]$ (**89**) (Fig. 21) [144] displays a very unconventional cubane structure with a $[Cu_4N_2O_2]$ core where the N atoms belong to azide groups and the O donors are from alkoxides provided by a pentadentate Schiff-base ligand, which also serves to complete the peripheral ligation around Cu(II). The coupling within the cubane core is dominated by antiferromagnetic interactions, which leads to a spin ground state of $S = 0$. The copper(II) complex containing $\mu_{1,1}$ azide nitrogen and μ_3-alkoxo oxygen in cubane type tetranuclear core is $[Cu_4(M_3)_2(\mu_3\text{-OEt})_2(\mu\text{-}N_3)_2(N_3)_2](MeOH)$ (**90**) [145] where M_3 is a deprotonated macrocycle ligand. This compound shows two dimeric units Cu_2O_2 associated in an axial fashion through two $\mu_{1,1}$ azides and two μ_3 alkoxides, to from a $Cu_4N_2O_4$ open 'boxkite' arrangement of two fused cubes, each missing one apex. In this dicubane type complex, the two Cu_2NO faces are in the opposite sides with respect to the Cu_2O_2 face, which they share in the tetranuclear core.

A one-dimensional molecular rail road copper(II) azido compound of formula $[Cu_4(bpm)_2(N_3)_8]_n$ (**91**) [146] with a Cu_4N_6 defective double cubane unit exhibited three different coordination, namely the $\mu_{\text{-}1,1}$, $\mu_{\text{-}1,1,1}$ and $\mu_{\text{-}1,1,3}$-N_3-bridging modes, lead to an unprecedented structure of the Cu(II) azide. In addition, the Cu–$N_{(azido)}$–Cu angles vary in the range 93.80(10)–102.31(9)°, values which lie within the domain where the magnetic coupling for azido-bridged copper(II) compounds is predominantly ferromagnetic [40].

5.4. Rare $\mu_{1,1,3,3}$-N_3-coordination in an Cu_4 cluster

Complex $[Cu_4(tpimim)_2(N_3)]Cl$ (**92**) [147] is the only Cu(II) species that contains azide in the $\mu_{\text{-}1,1,3,3}$ mode (Fig. 1i). The metals spanned by two of the opposite edges are not supported by any additional ligand, while the other two sides are spanned by two heptadentate tpimim ligands. The interaction between the ions bridged by the tpimim ligand (Fig. 22) is weakly ferromagnetic, most probably because of the imidazolidine bridge, rather than the azide. The coupling mediated by EE azide pathways is, as usual, antiferromagnetic.

5.5. Asymmetric μ_4 end-on bridging mode

Reaction of copper(II) perchlorate with di-2,6-(2-pyridylcarbonyl)pyridine (pyCOpyCOpy, dpcp) in the presence of sodium azide yields complex $Cu_4(N_3)_2\{pyC(OMe)(O)pyC(OMe)(O)py\}_2(MeOH)_2](ClO_4)\cdot 2MeOH$ (**93**) consisting of four Cu(II) ions in a rhombic topology with a new metal core of asymmetric μ_4-azido bridges adopting a $\mu_{1,1,1,1}$ (Fig. 1h) bridging mode [148]. This bridging mode for azides is very rare, and it is observed for the first time in complex **93**. Ferromagnetic interaction ($J = +26.8\,cm^{-1}$) in **93** is caused by the structural constraints imposed by the $\{pyC(OMe)(O)pyC(OMe)(O)py\}^{2-}$ ligand on the Cu(II) ions [148].

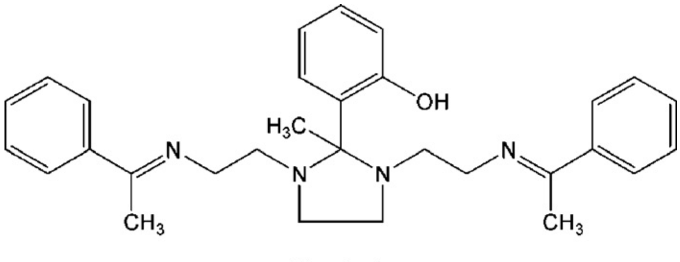

H_3tpimim

Fig. 22. The structure of the ligand H_3tpimim.

5.6. *A linear Cu^{II}_5 arrangement with azido linkage*

The compound $[Cu_5(terpy)_2(N_3)_{10}]$ (**94**) [149] comprises a linear central trinuclear unit held together by two double μ-N_3^- bridges, with each external copper ion of this unit linked by a single EO azido ligand to a $[Cu(terpy)(N_3)]^+$ moiety. Bulk magnetization studies reveal that the peripheral Cu(II) centers essentially do not interact with the central unit, and the latter exhibits weak ferromagnetic coupling.

5.7. *A hexanuclear Cu(II) cluster with azido linkage*

The employment of the di-2-pyridyl ketone $[(py)_2CO]/PhCO_2^-/N_3^-$ ligand provided a hexanuclear cluster $[\{Cu_6(O_2CPh)_4(N_3)_2\{(py)_2CO_2\}_2\{(py)_2C(OH)O\}_2]$ (**95**), and two coordination polymers $[Cu_4(O_2CPh)_2(N_3)_4\{(py)_2C(OMe)O\}_2]_n$ (**96**) and $[Cu_2(O_2CPh)(N_3)_2\{(py)_2\text{-}C(OMe)O\}]_n$ (**97**) [150]. Complex **95** has a $[Cu_6(\mu_3\text{-}OR^-)_2(\mu\text{-}OR^-)_4]^{6+}$ core based on a central defective cubane unit and two additional Cu(II) atoms across the missing edges. Complex **96** showed a zigzag chains while complex **97** showed an extended 2D networks that adopt the herringbone architecture which is not based on T-shaped nodes. Cluster (**95**) is antiferromagnetically coupled ($J_1 = -94(5)\,cm^{-1}$, $J_2 = -110(5)\,cm^{-1}$, $J_3 = -116(5)\,cm^{-1}$) with an $S = 0$ ground state [150].

The reactions of di-2-pyridyl ketone with $Cu(O_2CPh)_2$ in the presence of NaN_3 and LiOH afforded an antiferromagnetically coupled ($S = 0$; $J_1 = -94(5)\,cm^{-1}$, $J_2 = -110(5)\,cm^{-1}$, $J_3 = -116(5)\,cm^{-1}$) Cu^{II}_6 cluster with a novel core. $[Cu_6(O_2CPh)_4(N_3)_2\text{-}\{(py)_2CO_2\}_2\{(py)_2C(OH)O\}_2]\cdot 2H_2O4.5MeCN$ (**98**) and coordination polymers $[Cu_4(O_2CPh)_2(N_3)_4\{(py)_2C(OMe)O\}_2]_n$ (**99**) and $[Cu_2(O_2CPh)(N_3)_2\{(py)_2C(OMe)O\}]_n$ (**100**) have fascinating structures. The cluster or polymer formation depends on the solvent used during preparation [151].

5.8. *Azido clusters of transition metals and polyoxometallates*

A relatively new class of molecular magnetic materials is prepared by using polyoxometallates (POMs) and azide in combination with paramagnetic transition-metal ions [152]. Anionic clusters like $[(\gamma\text{-}SiW_{10}O_{36})_2Cu_4(N_3)_4]^{12-}$ (**101**) [149], $[(\gamma\text{-}SiW_{10}O_{36})_2Cu_4(H_2O)_2(N_3)_4]^{12-}$ (**102**) [153] and $[(SiW_8O_{31})_3Cu_9(OH)_3(H_2O)_6(N_3)_4]^{10-}$ (**103**) [154] are of this type. The complex (**103**) is especially remarkable because it features an unprecedented coordination mode for azide, namely $\mu_{1,1,1,3,3,3}$-N_3 (Fig. 1j) [154].

5.9. *Clusters with heterometallic azide bridges*

In comparison with the plethora of homometallic azido systems reported to date, compounds in which the azido ligand acts as a bridge between two different paramagnetic centers (excluding different oxidation states of the same metallic atom) are extremely rare. Low nuclearity systems such as one [CuNi] dinuclear complex with $\mu_{1,1}$-azido bridges [155]; one trinuclear cluster [FeCuFe] linked by means of $\mu_{1,3}$-azido bridges [156] are reported. The high nuclearity complex $[Cu_4(O_2cyclam2)_4Mn_2(N_3)_4]$ (**104**) [157] contains heterometallic azido bridges. The asymmetric unit of (**104**) consists of a [CuMnCu] trinuclear unit in which Mn atom is bridged to both Cu atoms by means of oxamide bridges. Each Cu(II) ion is embedded within a macrocycle that is a part of the oxamide moiety. The remaining coordination sites of the octahedral coordination sphere around Mn are occupied by two azido ligands. One of them acts as a terminal ligand where as the second azido binds to the axial position of the square pyramidal copper atom of a second trinuclear unit. The role of the azido bridges in the magnetism of the complex (**104**) is marginal since these are coordinated to the axial sites of the copper atoms.

6. One-dimensional azido systems

One-dimensional systems are of following types: (1) uniform systems with $\mu_{1,3}$ (EE) bridging, $\mu_{1,1}$ (EO) bridging and having both $\mu_{1,3}$ and $\mu_{1,1}$ bridging; (2) alternating systems with (EE/EO) bridging; (3) $\mu_{1,1,3}$-bridging and (4) having azide and other bridges. We will be discussing their structural and magnetic properties in the following sections.

6.1. *One-dimensional uniform systems with $\mu_{1,3}$-azido bridging ligands*

Uniform 1D system is understood to be those systems in which all ions have the same magnetic interaction pathway (Fig. 23).

A novel example of this category is one-dimensional Cu(II) compound $[Cu(L^{25})(\mu_{1,3}\text{-}N_3)(ClO_4)]_n$ (**105**) that exhibits ferromagnetic interaction through end-to-end azido linkages [158]. DFT calculation rationalized its exceptional magnetic behavior [158]. Two uniform single end-to-end azido-bridged 1D polymeric complexes $[Cu(L^{26})(N_3)]_n(ClO_4)_n$ (**106**) and $[Cu(L^{27})(N_3)]_n(ClO_4)_n$ (**107**) feature ferromagnetic interactions [159(a)]. Tridentate Schiff base complexes $[Cu(L^{28})(N_3)]_n(ClO_4)_n$ (**108**), $[Cu(L^{29})(N_3)]_n(ClO_4)_n$ (**109**) and $[Cu(L^{30})(N_3)]_n(ClO_4)_n$ (**110**) containing end-to-end azido bridge show weak ferromagnetic interaction [160]. $[Cu(L^{31})(N_3)]_n(ClO_4)_n$ (**111**) represents first example of structurally characterized ferromagnetically coupled 1D uniform system incorporating reduced Schiff base as co-ligand [119]. One-dimensional chiral copper(II) coordination polymers with single asymmetric end-to-end (EE) azide bridges $[Cu(R\text{-}L^{32})_2(N_3)]_n(ClO_4)_n$ (**112**) or $[Cu(S\text{-}L^{32})_2(N_3)]_n(ClO_4)$ (**112**) [161] were obtained using chiral Schiff bases as auxiliary ligands and azide ions as bridging ligand. In these complexes the central Cu(II) ion is exist in an elongated octahedron (Table 10a).

The complex $[Cu(R\text{-}L^{32})_2(N_3)]_n(ClO_4)_n$ (**112**) [161] exhibits very weak ferromagnetic interaction between copper(II) ions through the single end-to-end azido bridge with a J value equal to $0.70(3)\,cm^{-1}$. A doubly end-to-end (EE) azido-bridged 1D Cu(II) chain $Cu(L^{33})_2(N_3)_2$ (**113**) also exhibits ferromagnetic interaction [162]. In complex (**113**) Cu–N–N angles [123.0(4) and 115.7(4)°] are not close to 165° at which antiferromagnetic interaction is minimum and hence large $Cu\text{–}N_3\text{–}Cu$ torsion angle (−71°) is responsible for the orientation of the magnetic orbitals in orthogonal fashion to obtain the observed ferromagnetic interaction. The only reported copper(II) complexes $[Cu(L^{34})(N_3)]_n(H_2O)_{2n}$ (**114**) [112] and $[Cu(bpym)(N_3)_2]_n$ (**116**) [163] exhibit intrachain weak antiferromagnetic interactions through end-to-end azido coupler till date. The complex $Cu(L^{35})(N_3)]_n$ (**115**) [L^{35} = 1-(N-salicylideneimino)-2-(N,N-dimethyl)-aminoethane] (Fig. 24) reveals that the neutral $[Cu(L^{35})(N_3)_n]$ units in complex (**115**) are connected each other by the single $\mu_{1,3}$-azido ligands to form an infinite 1D polymeric chain [54]. The tridentate NNO donor Schiff-base ligand acts as a chelating ligand. The typical folded-knee shaped χ_M *versus* T curve indicates a bulk antiferromagnetic interaction is operative in the complex (**115**) (Fig. 25).

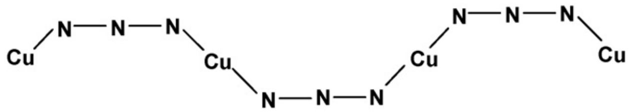

Fig. 23. Single end-to-end (EE) 1D azido bridging mode.

Table 10a
Structural parameters for one-dimensional systems with $\mu_{1,3}$-azido unit: Cu–N bond distances (Å) and Cu–N–N angles (°).

Complexes	Cu–N (Å)	Cu–N–N (Å)	Cu–N_3–Cu (Δ)	Ref.
$[Cu(L^{25})(N_3)]_n(ClO_4)_n$ (**105**)	1.936, 2.486	125.6	91.6	[158]
$[Cu(L^{26})(N_3)]_n(ClO_4)_n$ (**106**)	1.991, 2.266	134.4, 136.7	31.3	[159]
$[Cu(L^{27})(N_3)]_n(ClO_4)_n$ (**107**)	1.946, 2.398	122.5, 135.1	102.7	[159]
$[Cu(L^{28})(N_3)]_n(ClO_4)_n$ (**108**)	1.947, 2.355	126.5, 131.2	97.8	[160]
$[Cu(L^{29})(N_3)]_n(ClO_4)_n$ (**109**)	1.965, 2.311	131.2, 139.1	50.4	[160]
$[Cu(L^{30})(N_3)]_n(ClO_4)_n$ (**110**)	1.951, 2.270	139.0, 132.2	40.4	[160]
$[Cu(L^{31})(N_3)]_n(ClO_4)_n$ (**111**)	1.955, 2.880	133.5, 100.3	92	[119]
$[Cu(R\text{-}L^{32})_2(N_3)]_n(ClO_4)_n$ (**112**) or $[Cu(S\text{-}L^{32})_2(N_3)]_n(ClO_4)_n$ (**112**)	1.975, 2.683 1.971, –	127.7, 128.0	–	[161]
$[Cu(L^{33})_2(N_3)_2]_n$ (**113**)	2.029, 2.611	115.7, 123.0	−71	[162]
$[Cu(L^{34})(N_3)]_n(H_2O)_{2n}$ (**114**)	1.948, 2.563	129.0	17.0	[112]
$[Cu(L^{35})(N_3)]_n$ (**115**)	1.980, 2.473	–	–	[54]

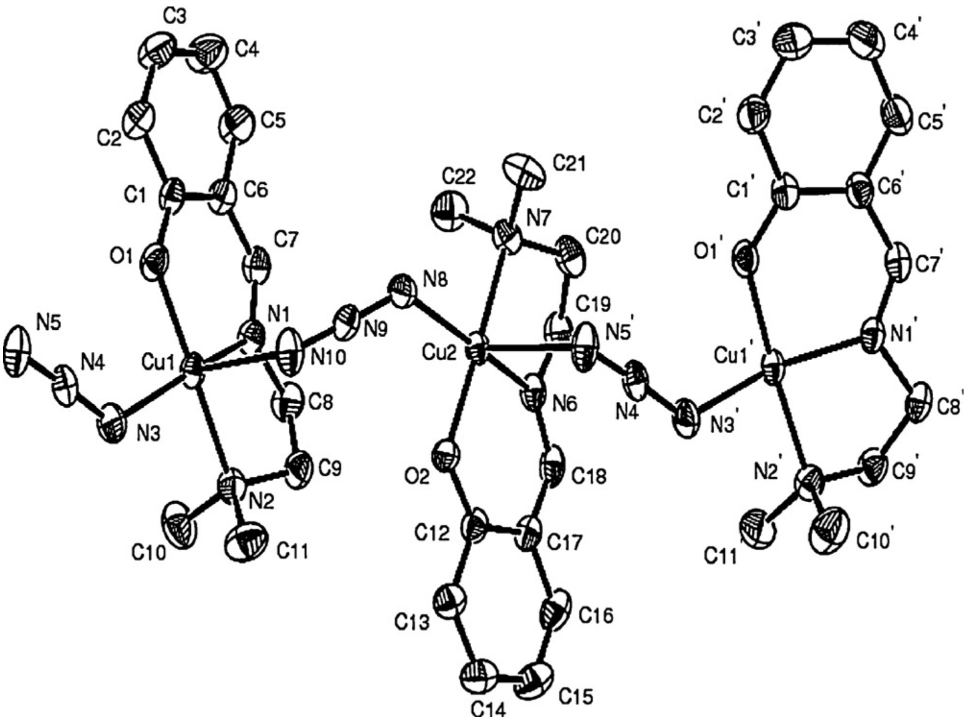

Fig. 24. Ortep diagram of complex $[Cu(L^{35})(N_3)]_n$ (**115**) showing part of the 1D infinite chain with atom numbering scheme (reprinted with permission from Elsevier© [54].

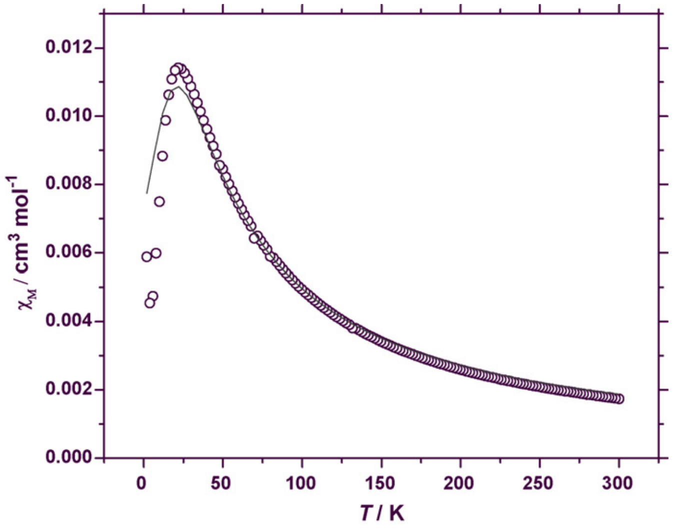

Fig. 25. χ_M *versus* T (Δ) plot for complex $[Cu(L^{35'})(N_3)]_n$ (**115**). Solid lines represent the best fit of the data (reprinted with permission from Elsevier© [54].

A polymeric chain complex $[L^{36}Cu_2(N_3)_2]_n(ClO4)_{2n}\cdot n(H_2O)$ (**117**) [L^{36} = the dinucleating macrocyclic ligand bis-p-xylyl-BISDIEN] having end-to-end azido-bridged cationic $[L^{36}Cu_2(N_3)_2]^{2+}$ unit, consists of non-coordinated perchlorate anions and crystallized water molecules [164]. Magnetic moments vary from 2.05 (B.M.) at 300 K to 2.01 (B.M.) at 80 K suggesting that very weak interactions exist between the metal centers.

A look at Table 10b reveals that most of the complexes listed there are ferromagnetic in nature. However, the coupling parameters are small. For copper(II) systems, the magnitude of the super exchange parameter J is strongly dependent on main two factors, *viz.* the atomic orbitals of the copper atoms involved and the ∠Cu–N–N and Cu–N_3–Cu torsion angle in the bridging region. The coupling may be strongly AF when the end-to-end azido ligands are bonded to the equatorial coordination sites of the two copper atoms, in which case two $d_{x^2-y^2}$ orbitals is involved in the super exchange mechanism. In contrast, very weak coupling should be expected when the interaction is axial-equatorial in nature involving $d_{x^2-y^2}$ and d_{z^2} atomic orbitals.

The different magnetic behavior is related to the low unpaired electronic density found in the d_{z^2} atomic orbital in the square pyramidal or octahedrally coordinated copper atoms. Classical attempts to relate the magnitude of the super exchange cou-

Table 10b
Magnetic parameters for one-dimensional systems with $\mu_{1,3}$-azido bridge.

Complexes	J (cm^{-1})	Ref.
$[Cu(L^{25})(N_3)]_n(ClO_4)_n$ (**105**)	1.36	[158]
$[Cu(L^{26})(N_3)]_n(ClO_4)_n$ (**106**)	2.69	[159]
$[Cu(L^{27})(N_3)]_n(ClO_4)_n$ (**107**)	2.02	[159]
$[Cu(L^{28})(N_3)]_n(ClO_4)_n$ (**108**)	2.15	[160]
$[Cu(L^{29})(N_3)]_n(ClO_4)_n$ (**109**)	3.61	[160]
$[Cu(L^{30})(N_3)]_n(ClO_4)_n$ (**110**)	2.06	[160]
$[Cu(L^{31})(N_3)]_n(ClO_4)_n$ (**111**)	1.60	[119]
$[Cu(R\text{-}L^{32})_2(N_3)]_n(ClO_4)_n$ (**112**)	0.70	[161]
$[Cu(L^{33})_2(N_3)_2]_n$ (**113**)	1.6	[162]
$[Cu(L^{34})(N_3)]_n(H_2O)_{2n}$ (**114**)	−4.30	[112]
$[Cu(L^{35})(N_3)]_n$ (**115**)	−22.5	[54]
$[Cu(bpym)(N_3)_2]_n$ (**116**)	−3.8	[163]
$[L^{36}Cu_2(N_3)_2]_n(ClO_4)_{2n}\cdot n(H_2O)$ (**117**)	WAF	[164]

pling and the structural data for the axial-equatorial case conclude a greater AF coupling for the trigonal bipyramidal arrangement which is in agreement with the greater mixing of the $d_{x^2-y^2}$ and d_{z^2} atomic orbitals in such cases [118]. In a recent study the electronic structures of two asymmetrical EE azido-bridged copper(II) complexes $[Cu(L^{26})(N_3)]_n(ClO_4)_n$ (**106**) and $[Cu(L^{27})(N_3)]_n(ClO_4)_n$ (**107**) [159(b)] were studied. The result shows that the spin population in these two complexes is largely distributed on the equatorial plane of the square pyramid surrounding the copper(II) ions. Ferromagnetic coupling through the asymmetrical azido ligand in these two complexes has been mainly attributed to the spin delocalization and weak spin polarization effect.

6.2. One-dimensional uniform systems with $\mu_{1,1}$-azido bridging ligands

The structural and magnetic information of the 1D Cu(II) complexes containing single EO azide bridges (Fig. 26) are summarized in Tables 11a and 12.

The Cu(II) ions in these complexes assume the pseudo-square-pyramidal geometry. The single EO azido bridge in $[Cu_2(\mu\text{-trans-oxen})(\mu_{1,1}\text{-}N_3)_2(Br)]_n$ (**118**) [165] adopts a quasi-symmetric basal–basal disposition between metal ions and mediates a relatively strong antiferromagnetic interaction.

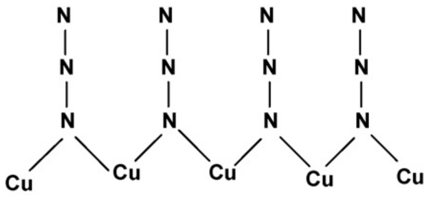

Fig. 26. Single end-on (EO) 1D azido bridging mode.

Both symmetric and asymmetric single EO azido bridges are present in $[Cu_4(\mu\text{-trans-oxen})_2(\mu_{1,1}\text{-}N_3)_2(\mu_{1,3}\text{-}N_3)]_n(ClO_4)_n$ (**119**) [166] where the interactions mediated by these bridges were not quantified, but the overall antiferromagnetic interaction between the binuclear Cu(oxen)Cu units has been mainly attributed to the symmetric bridges. Further the single EO azido bridges in the other complexes adopt the asymmetric basal–apical disposition and mediate relatively weak magnetic interactions those are either antiferromagnetic or ferromagnetic. As can been seen from Tables 11a and 11b, the dependence of the interaction upon the Cu–N–Cu bridging angle observed in the symmetric EO azido bridge is not apparent in the asymmetric varieties. In fact it is impossible to find any general magneto-structural correlation with these limited experimental data.

6.3. One-dimensional uniform systems with both kinds of azido (EO and EE) bridges

Examples of 1D uniform system having both types of azido bridges are limited in the literature. There are only two reported complexes fall in this variety: one having single EO and double EE azido bridges (Fig. 27) and other having mixed EO and EE bridges together with double EO bridges (Fig. 28).

In complex $[NMe_4][Cu(N_3)_3]$ (**127**) [172] the Cu(II) ions are simultaneously bridged by one EO and two EE azido bridges mediating antiferromagnetic coupling with exchange parameter $J/k = -3.6$ K, $g = 2.1$.

The one-dimensional chain of $[Cu(3\text{-Clpy})_2(\mu\text{-}N_3)_2]_n$ (**128**) (3-Clpy = 3-chloropyridine) consists of two groups of the mixed end-to-end and end-on bridges along with two groups of double

Table 11a
Structural parameters for the single EO azido bridges 1D Cu(II) complexes.

Complex	Cu–Cu (Å)	Cu–N (Å)	Cu–N–Cu (°)	Ref.
$[Cu_2(\mu\text{-oxen})(\mu\text{-}N_3)_2(Br)]_n$ (**118**)	3.27	1.98, 1.95(bb)	112.5	[165]
$[Cu_4(\mu\text{-oxen})_2(\mu_{1,1}\text{-}N_3)_2(\mu_{1,3}\text{-}N_3)]_n(ClO_4)_n$ (**119**)	3.27	1.98, 1.98(bb)	111.8	[166]
	3.28	2.41, 1.95(ba)	97.3	
$[Cu_2(L^{37})_2(N_3)_2(\mu\text{-}N_3)_2]_n$ (**120**)	3.69	2.34, 1.99(ba)	116.6	[167]
$[Cu_2(Me\text{-}L^{37})(\mu\text{-}N_3)_4]_n$ (**121**)	3.52	2.30, 1.97(ba)	110.9	[167]
$[Cu(L^{38})(N_3)(\mu\text{-}N_3)]_n$ (**122**)	3.67	2.42, 1.96(ba)	113.6	[168]
$[Cu(L^{39})(N_3)(\mu\text{-}N_3)]_n$ (**123**)	3.68	2.60, 1.95(ba)	107.1	[168]
$[Cu(L^{40})(\mu\text{-}N_3)_2]_n$ (**124**)	3.90	2.48, 1.99(ba)	126.33	[169]
	3.99		125.50	
$[Cu(L^{41})(N_3)]_n$ (**125**)	4.29	1.97, 2.72(ba)	–	[170]
$[Cu(dpa)(N_3)_2]_n$ (**126**)	3.86	2.34, 2.04(ba)	123.3	[171]

Table 11b
Magnetic parameters for the single EO azido bridges 1D Cu(II) complexes.

Complex	J (cm^{-1})	τ	Ref.
$[Cu_2(\mu\text{-oxen})(\mu\text{-}N_3)_2(Br)]_n$ (**118**)	−85.7	0.05, 0.08	[165]
$[Cu_4(\mu\text{-oxen})_2(\mu_{1,1}\text{-}N_3)_2(\mu_{1,3}\text{-}N_3)]_n(ClO_4)_n$ (**119**)	–	0.02, 0.19	[166]
$[Cu_2(L^{37})_2(N_3)_2(\mu\text{-}N_3)_2]_n$ (**120**)	14.1	0.21, 0.10	[167]
$[Cu_2(Me\text{-}L^{37})(\mu\text{-}N_3)_4]_n$ (**121**)	–	0.21, 0.28	[167]
$[Cu(L^{38})(N_3)(\mu\text{-}N_3)]_n$ (**122**)	−2.2	0.32	[168]
$[Cu(L^{39})(N_3)(\mu\text{-}N_3)]_n$ (**123**)	−3.7	0.22	[168]
$[Cu(L^{40})(\mu\text{-}N_3)_2]_n$ (**124**)	−0.2, −0.1	–	[169]
$[Cu(L^{41})(N_3)]_n$(**125**)	2.5	–	[170]
$[Cu(dpa)(N_3)_2]_n$ (**126**)	−4.6	0.51	[171]

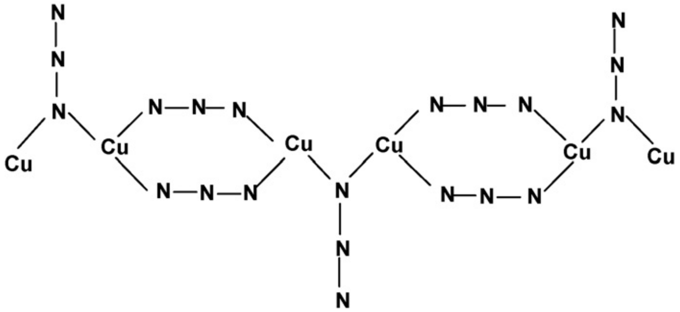

Fig. 27. Single EO and double EE azido bridiging mode.

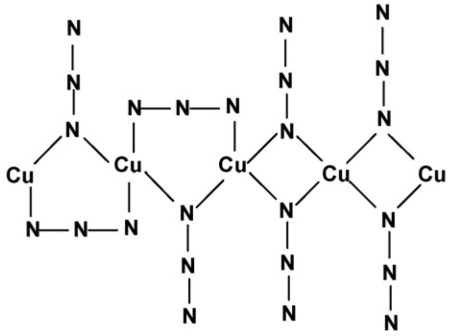

Fig. 28. Mixed EO and EE along with double EO azido bridging mode.

end-on bridges [173]. From the magnetic view-point, this is a singular ferromagnetic chain with local $S_A = S_B$. The chain shows regular alternating of two ferromagnetic and two antiferromagnetic interactions, with a global ferromagnetic coupling.

6.4. One-dimensional uniform and alternating systems with $\mu_{1,1}$ and $\mu_{1,3}$-azido bridging ligands

A schematic diagram of 1D system with single EO and single EE azido bridges is depicted in the Fig. 29.

The copper(II) chain compound $[Cu(hppz)(\mu_{1,1}\text{-}N_3)(\mu_{1,3}\text{-}N_3)]_n$ (**129**), has an unusual structure with alternate single end-on and single end-to-end azido bridges [174]. It shows a very high Cu–N–Cu bond angle (129.98°) for the end-on azido-bridging mode. A model of an alternating AF chain with $S = 1/2$ can explain the overall AF behavior of (**129**), and affords a set of parameters: $J_1 = -11.5\,cm^{-1}$, $J_2 = -2.7\,cm^{-1}$. $[Cu_2(bben)_2(N_3)_4]_n$ (**130**) is an unusual alternating ferro- and antiferromagnetic 1D hydrogen-bonded $\mu_{1,3}$-azide bridged copper(II) complex [175]. The complex **130** consists of double asymmetric $\mu_{1,3}$-azido-bridged dimeric Cu(II) moieties in which each Cu(II) coordinates with one bben, one terminal azido, and the two bridging azido ligands. Magnetic measurements showed a dominant ferromagnetic interaction in this complex with exchange coupling parameters $J_F = 16.8\,cm^{-1}$, and $J_{AF} = -3.6\,cm^{-1}$. Complex $[Cu(NITmPy)(N_3)_2(CH_3OH)]$ (**131**) [176] is a novel 1D copper(II)–radical complex in which copper(II) ions are alternatively bridged by double symmetric end-on and asymmetric end-to-end azido groups. The magnetic study of complex (**131**) reveals ferromagnetic interactions between the copper(II) ions through both end-on and end-to-end azido bridging ligands; coupling between the copper(II) ion and NITmPy radical is also ferromagnetic in nature [176]. In $[Cu(bnm)(N_3)_{2n}]$ (**132**), Cu(II) ions are alternatively bridged by end-on and asymmetric end-to-end (EE) azido ligands [177]. Complex $[Cu(4,4'\text{-}dmbpy)(N_3)_2]_n$ (**133**) [178] is a neutral chain complex where Cu(II) ions are alternately bridged by double asymmetrical end-on and end-to-end azide groups. Magnetic measurement of (**133**) suggests an alternating ferro- and antiferromagnetic coupling exists in this compound with $J_1 = 297.1\,cm^{-1}$ and $J_2 = -191\,cm^{-1}$.

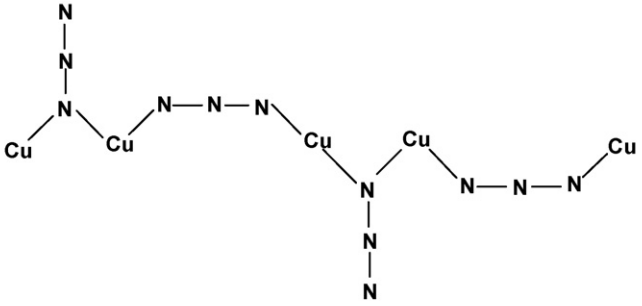

Fig. 29. Single EO and single EE azido bridiging mode.

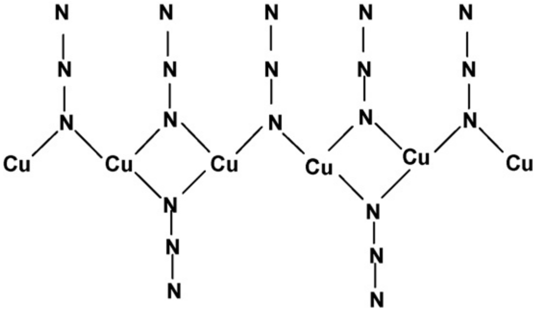

Fig. 30. Single EO and double EO azido bridiging mode.

6.5. One-dimensional uniform and alternating systems with single $\mu_{1,1}$ and double $\mu_{1,1}$ azido bridging ligands

1D polymer having uniform and alternating systems with single EO and double EO azide are unusual. Fig. 30 depicts such unusual coordination of azide ligand.

Complex $[Cu_2(L^{42})_2(H_2O)(N_3)_4]_n$ (**134**) (L^{42} = 5-methylpyrimidin-2-amine) [179] consists of 1D chain in which the Cu(II) ions with a square-pyramidal geometry are alternately bridged by asymmetric single and symmetric double end-on (EO) azido ligands. Magnetic analysis reveals that the dominating ferromagnetic interaction is mediated by the symmetric double azido bridge with the exchange parameter $J = 55.17\,cm^{-1}$ [179].

6.6. Mixed co-ligand one-dimensional uniform and alternating systems with single $\mu_{1,1}$ and double $\mu_{1,1}$-azide linkage

Mixed-ligand copper(II) complexes $[\{Cu(L^{43})(\mu_{1,3}\text{-}N_3)\}\{Cu(L^{44})(\mu_{1,3}\text{-}N_3)(\mu_{1,1}\text{-}N_3)\}]_n$ (**135**) and $[\{Cu(L^{45})(\mu_{1,3}\text{-}N_3)\}\{Cu(L^{44})(\mu_{1,3}\text{-}N_3)(\mu_{1,1}\text{-}N_3)\}]_n$ (**136**) [180] contain single end-to-end ($\mu_{1,3}$) azido-bridged 1D infinite chains (rail) which propagate parallel to the crystallographic *b*-axis. The neighboring chains are interconnected by pairs of double asymmetric end-on ($\mu_{1,1}$) azido bridges (rung) to yield a ladder-like structure (Fig. 31). However, in these complexes rungs (end-on azido bridges) do not connect each of the copper centers of the chains like in a regular ladder; instead they connect only the alternating copper sites of the 1D chain. In a chain the coordination environment around copper(II) ions

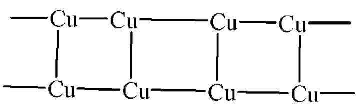

Fig. 31. Ladder-like arrangement.

Table 12
Structural and magnetic parameters for Cu(II) $\mu_{1,1,3}$-N_3 bridges (J_1, J_2 = singlet–triplet separations); $H = -J\Sigma(S_{2i}S_{2i-1} - \alpha S_{2i}S_{2i+1})$ with $\alpha = (J_F/J_{AF})$ Cu–N/Å.

Compounds	$\mu_{1,1}$(e o)			$\mu_{1,3}$ (e e)			
	Short	Long	J_2 (cm^{-1})	Short	Long	J_1 (cm^{-1})	Ref.
$[Cu(2,2'\text{-bpy})(N_3)_2]_n$ (**137**)	1.97	2.60	4.6	1.97	2.84	−2.9	[181]
$[Cu(phen)(N_3)_2]_n$ (**138**)	1.99	2.45	12.8	1.99	2.71	−6.6	[182]
$[Cu(aepy)(N_3)_2]_n$ (**139**)	2.01	2.65	0.2	2.01	2.66	−2.8	[183]
	2.01	2.58	−3.2	2.01	2.58	17	[105]
$[(\mu_{1,1,3}\text{-}N_3)_2\{Cu_2(Me_2Eten)_2(N_3)_2\}]_n$ (**140**)	2.02	2.85	24.7	2.02	2.65	−7.0	[184]
	2.02	2.61		2.02	2.47	17	
$[Cu(pn)(N_3)_2]_n$ (**141**)	2.01	2.47	3.1	2.01	2.85	−3.7	[41]

are not the same: while the $\{Cu(L^{43})(\mu_{1,3}\text{-}N_3)\}$ and $\{Cu(L^{45})(\mu_{1,3}\text{-}N_3)\}$ moieties have a penta-coordinated copper(II) center, the copper(II) ion of the neighboring $\{Cu(L^{43})(\mu_{1,3}\text{-}N_3)(\mu_{1,1}\text{-}N_3)\}$ or $\{Cu(L^{45})(\mu_{1,3}\text{-}N_3)(\mu_{1,1}\text{-}N_3)\}$ moiety has an octahedral coordination environment. The variable temperature (2–300 K) magnetic susceptibility measurements showed that the magnetic interaction between the metal centers in complexes (**135**) ($J = -1.27$ cm^{-1}, $zJ' = -0.12$ cm^{-1}) and (**136**) ($J = -1.82$ cm^{-1}, $zJ' = -0.19$ cm^{-1}) is dominantly antiferromagnetic [180].

6.7. One-dimensional alternating systems with $\mu_{1,1,3}$-azido bridging ligands

There are large numbers of copper(II) coordination polymers with alternating asymmetric azido bridges (both end-on and end-to-end bridges). Fig. 31 shows a schematic diagram of such $\mu_{1,1,3}$-azido coordination environment. Structural and magnetic parameters of this variety of copper(II) complexes [41,181–185] are gathered in Table 12 and Fig. 32.

Generally a weak ferromagnetic and a weak antiferromagnetic exchange interactions are assigned to end-on and end-to-end Cu azido bridges, respectively. However, the complex $[Cu_2(pn)_2(N_3)_4]$ (**141**) [41] is an exception amongst them as magnetic study reveals that the antiferromagnetic behavior for both the coordination mode of azide showing $J_1 = -3.7$ cm^{-1} and $J_2 = -3.1$ cm^{-1}. For the other reported examples, the ferromagnetic exchange coupling (J_2) was assigned to the double asymmetric $\mu_{1,1}$-N_3 bridges, while the antiferromagnetic one (J_1) was assigned to the double asymmetric $\mu_{1,3}$-N_3 bridges. Triki et al. reported the DFT calculations of such systems to address this apparently paradoxical nature of magnetic interaction [41].

Azido-bridged copper(II) coordination polymers $[(\mu_{1,1,3}\text{-}N_3)_2\{Cu_2(R\text{-}L^{46})_2(N_3)_2\}]_n$ (**142**) and $[(\mu_{1,1,3}\text{-}N_3)_2\{Cu_2(S\text{-}L^{46})_2(N_3)_2\}]_n$ (**143**) [185] consist of one-dimensional chiral structures in which the copper(II) ions have a distorted octahedral geometry. Copper(II) centers are interlinked by the unusual $\mu_{1,1,3}$-azido ligands. The magnetic study reveals that there is antiferromagnetic coupling ($J = -2.06$ cm^{-1}, $zJ' = -0.0309$ cm^{-1}) between the copper(II) ions through $\mu_{1,1,3}$-N_3-azido bridges [185].

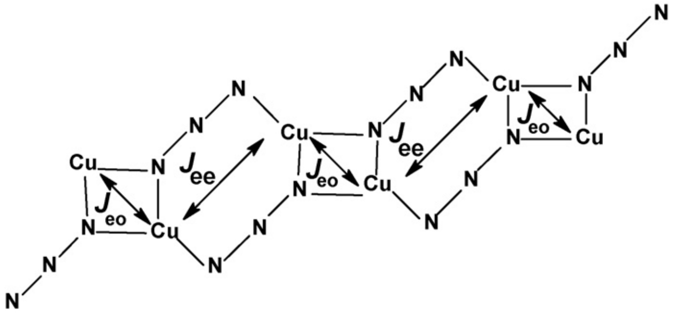

Fig. 32. 1D alternating system with $\mu_{1,1,3}$-azido bridges.

6.8. One-dimensional systems with azido and other bridging ligands

Fig. 33 models a typical 1D system in which azide as well as other bridging ligands binds simultaneously the same copper(II) center.

Complex $[\{Cu_2(\mu\text{-}N_3)(\mu\text{-}ox)(deen)_2\}_n](ClO_4)_n$ (**144**) is a mixed bridged alternating μ-oxalato μ-azido chain complex which exhibits a strong antiferromagnetic coupling [186]. The mixed bridged complex $\{[Cu(Hhpt)(N_3)]\cdot nH_2O\}$ (**145**) was formed by chains of copper atoms simultaneously bridged by *syn–syn* carboxylato and end-on azido ligands [187]. The copper chains are further linked by a second carboxylato bridge, giving a 2D compound showing strong ferromagnetic coupling due to the counter complementary of the superexchange pathways by the two bridging ligands. One-dimensional chain complex $[Cu_2(\mu_{2\text{-}1,1}\text{-}N_3)_2(\mu_{2\text{-}1,3}\text{-}NO_3)_2(\mu_{2\text{-}1,3}\text{-}Me_3CH_2CO_2)_2]_n$ (**146**) contains three different bridging groups, $\mu_{1,1}$-azido (end-on), $\mu_{1,3}$-nitrato, and μ-*syn,syn* carboxylato and they are so disposed that the azido and carboxylato groups occupy the equatorial positions. This, in fact, dictates the intrachain magnetic interaction between the copper(II) ions [188]. The structure has been rationalized in terms of a layered magnetic model with antiferromagnetic coupling between ferromagnetically coupled layers, leading to metamagnetic behavior. In $[Cu(atrz)_2(N_3)](NO_3)$ (**147**) the Cu(II) ions are linked by one end-on azido and two triazole bridges forming a cationic chain showing weakly antiferromagnetic interaction $J = -17.7$ cm^{-1} [132].

Magneto-structural correlations of coordination polymers $[Cu(\mu_{1,1}\text{-}N_3)(\mu_{1,3}\text{-}(C_4H_3S\text{-}CH_2COO))(\mu\text{-}DMSO)]_n$ (**148**) and $[Cu_3(\mu_{1,1}\text{-}N_3)_4(\mu_{1,3}\text{-}(C_4H_3S\text{-}COO)_2)(\mu\text{-}DMSO)_2]_n$ (**149**) having bridging azido, carboxylato and DMSO have been established [189]. The Cu(II) atoms in (**148**) are triply bridged by an EO type azide, a *syn–syn* carboxylate and a μ-O DMSO molecule. Complex (**149**) presents a trinuclear repeating unit in which the Cu(II) atoms are triply bridged in a fashion identical to (**148**). In addition, the trinuclear moieties in (**149**) are linked through two centro-symmetrically related EO azides. The variable-temperature magnetic susceptibilities of complexes (**148**) and (**149**) have been

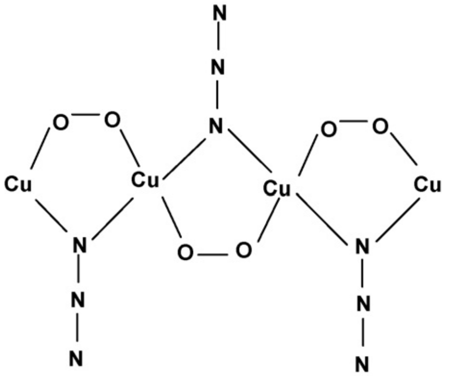

Fig. 33. 1D system with azide and other bridging ligand.

measured in the range 2–300 K under various external fields in the range 0.02–1.0*T*. Both curves are almost superimposable with small differences in the low temperature range and reflect the same ferromagnetic behaviour in almost all the temperature range. Quantum Monte Carlo (QMC) calculations were carried out in order to fit the susceptibility curves of the two compounds. The simulated parameters were $J = 126(2)\,\mathrm{cm}^{-1}$, $g = 2.15(1)$ for compound (**148**) and $J_1 = 126(2)\,\mathrm{cm}^{-1}$, $J_2 = 80(3)\,\mathrm{cm}^{-1}$ $g = 2.17(1)$ for compound (**149**), proving that large ferromagnetic interactions exist in both compounds [189].

The complex $[\mathrm{Cu(benzoate)(N_3)}]_n$ (**150**), displays an isolated 1D azido copper chain structure [190]. The asymmetric unit of this complex consists of half of a Cu(II) ion, half of an azide anion, and half benzoate ligand. The azido takes the EO mode linking two Cu(II) ions, while the carboxylato bridges two Cu(II) ions together with the azido anions forming a carboxylato/EO-azido mixed-bridged copper chain. The magnetic behavior of **150** is that of an isolated ferromagnetic chain ($J = 39\,\mathrm{cm}^{-1}$) [190]. Reactions between potentially pentadentate (N_2O_3), trianionic double Schiff-base ligand 2,6-bis[[(2-hydroxyethyl)imino]methyl]-4-methylphenol (H_3L^{47}) and $Cu(CH_3CO_2)_2$ or $Cu(ClO_4)_2$, in the presence of NaN_3, give novel coordination polymers with chain $\{[Cu_2(H_2L^{47})(N_3)_3]_2{\cdot}H_2O\}_n$ (**151**) or sheet-like structures $[Cu_2(H_2L^{47})(N_3)_3]_n$ (**152**) and $[Cu_2(HL^{47})(N_3)]_n[ClO_4]_n$ (**153**) [191]. These clusters are comprised of repeating dinuclear units (**151**) or their dimers (**152**) and (**153**). In these compounds, H_3L^{47} acts as a tridentate (N_2O) monoanionic (**151**), tetradentate (ON_2O) monoanionic (**152**), or pentadentate (O_3N_2) dianionic (**153**) ligand. Compound $[Cu_2(HL^{47})(N_3)_2(H_2O)]{\cdot}0.5CH_3OH$ (**154**) is isolated from the reaction of $Cu(CH_3CO_2)_2$ with H_3L^{47} under reflux, however, it did not afford crystals suitable for X-ray studies. X-ray structure determination revealed that the basic building block in (**151**–**153**) comprises two copper centers bridged through one μ-phenolate O atom from H_2L^{47} or $HL_2{}^{47}$ and one μ-azido (N1,N1) ion. Compounds (**151**–**153**) exhibit three different ways in which the Cu_2 basic unit may be organized in the crystalline phase at the supramolecular level through a variety of bridging interactions involving additional azide ligands or alkoxide groups from the side arms of the ligand H_3L^{47}. Bulk magnetization measurements demonstrate that the magnetic interactions ($H = -JS_1S_2$) are completely dominated by the strong antiferromagnetic coupling occurring within the Cu_2 building block, with coupling constants −512(1), −330(20), $-347(3)\,\mathrm{cm}^{-1}$ for **151**, **152** and **153**, respectively [191].

6.9. One-dimensional systems of copper(II) macrocycle

Synthesis of azide complexes with the copper(II) macrocycle complex $Cu(14ane)^{2+}$ has yielded two compounds. $Cu(14ane)Cu(N_3)_4$ (**155**) [192] contains $\mu_{1,3}$-azido-bridged chains of $Cu(14ane)^{2+}$ cations and $Cu(N_3)_4{}^{2-}$ anions. Magnetic studies reveal the presence of ferromagnetic interactions within the chains with $J/k = 0.635(4)$ K. $[Cu(14ane)N_3]BF_4$ (**156**) contains $[Cu(14ane)N_3]^+$ cations with elongated square-pyramidal geometry [192].

6.10. Heterometallic copper-lanthanide azido-derivative containing alternating EE/EO chain

The complex $[GdCu_2(IN)_5(N_3)_2(H_2O)_3]{\cdot}2H_2O$ (**157**) [193] is the first example of 3d–4f heterometallic azido-derivative synthesized by synergistic coordination. The alternating EE and EO chain in this complex can be regarded as isolated monomeric copper units linked by weak coordination interactions, which result in the alternating ferromagnetic/antiferromagnetic interactions that will give a total $S = 0$ for the chain.

6.11. Molecular tapes: azido-bridged eight-membered copper rings

Two exotic 1D molecular tapes with serial and parallel cyclic azido-bridged eight-membered copper rings $[Cu_4(N_3)_8(CH_3CN)_3(bzp)_2]_n$ (**158**) and $[Cu_5(N_3)_{10}(bzp)_2]_n$ (**159**) [194] are known. The EO bridge in (**158**) transmits ferromagnetic interactions whereas the central copper center of the linear pentanuclear $\{Cu_5\}$ unit in (**159**) is antiferromagnetically coupled with its neighboring Cu ions and has a ground state $S = 3/2$ [194].

6.12. Cu(I) coordination polymer $[Cu(\mu\text{-}N_3)(\mu\text{-}PTA)]_n$

The aqueous medium self-assembly reactions of copper(II) nitrate with 1,3,5-triaza-7-phosphaadamantane (PTA) as a main ligand and sodium azide or iodide as an auxiliary ligand lead to the new water-soluble Cu(I) coordination polymer $[Cu(\mu\text{-}N_3)(\mu\text{-}PTA)]_n$ (**160**) [195]. The complex (**160**) represents the first example of a copper compound with P,N-coordination of PTA. The crystal structure of (**160**) consists of neutral symmetry equivalent $[Cu(\mu\text{-}N_3)(\mu\text{-}PTA)]$ units, which are connected to each other to form infinite 1D double chains. This compound also represents the first example of a homometallic 1D coordination polymer bearing any cage-like PTA derivative.

7. Two-dimensional systems with azide blocker

A neutral molecule $[Cu(benzylamine)(N_3)_2]_n$ (**161**) has a sheet-like 2D structure. A double EO bridging Cu_2 unit is further connected to four neighboring Cu_2 units through four single EE azido bridges to form a 2D layer. Magnetic study reveals a long-range ordering with ferromagnetic ground state at $T_c = 7$ K [196]. In $[Cu(4\text{-}Etpy)_2(N_3)_2]_n$ (**162**) [64], each copper atom in the asymmetric unit is coordinated through two end-to-end ($\mu_{1,3}$) azido ligands, a pair of trans 4-Etpy molecules and a nitrogen atom of a terminal azide group. The terminal azido group further links a neighboring copper atom at a long Cu–N distance of 2.92 Å, thus interconnecting the asymmetric units giving rise to a 2D structure.

$[Cu(bpds)(N_3)]_n(ClO_4)_n(H_2O)_{25n}$ (**163**) [197] is another 2D network of 4,4′ topology in which nodes are occupied by the Cu(II) ions and edges formed by single azide and double bpds connectors. Very weak antiferromagnetic coupling ($J = -1.21 \pm 0.2\,\mathrm{cm}^{-1}$) through the $\mu_{1,3}$-azido bridging can be interpreted as a consequence of the almost no overlap through the $\mu_{1,3}$-azido bridging ligands in the apical(long)–apical(long) coordination mode. The copper(II) complex $[Cu(\mu_{1,3}\text{-}N_3)(N_3)(bpp)]_n$ (**164**) exhibits a 2D network formed by the bpp ligands interlinking copper(II) chains, in which the single azido bridge assumes an asymmetric $\mu_{1,3}$ mode with equatorial-axial disposition between Cu(II) ions that mediates a weak ferromagnetic coupling [198]. Magnetic investigation of a 2D grid-like copper(II) complex $[Cu(N_3)_2(pyz)]$ (**165**) showed that the presence of an overall antiferromagnetic interaction between the copper(II) ions was mainly mediated *via* pyrazine bridge [199].

Complex $[Cu_3(N_3)_6(DMF)_2]_n$ (**166**), a 2D coordination polymer, contains $\mu_{1,1,1}$ and $\mu_{1,1,3}$-azido ligands. Its structure consists of $[Cu_3(N_3)_6(DMF)_2]$ repeating units, which form chains that propagate parallel to the crystallographic *a* axis; their bridging is achieved through end-on azides [200]. The chains form sheets parallel to the *ab* plane through end-to-end azido bridges. Complex (**166**) exhibits ferromagnetic interaction with a ground state $S = 3/2$ (based on a Cu_3 repeating unit). Ferromagnetic chains are coupled through antiferromagnetic interaction, which is weak enough to be overcome by moderate magnetic fields at 2 K leading to a metamagnetic spin-flop transition at 2.7*T*. The transition is first-order, leading to hysteresis of the order of 0.2*T*. A new two-dimensional polymeric copper(II) complex $[Cu_2(heae)(N_3)_2]_n$ (**167**) (heae represents the dianion of N,N′-bis(N-hydroxyethylaminoethyl)oxamide) assembled by bis-tridentate chelated $[Cu(trans\text{-}heae)Cu]^{2+}$ building blocks and end-on azido ligands [201]. The DNA-binding properties of the said species were investigated by emission spectroscopic and electrochemical techniques, indicating the binuclear copper(II) complex binds to HS-DNA *via* a groove mode azido-bridged 2D Cu(I)–Cu(II) mixed valence compound $[Cu_2(2,2'\text{-}bpy)(N_3)_3]_n$ (**168**) obtained by hydrothermal reaction features a honeycomb-type networked structure [202]. In this case Cu(II) ions are partly reduced to Cu(I) by 2,2′-bpy and N_3^- ligands. Cu(I) ions are then bridged by N_3^- ions to give the infinitely helical chain $[Cu(N_3)]_n$. The chains are subsequently connected by the $[Cu(2,2'\text{-}bpy)(N_3)_2]_2$ fragments to furnish the 2D honeycomb-type network. In this network Cu(I) ions act as 3-connected nodes and the Cu(II) ions locate on the edge. The magnetic measurement suggests an antiferromagnetic ($J = -8.71\,cm^{-1}$) interaction of the dinuclear copper fragment mediated by EO azido bridges [202]. Substitution of some positions of hydroxyl with azide has resulted in an unprecedented 2D inorganic azido copper-hydroxyl compound $[Cu(H_2O)_6][\{Cu_2(N_3)_{4/3}(OH)(pta)_6\}]$ (**169**) [199]. The $[Cu_{24}]$ macrocycles that form the 2D layers in the complex are likely templated around $[Cu(H_2O)_6]^{2+}$ cations *via* strong hydrogen bonds. The crystal structure of complex (**169**) consists of a new anionic 2D layer network containing two Cu(II) ions, one phthalic anion (in μ_4-O,O′,O″,O‴ bridging mode), one μ_3 hydroxyl anion, and 4/3 azide anions, which take $\mu_{1,1}$ and $\mu_{1,1,1}$ bridging modes. This complex shows a clear average antiferromagnetic interaction leading to an $S = 0$ ground state [203].

$[Cu(4\text{-}bromopyridine)(N_3)_2]_n$ (**170**) [204] features a sheet-like structure formed by a uni-nodal 2D net which has both EO and EE azido bridging with additional Br...Br (mean 3.903(2) Å) and Br···N(azide) (3.035(5) Å) contacts. Magnetic measurement of complex (**170**) affords $J_1 = 36(6)\,cm^{-1}$ for the end-on azido interactions and $J_2 = 2.5(1)\,cm^{-1}$ for the orthogonal end-to-end azido interactions.

Homochiral layered neutral 2D brick-wall networks with exclusively end-on azido bridging complexes $[Cu_3(R\text{-}chea)_2(N_3)_6]_n$ (**171**), $[Cu_3(S\text{-}chea)_2(N_3)_6]_n$ (**172**) and $[Cu_3(S\text{-}phpa)_2(N_3)_6]_n$ (**173**) [205] were synthesized by the self-assembly reactions of $Cu(NO_3)_2{\cdot}3H_2O$, NaN_3 and small organic amine ligands. Magnetic studies show that complexes (**171**–**173**) are interesting chiral ferromagnets with the magnetic transition temperature at *ca.* 5.0 K [205]. $[Cu(2\text{-}methyl\text{-}benzoate)(N_3)]_n$ (**174**) and $[Cu(1\text{-}naphthoate)(N_3)]_n$ (**175**) are 2D azido copper networks displaying $\mu_{1,1,3,3}$ and $\mu_{1,1,3}$-azido coordination modes and exhibiting new azido copper networks with (4^4) and $(4{\cdot}\times8^2)$ topologies [190]. (**174**) and (**175**) showed spontaneous magnetization with characteristics of soft ferromagnetic magnetism with phase transition temperatures of 13 and 10 K, respectively [190].

$\{[Cu_2(\mu\text{-}O_2CMe)(\mu\text{-}MedapO)(\mu_{1,1}\text{-}N_3)_2]_n(CH_3OH)_n\}$ (**176**), consists of neutral alternate 1D chains formed by the sequence of $[Cu(1)–(\mu_{1,1}\text{-}N_3)_2–Cu(1)–(MedapO/acetate)–Cu(2)–(\mu_{1,1}\text{-}N_3)_2–Cu(2)]$ [206]. Each dinuclear [Cu(1)–Cu(2)] unit interacts with similar dinuclear units of neighbor chains through long Cu–N(azido) bonds to give a 2D arrangement. The magnetic behavior of (**176**) has been studied which showed an overall ferromagnetic coupling. The complex affords a J value of $53.0\,cm^{-1}$ as a consequence of the orbital counter-complementarity phenomenon [206].

8. Three-dimensional azido-bridged complexes

A 3D mixed valence copper azido coordination polymer $[Cu(I){\cdot}Cu(II)(N_3)(pzc)_2\,(H_2O)]_n$ (**177**) [207] containing rare asymmetric $\mu_{1,1,3}$-bridging mode ($J = 0.06 \pm 0.001\,cm^{-1}$) has been characterized. In this complex azido ligands and the Cu(2) ions act as 3-center nodes, and the Cu(1) ions act as 4-center nodes. Three-dimensional coordination polymers $[Cu_6(N_3)_{12}(N\text{-}Eten)_2]_n$ (**178**) and $\{[Cu_9(N_3)_{18}(1,2\text{-}pn)_4]{\cdot}H_2O\}_n$ (**179**) have been synthesized in a reaction of $Cu(NO_3)_2{\cdot}3H_2O$, NaN_3 and diamine ligands [208]. Complex (**178**) is composed of a neutral 3D coordination framework based on unprecedented hexanuclear copper(II) clusters which features three types of bridging modes for azide ($\mu_{1,1}$, $\mu_{1,3}$ and $\mu_{1,1,3}$). Complex $\{[Cu_9(N_3)_{18}(1,2\text{-}pn)_4]{\cdot}H_2O\}_n$ (**179**) is a novel 3D coordination polymer featuring octanuclear copper azido clusters in which $Cu(diamine)_2]^{2+}$ units are linked by azido bridges. Magnetic studies of complex $[Cu_6(N_3)_{12}(N\text{-}Eten)_2]_n$ (**178**) showed ferromagnetic ordering at 3.5 K, where the azido bridges mediate ferromagnetic coupling between adjacent Cu(II) ions. The magnetic data for $[Cu_6(N_3)_{12}(N\text{-}Eten)_2]_n$ (**178**) were fitted to a uniform hexanuclear copper model which yielded $g = 2.21$, $J = 6.26\,cm^{-1}$, $zJ' = 0.39\,cm^{-1}$. Complex $\{[Cu_9(N_3)_{18}(1,2\text{-}pn)_4]{\cdot}H_2O\}_n$ (**179**) shows ferromagnetic coupling in the nonanuclear unit and antiferromagnetic interaction between neighboring units [208].

3D copper(II) azido isomers $[Cu(N_3)(nic)]_n$ (**180** and **181**) were formed by hydrothermal method with the aid of 'non-innocent' reagent that does not exist in the final compound [209]. The complex (**180**) is the first metal azido complex showing rutile-type topology. It showed strong intradimer ferromagnetic $J = 132\,cm^{-1}$ coupling with weak interdimer and interchain antiferromagnetic interactions. Complex (**181**) shows an intrachain weak ferromagnetic coupling between the Cu(II) ions, as is expected for the presence of EO azido bridges together with (*syn*,*syn*)-carboxylate bridges featured in the chain. The EO azido bridge usually mediate a ferromagnetic exchange, while the *syn*,*syn*-carboxylate provides antiferromagnetic coupling between the Cu(II) centers. The chains are not isolated; they are linked *via* the pyridine group of the nic ligand to form a 3D network [209]. Complex $[Cu(trz)(N_3)]_n$ (**182**) is a first metal-triazolate coordination polymer which displays a rare three-dimensional non-interpenetrated utp-type topological network structure and exhibits spin-canted antiferromagnetism at low temperature [210].

Synthesis, crystal engineering, and magnetic properties of an anionic 4-terpyridone (L^{48}) based three-dimensional supramolecule, $[Cu_2(L^{48})_2(N_3)_2]{\cdot}2[Cu(L^{48})(N_3)(H_2O)]{\cdot}6H_2O$ (**183**), have been described in which one dinuclear $[Cu_2(L^{48})_2(N_3)_2]$ unit is co-crystallized with two mononuclear $[Cu(L^{48})(N_3)(H_2O)]$ units [211]. In both the dinuclear and mononuclear species chelated 4-terpyridone in its anionic form. The coordination environment of the metal ions is distorted square pyramidal. Eight O–H–O type strong hydrogen bonds involving the oxygen of anionic 4-terpyridone ligand and water molecules link the components of (**183**) into a three-dimensional framework. Excluding the atoms except for the water molecules and ligand oxygens, the topology is merely a two-dimensional. The mononuclear $[Cu(L^{48})(N_3)(H_2O)]$ moiety is appended from this sheet, while the neighboring sheets are interlinked by the dinuclear $[Cu_2(L^{48})_2(N_3)_2]$ unit to the third affords an overall three-dimensional structure. The complex (**183**) exhibits a weak ferromagnetic ($J = 15\,cm^{-1}$) interaction [211]. Reaction between 2,6-diformyl-4-methylphenol (DFMP) and tris(hydroxymethyl)aminomethane (THMAM) with copper(II) acetate and sodium azide formed the antiferromagnetically ($J_1 = -113.5(4)\,cm^{-1}$) coupled, polymeric copper(II) coordination cluster $\{[(H_5L^{49})Cu_2(\mu\text{-}N_3)]_2[Cu(N_3)_4]{\cdot}2CH_3OH\}_n$ (**184**). It has a novel double-stranded ladder-like structure in which $[Cu(N_3)_4]^{2-}$ anions link single-chains comprised of dinuclear subunits. The compound forms a 3D-structure with interconnected ladders through H-bonding. The 3D-structure is the result of coordinatively driven and hydrogen-bonding directed self-assembly [212].

In a 3D mixed valence copper azido coordination polymer $[Cu^{I}{\cdot}Cu^{II}(N_3)(pzc)_2\,(H_2O)]_n$ (**185**) azide acts as a rare asymmetric

Table 13
Summary of the main features of copper-azido compounds described in the present review.

Compound	Azide binding	Magnetic Properties	J (cm^{-1})	Ref.
Mononuclear copper (II) complexes with monodentate azide coordination				
$[Cu(L^1)(N_3)]$ (**1**)	Terminal	Para	–	[4]
$[Cu(L^2)(N_3)]$ (**2**)	Terminal	Para	–	[55]
$[Cu(pbpd)(N_3)]PF_6$ (**3**)	Terminal	Para	–	[56]
$[Cu(pfbd)(N_3)]ClO_4$ (**4**)	Terminal	Para	–	[56]
$[Cu_2(1,3\text{-}tpbd)(N_3)_4]$ (**5**)	Terminal	Para	–	[57]
$[Cu(N_3)(pyrazinato)(H_2O)]_n$ (**6**)	Terminal	Para	–	[58]
$[Cu(pmp)(N_3)(ClO_4)]_n$ (**7**)	Terminal	Para	–	[59]
$[Cu(N_3)_2(sparteine)]$ (**8**)	Terminal	Para	–	[60]
$[Cu(\beta\text{-}collidine)_4(N_3)](ClO_4)$ (**9**)	Terminal	Para	–	[61]
$[Cu(s\text{-}collidine)_2(N_3)_2]$ (**10**)	Terminal	Para	–	[62]
$[Cu(3,4\text{-}lutidine)(N_3)_2]$ (**11**)	Terminal	Para	–	[63]
$[Cu(3\text{-}Etpy)_2(N_3)_2]_n$ (**12**)	Terminal	Para	–	[64]
$[Cu(terpy)(N_3)Cl]$ (**13**)	Terminal	Para	–	[65]
$[Cu(pmap)(N_3)]ClO_4$ (**14**)	Terminal	Para	–	[66]
$[Cu_2(\mu\text{-}Hbdea)_2(N_3)_2]$ (**15**)	Terminal	Para	–	[67]
Dinuclear copper(II) complexes with bridging azido coordination				
$[Cu_2(N_3)_2(4\text{-}Etpy)_4(\mu\text{-}NO_3)_2]$ (**16**)	Double EO	Ferro	230.1	[68]
$[Cu_2(N_3)_2(3\text{-}ampy)_4(\mu\text{-}NO_3)_2]\cdot EtOH$ (**17**)	Double EO	Ferro	223.2	[68]
$[Cu_2(4\text{-}pya)_2(N_3)_2(DMF)_2$ (**18**)	Double EO	Ferro	145	[69]
$[Cu_2(N_3)_2(t\text{-}Bupy)_4](ClO_4)_2$ (**19**)	Double EO	Ferro	105 ± 20 (235)	[36,70]
$[Cu_4(N_3)_4(Dur)][PF_6)_4\cdot 4H_2O\cdot 6CH_3CN$ (**20**)	Double EO	Ferro	94	[71]
$[Cu_2(DMPTD)_2(\mu\text{-}N_3)_2(N_3)_2]$ (**21**)	Double EO	Ferro	85 ± 1	[72]
$[Cu_2(N_3)_2(N_3)_2([24]ane\text{-}N_2O_6)]\cdot H_2O$ (**22**)	Double EO	Ferro	70 ± 20	[34]
$[Cu_2(N_3)_2(O_2CCH_3)_2(dpyam)_2]$(**23**)	Double EO	Ferro	64	[73]
$[Cu_2(N_3)_2(O_2CH)_2(dpyam)_2]$ (**24**)	Double EO	Ferro	63	[73]
$[Cu_2(N_3)_2(N_3)_2(phprpy)_2]$ (**25**)	Double EO	Ferro	25.6	[74]
$[Cu_2(N_3)_2(N_3)_2(tbz)_2]\cdot 2CH_3OH$ (**26**)	Double EO	Ferro	23	[75]
$[Cu_2(N_3)_2(tacn)_2](ClO_4)_2\cdot CH_3OH$ (**27**)	Double EO	Ferro	2.5	[76]
$[Cu(Him2\text{-}py)(N_3)]_2$(**28**)	Double EO	Antiferro	−0.3	[78]
$[Cu(L^3)(N_3)]_2$ (**29**)	Double EO	Antiferro	−1.29	[79]
$[Cu_2(dipn)_2(\mu\text{-}N_3)_2]$ (**30**)	Double EO	Antiferro	−2.1	[80]
$[Cu(L^4)(N_3)]_2$ (**31**)	Double EO	Antiferro	−8.5	[81]
$[Cu(L^5)(N_3)]_2\cdot CH_3OH\cdot H_2O$ (**32**)	Double EO	Antiferro	−4.2	[82]
$[Cu(L^6)(N_3)]_2$ (**33**)	Double EO	Antiferro	−1.8	[83]
$[Cu(L^7)(N_3)]_2$ (**34**)	Double EO	Antiferro	−3.1	[83]
$[Cu(L^8)(N_3)]_2$ (**35**)	Double EO	Antiferro	−1.8	[84]
$[Cu(L^9)(N_3)]_2$ (**36**)	Double EO	Antiferro	−2.6	[84]
$[Cu(L^{10})(N_3)]_2$ (**37**)	Double EO	Antiferro	−5.4	[84]
$[Cu(L^{11})(N_3)]_2\cdot CH_3OH$ (**38**)	Double EO	Antiferro	–	[101]
$[Cu(L^{12})(N_3)]_2(NO_3)_2$ (**39**)	Double EO	Antiferro	−1.3	[102]
$[Cu(L^{13})(N_3)]_2$ (**40**)	Double EO	Antiferro	−146	[103]
$[Cu(terpy)(N_3)(H_2O)]_2(PF_6)_2$ (**41**)	Double EO	Antiferro	–	[104]
$[Cu(dpt)(N_3)]_2\ (ClO_4)_2$ (**42**)	Double EO	Antiferro	−2.9	[59]
$[Cu(aepi)(N_3)_2]_2$ (**43**)	Double EO	Antiferro	−3.1	[105]
$[Cu(L^{14})(N_3)]_2(ClO_4)_2$ (**44**)	Double EO	Antiferro	−3.2	[106]
$[Cu(Medien)(N_3)]_2(ClO_4)_2$ (**45**)	Double EO	Antiferro	−16.8	[107]
$[Cu(DMP)(N_3)_2]_2$ (**46**)	Double EO	Antiferro	−27.6	[108]
$[Bu_4N]_2[Cu_2(\mu_{1,1}\text{-}N_3)_2(N_3)_4]$ (**47**)	Double EO	Antiferro	−36.0	[109]
$[Cu(L^{15})(N_3)]_2$ (**48**)	Double EE	Antiferro	2.9	[83]
$[Cu(L^{16})(N_3)]_2(ClO4)_2$ (**49**)	Double EE	W. Ferro	–	[110]
$[Cu(L^{17})(N_3)]_2$ (**50**)	Double EE	Ferro	24	[111]
$[Cu(PAP)(N_3)_2]_2$ (**51**)	Double EE	Ferro	35	[108]
$Cu_2(NiL^{18})_2(N_3)_4$ (**52**)	Double EE	Ferro	20.3	[112]
$Cu_2(dmterpy)_2(N_3)]_2(N_3)_2(NO_3)(H_2O)_2$ (**53**)	Double EE	Ferro	2.9	[113]
$[Cu(Hz)(N_3)]_2$ (**54**)	Double EE	Ferro	0.75	[114]
$[Cu(Medpt)(\mu\text{-}N_3)]_2(ClO_4)_2$ (**55**)	Double EE	Antiferro	−105	[107]
$[Cu(Et_5dien)(\mu\text{-}N_3)]_2(ClO_4)_2$ (**56**)	Double EE	Antiferro	−28	[117]
$[Cu(Me_5dien)(\mu\text{-}N_3)]_2(BPh_4)_2$ (**57**)	Double EE	Antiferro	−13	[118]
$[Cu(Me_5dien)(\mu\text{-}N_3)]_2(ClO_4)_2$ (**58**)	Double EE	Antiferro	−7.5	[117]
$[Cu(L^{19})(\mu\text{-}N_3)]_2(ClO_4)_2$ (**59**)	Double EE	Antiferro	−3.4	[119]
$[Cu(N_3)(tmen)(\mu\text{-}N_3)]_2$ (**60**)	Double EE	Ferro	≈0	[120]
$[Cu(L^{20})(\mu\text{-}N_3)]_2(ClO_4)_2$ (**61**)	Double EE	Ferro	2.4	[121]
$[Cu(Et_3dien)(\mu\text{-}N_3)]_2(ClO_4)_2$ (**62**)	Double EE	Ferro	9	[107]
$[Cu(L^{21})(\mu\text{-}N_3)]_2(ClO_4)_2$ (**63**)	Double EE	Ferro	90.7, 185.6	[59]
$[Cu(L^{22})(\mu\text{-}N_3)]_2$ (**64**)	Double EE	Ferro	13.6	[122]
$[\{Cu(phen)(N_3)_2\}(4,4'bpy)](ClO_4)_2$ (**65**)	Double EE	Ferro	≈0	[123]
$[CuL^{23}(\mu\text{-}N_3)]_2$(**66**)	Double EE	Ferro	2.4	[124]
Trinuclear copper(II) azido complexes with bridging azido coordination				
$\{[Pr_4N]_2[Cu_3(\mu_{1,1}\text{-}N_3)_4(N_3)_4]\}_n$ (**67**)	Double EO, terminal	Ferro	7.0	[109]
$[Cu_3(\mu_{1,1}\text{-}N_3)_4(N_3)_2(Meinic)_2(DMF)_2]$ (**68**)	EO, EE	Bulkferro	–	[68]
$[L^{24}Cu(\mu\text{-}N_3)_2Cu(\mu\text{-}N_3)_2CuL^{24}]$ (**69**)	EO, EE	W. Antiferro	–	[125]
$[Cu_3(dien)_2(N_3)_6]$ (**70**)	Double EO	Antiferro	−2.1	[126]

Table 13 (*Continued*)

Compound	Azide binding	Magnetic Properties	J (cm^{-1})	Ref.
$[\mathrm{Cu_3(msalen)_2(N_3)_4(DMF)_2}]$ (**71**)	Single EO	Ferro	32.6	[127]
$[\mathrm{Cu_3(ampym)_2(\mu_{1,1}\text{-}N_3)_4(\mu_{1,3}\text{-}N_3)_2(dmf)_2}]_n$ (**72**)	EO, EE	Ferro	–	[128]
$[\mathrm{Cu_3(N_3)_6(2,2'\text{-}tpcb)(DMF)_2}]_n$ (**73**)	EO	–	+70(3), −3(2)	[129]
$[\mathrm{Cu_3(dpyam)_2(\mu_{1,1}\text{-}N_3)_2(\mu\text{-}CH_3COO\text{-}\kappa\text{-}O1)_2(\mu\text{-}CH_3COO\text{-}\kappa\text{-}O^1,O^2)_2}]\cdot\mathrm{2(H_2O)}$ (**74**)	Double EO	Antiferro	−10.2	[130]
$[\mathrm{Cu_3(hnta)_4(N_3)_2(H_2O)_3}]$ (**75**)	EO	L. Ferro	–	[131]
$[\mathrm{Cu_3(atrz)_2(N_3)_6}$ (**76**)	EO	Antiferro	−108.8	[132]
Tetranucler and other high nuclearity array of copper(II) azido coordination				
$[\mathrm{Cu_4(pap)_2(N_3)_8(MeOH)_2}]$ (**77**)	EE	Antiferro	–	[133]
$[\mathrm{Cu_4(papMe)_2(N_3)_4(H_2O)_2(NO_3)_2}](\mathrm{NO_3})_2$ (**78**)	EE	Antiferro	–	[134]
$[\mathrm{Cu_4(macy2)(N_3)_4}]$ (**79**)	EE	–	–	[135]
$[\mathrm{Cu_4(msalen)_2(N_3)_2(H_2O)(MeOH)}]$ (**80**)	EO	–	–	[136]
$[\mathrm{Cu_4(msalen)_2\ (N_3)_2(DMSO)_2}]$ (**81**)	EO	–	–	[137]
$[\mathrm{Cu_4(salen)_2(N_3)_4}]$ (**82**)	EO	Antiferro	−12.8, −10	[138]
$[\mathrm{Cu_4(bpt\text{-}H)_4(N_3)_4}]\cdot\mathrm{4.5H_2O}$ (**83**)	Terminal	Antiferro	–	[139]
$[\mathrm{Cu_4(bmdp)_2(OAc)_2(N_3)}](\mathrm{ClO_4})_3$ (**84**)	EE	Ferro	–	[140]
$[\mathrm{Cu_4(O_2cyclam1)_2(tmen)_2(N_3)}](\mathrm{ClO_4})_3$ (**85**)	Terminal	–	–	[141]
$[\mathrm{Cu_4(acac)_2(phen)_4(N_3)_4(ClO_4)_2}]$ (**86**)	EO	Ferro	$S=2$	[142]
$[\mathrm{Cu_4(\mu_2\text{-}PhCOO)_2(\mu\text{-}bdmap)_2(\mu_{1,3}\text{-}N_3)_2(N_3)_2(H_2O)_2}]$ (**87**)	Double EE	B. antiferro	−85.4	[143]
$[\mathrm{Cu_4(\mu_2\text{-}PhCOO)_2\text{-}(\mu\text{-}bdmap)_2(\mu_{1,3}\text{-}N_3)_2(PhCOO)_2(CH_3OH)_2}]$ (**88**)	Double EE	B. antiferro	−89.5	[143]
$[\mathrm{Cu_4(bsi)_2(N_3)_2}]$ (**89**)	Double EO	Antiferro; W. Ferro ($\mathrm{N_3}^-$)	$S=0$	[144]
$[\mathrm{Cu_4(M_3)_2(\mu_3\text{-}OEt)_2(\mu\text{-}N_3)_2(N_3)_2}](\mathrm{MeOH})$ (**90**)	EO	–	–	[145]
$[\mathrm{Cu_4(bpm)_2(N_3)_8}]_n$ (**91**)	EO, $\mu_{-1,1}$, $\mu_{-1,1,3}$	Ferromag	–	[146]
$[\mathrm{Cu_4(tpimim)_2(N_3)}]\mathrm{Cl}$ (**92**)	$\mu_{-1,1,3,3}$	Antiferro	–	[147]
$\mathrm{Cu_4(N_3)_2\{pyC(OMe)(O)pyC(OMe)(O)py\}_2(MeOH)_2}](\mathrm{ClO_4})\cdot\mathrm{2MeOH}$ (**93**)	$\mu_{1,1,1,1}$	Ferromag	26.8	[148]
$[\mathrm{Cu_5(terpy)_2(N_3)_{10}}]$ (**94**)	Single EO	Weakferro	–	[149]
$[\mathrm{Cu_6(O_2CPh)_4(N_3)_2\{(py)_2CO_2\}_2\{(py)_2C(OH)O\}_2}]$ (**95**)	EO	Antiferro $S=0$	−94(5); −110(5); −116(5)	[150]
$[\mathrm{Cu_4(O_2CPh)_2(N_3)_4\{(py)_2C(OMe)O\}_2}]_n$ (**96**)	EO	–	–	[150]
$[\mathrm{Cu_2(O_2CPh)(N_3)_2\{(py)_2\text{-}C(OMe)O\}}]_n$ (**97**)	EO	–	–	[150]
$\mathrm{Cu_6(O_2CPh)_4(N_3)_2\{(py)_2CO_2\}_2\{(py)_2C(OH)O\}_2}]\cdot\mathrm{2H_2O}\cdot\mathrm{4.5MeCN}$ (**98**)	EO	Antiferro	−94(5); −110(5); −116(5)	[151]
$[\mathrm{Cu_4(O_2CPh)_2(N_3)_4\{(py)_2C(OMe)\ O\}_2}]_n$ (**99**)	EO	–	–	[152]
$[\mathrm{Cu_2(O_2CPh)(N_3)_2\{(py)_2C(OMe)O\}}]_\mathrm{n}$ (**100**)	EO	–	–	[152]
$[(\gamma\text{-}\mathrm{SiW_{10}O_{36})_2Cu_4(N_3)_4}]^{12-}$ (**101**)	EO	–	–	[153]
$[(\gamma\text{-}\mathrm{SiW_{10}O_{36})_2Cu_4(H_2O)_2(N_3)_4}]^{12-}$ (**102**)	EO	–	–	[153]
$[\mathrm{(SiW_8O_{31})_3Cu_9(OH)_3(H_2O)_6(N_3)_4}]^{10-}$ (**103**)	$\mu_{1,1,1,3,3,3}$	–	–	[154]
$[\mathrm{Cu_4(O_2cyclam2)_4Mn_2(N_3)_4}]$ (**104**)	EO	–	–	[157]
1D copper(II) complexes with different azide binding				
$[\mathrm{Cu(L^{25})(N_3)}]_n(\mathrm{ClO_4})_n$ (**105**)	EE	Ferro	1.36	[158]
$[\mathrm{Cu(L^{26})(N_3)}]_n(\mathrm{ClO_4})_n$ (**106**)	EE	Ferro	2.69	[159]
$[\mathrm{Cu(L^{27})(N_3)}]_n(\mathrm{ClO_4})_n$ (**107**)	EE	Ferro	2.02	[159]
$[\mathrm{Cu(L^{28})(N_3)}]_n(\mathrm{ClO_4})_n$ (**108**)	EE	Ferro	2.15	[160]
$[\mathrm{Cu(L^{29})(N_3)}]_n(\mathrm{ClO_4})_n$ (**109**)	EE	Ferro	3.61	[160]
$[\mathrm{Cu(L^{30})(N_3)}]_n(\mathrm{ClO_4})_n$ (**110**)	EE	Ferro	2.06	[160]
$[\mathrm{Cu(L^{31})(N_3)}]_n(\mathrm{ClO_4})_n$ (**111**)	EE	Ferro	1.60	[119]
$[\mathrm{Cu(R\text{-}L^{32})_2(N_3)}]_n(\mathrm{ClO_4})_n$ (**112**)	EE	Ferro	0.70	[161]
$[\mathrm{Cu(L^{33})_2(N_3)_2}]_n$ (**113**)	EE	Ferro	1.6	[162]
$[\mathrm{Cu(L^{34})(N_3)}]_n(\mathrm{H_2O})_{2n}$ (**114**)	EE	Antiferro	−4.30	[112]
$[\mathrm{Cu(L^{35})(N_3)}]_n$ (**115**)	EE	Antiferro	−22.5	[54]
$[\mathrm{Cu(bpym)(N_3)_2}]_n$ (**116**)	EE	Antiferro	−3.8	[163]
$[\mathrm{L^{36}Cu_2(N_3)_2}]_n(\mathrm{ClO_4})_{2n}\cdot\mathrm{n(H_2O)}$ (**117**)	EE	W. antiferro	–	[164]
$[\mathrm{Cu_2(\mu\text{-}oxen)(\mu\text{-}N_3)_2(Br)}]_n$ (**118**)	EO	Antiferro	−85.7	[165]
$[\mathrm{Cu_4(\mu\text{-}oxen)_2(\mu_{1,1}\text{-}N_3)_2(\mu_{1,3}\text{-}N_3)}]_n(\mathrm{ClO_4})_n$ (**119**)	EO, EE	–	–	[166]
$[\mathrm{Cu_2(L^{37})_2(N_3)_2(\mu\text{-}N_3)_2}]_n$ (**120**)	Single EO	Ferro	14.1	[167]
$[\mathrm{Cu_2(Me\text{-}L^{37})(\mu\text{-}N_3)_4}]_n$ (**121**)	Single EO	–	–	[167]
$[\mathrm{Cu(L^{38})(N_3)(\mu\text{-}N_3)}]_n$ (**122**)	Single EO	Antiferro	−2.2	[164]
$[\mathrm{Cu(L^{39})(N_3)(\mu\text{-}N_3)}]_n$ (**123**)	Single EO	Antiferro	−3.7	[168]
$[\mathrm{Cu(L^{40})(\mu\text{-}N_3)_2}]_n$ (**124**)	Single EO	Antiferro	−0.2, −0.1	[169]
$[\mathrm{Cu(L^{41})(N_3)}]_n$ (**125**)	Single EO	Ferro	2.5	[169]
$[\mathrm{Cu(dpa)(N_3)_2}]_n$ (**126**)	Single EO	Antiferro	−4.6	[171]
$[\mathrm{NMe_4}][\mathrm{Cu(N_3)_3}]$ (**127**)	EO, EE	Antiferro	−3.6	[172]
$[\mathrm{Cu(3\text{-}Clpy)_2(\mu\text{-}N_3)_2}]_n$ (**128**)	EO, EE	Globalferro	–	[173]
$[\mathrm{Cu(hppz)(\mu_{1,1}\text{-}N_3)(\mu_{1,3}\text{-}N_3)}]_n$ (**129**)	EO, EE	Antiferro	−11.5 −2.7	[174]
$[\mathrm{Cu_2(bben)_2(N_3)_4}]_n$ (**130**)	Double EE	Ferro antiferro	16.8 −3.6	[175]
$[\mathrm{Cu(NITmPy)(N_3)_2(CH_3OH)}]$ (**131**)	EO, EE	Ferro	–	[176]
$[\mathrm{Cu(bnm)(N_3)_{2n}}]$ (**132**)	EO, EE	–	–	[177]
$\mathrm{Cu(4,4'\text{-}dmbpy)(N_3)_2}]_n$ (**133**)	EO, EE	Ferromag antiferro	297.1 −191	[178]
$[\mathrm{Cu_2(L^{42})_2(H_2O)(N_3)_4}]_n$ (**134**)	Single EO double EO	Ferro	55.17	[179]

Table 13 (*Continued*)

Compound	Azide binding	Magnetic Properties	J (cm^{-1})	Ref.
$[\{Cu(L^{43})(\mu_{1,3}\text{-}N_3)\}\{Cu(L^{44})(\mu_{1,3}\text{-}N_3)(\mu_{1,1}\text{-}N_3)]_n$ (**135**)	EO, EE	Antiferro	−1.27 −0.12	[180]
$[\{Cu(L^{45})(\mu_{1,3}\text{-}N_3)\}\{Cu(L^{44})(\mu_{1,3}\text{-}N_3)(\mu_{1,1}\text{-}N_3)]_n$ (**136**)	EO, EE	Antiferro	−1.82 −0.19	[181]
$[Cu(2,2'\text{-}bpy)(N_3)_2]_n$ (**137**)	$\mu_{1,1,3}$	Ferro antiferro	4.6 −2.9	[181]
$[Cu(phen)(N_3)_2]_n$ (**138**)	$\mu_{1,1,3}$	Ferro antiferro	12.8 −6.6	[182]
$[Cu(aepy)(N_3)_2]_n$ (**139**)	$\mu_{1,1,3}$	Ferro antiferro	0.2, −2.8	[183]
$[(\mu_{1,1,3}\text{-}N_3)_2\{Cu_2(Me_2Eten)_2(N_3)_2\}]_n$ (**140**)	$\mu_{1,1,3}$	Ferro antiferro	24.7 −7.0	[184]
$[Cu(pn)(N_3)_2]_n$ (**141**)	$\mu_{1,1,3}$	Ferro antiferro	3.1 −3.7	[41]
$[(\mu_{1,1,3}\text{-}N_3)_2\{Cu_2(R\text{-}L^{46})_2(N_3)_2\}]_n$ (**142**)	$\mu_{1,1,3}$	Antiferro	−2.06 −0.03	[185]
$[(\mu_{1,1,3}\text{-}N_3)_2\{Cu_2(S\text{-}L^{46})_2(N_3)_2\}]_n$ (**143**)	$\mu_{1,1,3}$	Antiferro	−2.06 −0.03	[185]
$[\{Cu_2(\mu\text{-}N_3)(\mu\text{-}ox)(deen)_2\}_n](ClO_4)_n$ (**144**)	EE	Antiferro	–	[186]
$[Cu(Hhpt)(N_3)]\cdot nH_2O$ (**145**)	EO	Ferro	–	[187]
$[Cu_2(\mu_{2\text{-}1,1}\text{-}N_3)_2(\mu_{2\text{-}1,3}\text{-}NO_3)_2(\mu_{2\text{-}1,3}\text{-}Me_3CH_2CO_2)_2]_n$ (**146**)	EO, EE	Metamag	–	[188]
$[Cu(atrz)_2(N_3)]NO_3$ (**147**)	Single EO	Antiferro	−17.7	[132]
$[Cu(\mu_{1,1}\text{-}N_3)(\mu_{1,3}\text{-}(C_4H_3S\text{-}CH_2COO))(\mu\text{-}DMSO)]_n$ (**148**)	EO, EE	Ferro	126(2)	[187]
$[Cu_3(\mu_{1,1}\text{-}N_3)_4(\mu_{1,3}\text{-}(C_4H_3S\text{-}COO)_2)(\mu\text{-}DMSO)_2]_n$ (**149**)	EO, EE	Ferro	80(3)	[187]
$[Cu(benzoate)(N_3)]_n$ (**150**)	EO	Ferro	39	[190]
$\{[Cu_2(H_2L^{47})(N_3)_3]_2\cdot H_2O\}_n$ (**151**)	EE	Antiferro	−512(1)	[191]
$[Cu_2(H_2L^{47})(N_3)_3]_n$ (**152**)	EO, EE	Antiferro	−330(20)	[191]
$[Cu_2(HL^{47})(N_3)]_n[ClO_4]_n$ (**153**)	EE	Antiferro	−347(3)	[191]
$[Cu_2(HL^{47})(N_3)_2(H_2O)]\cdot 0.5CH_3OH$ (**154**)	–	–	–	[191]
$Cu(14ane)Cu(N_3)_4$ (**155**)	EE	Ferro	0.635	[192]
$[Cu(14ane)N_3]BF_4$ (**156**)	Terminal	–	–	[193]
$[GdCu_2(IN)_5(N_3)_2(H_2O)_3]\cdot 2H_2O$ (**157**)	EO, EE	Ferro, antiferro	–	[194]
$[Cu_4(N_3)_8(CH_3CN)_3(bzp)_2]_n$ (**158**)	EO	Ferro	–	[194]
$[Cu_5(N_3)_{10}(bzp)_2]_n$ (**159**)	EO	Antiferro	–	[194]
$[Cu(\mu\text{-}N_3)(\mu\text{-}PTA)]_n$ (**160**)	HM	–	–	[195]
2D copper(II) azido complexes				
$[Cu(benzylamine)(N_3)_2]_n$ (**161**)	Double EO Single EE	L. ferro	– T_c = 7 K	[196]
$[Cu(4\text{-}Etpy)_2(N_3)_2]_n$ (**162**)	EE	–	–	[64]
$[Cu(bpds)(N_3)]_n(ClO_4)_n(H_2O)_{25n}$ (**163**)	EE	Antiferro	−1.21 ± 0.2	[197]
$[Cu(\mu_{1,3}\text{-}N_3)(N_3)(bpp)]_n$ (**164**)	EE	Weakferro	–	[198]
$[Cu(N_3)_2(pyz)]$ (**165**)	Terminal	Antiferro	–	[199]
$[Cu_3(N_3)_6(DMF)_2]_n$ (**166**)	$\mu_{1,1,1}$	Metamag	– T = 7 K	[200]
$[Cu_2(heae)(N_3)_2]_n$ (**167**)	EO	–	–	[201]
$[Cu_2(2,2'\text{-}bpy)(N_3)_3]_n$ (**168**)	EO	Antiferro	−8.71	[202]
$[Cu(H_2O)_6][\{Cu_2(N_3)_{4/3}(OH)(pta)_6]$ (**169**)	EO, $\mu_{3\text{-}1,1,1}$	Antiferro	– S = 0	[203]
$[Cu(4\text{-}bromopyridine)(N_3)_2]_n$ (**170**)	EO, EE	Ferro	36(6) 2.5(1)	[204]
$[Cu_3(R\text{-}chea)_2(N_3)_6]_n$ (**171**)	–	Chiralferro	–T = 5.0	[205]
$[Cu_3(S\text{-}chea)_2(N_3)_6]_n$ (**172**)	–	Chiralferro	– T = 5.0	[205]
$[Cu_3(S\text{-}phpa)_2(N_3)_6]_n$ (**173**)	–	Chiralferro	– T = 5.0	[205]
$[Cu(2\text{-}methyl\text{-}benzoate)(N_3)]_n$ (**174**)	$\mu_{1,1,3,3}$	Softferro	– T = 13 K	[190]
$[Cu(1\text{-}naphthoate)(N_3)]_n$ (**175**)	$\mu_{1,1,3}$	Softferro	–T = 10 K	[190]
$\{[Cu_2(\mu\text{-}O_2CMe)(\mu\text{-}MedapO)(\mu_{1,1}\text{-}N_3)_2]_n(CH_3OH)_n\}$ (**176**)	EO, EE	Ferro	53.0	[206]
3D copper(II) azido complexes				
$[Cu(I)\cdot Cu(II)(N_3)(pzc)_2(H_2O)]_n$ (**177**)	$\mu_{1,1,3}$	Ferro	0.06 ± 0.001	[207]
$[Cu_6(N_3)_{12}(N\text{-}Eten)_2]_n$ (**178**)	$\mu_{1,1}$, $\mu_{1,3}$ $\mu_{1,1,3}$	Ferro	6.26, 0.39 T = 3.5 K	[208]
$\{[Cu_9(N_3)_{18}(1,2\text{-}pn)_4]\cdot H_2O\}_n$ (**179**)	–	Ferro	–	[208]
$[Cu(N_3)(nic)]_n$ (**180**)	–	Ferro	132	[209]
$[Cu(N_3)(nic)]_n$ (**181**)	EO	Ferro	–	[209]
$[Cu(trz)(N_3)]_n$ (**182**)	–	Spin-canted antiferro	–	[210]
$[Cu_2(L^{48})_2(N_3)_2]\cdot 2[Cu(L^{48})(N_3)(H_2O)]\cdot 6H_2O$ (**183**)	–	Ferro	15	[211]
$\{[(H_5L^{49})Cu_2(\mu\text{-}N_3)]_2[Cu(N_3)_4]\cdot 2CH_3OH\}_n$ (**184**)	EO	Antiferro	−113.5	[212]
$[Cu^{I}\cdot Cu^{II}(N_3)(pzc)_2(H_2O)]_n$ (**185**)	$\mu_{1,1,3}$	–	–	[207]
$[Cu(4\text{-}abpt)(N_3)_2]_n\cdot 2nH_2O$ (**186**)	EE	–	–	[213]
$[(Cu(N_3)_2)_2Cu(N_3)_2(methylpyrazine)_2]_n$ (**187**)	EO EE	Ferro antiferro	14.9 −1.7	[204]
$[Cu_6(1,2\text{-}pn)_4(N_3)_{12}]_n$ (**188**)	–	Ferro	–	[205]
$\{[Cu_8(en)_4(N_3)_{16}]H_2O\}_n$ (**189**)	–	Ferro	–	[205]
$[Cu_6(N\text{-}Ipren)_2(N_3)_{12}]_n$ (**190**)	–	Ferro	– T = 3.2 K	[205]
$[Cu(\mu\text{-}pymca)N_3]$ (**191**)	Double EO	Ferro	71	[214]

W = weak; B = bulk; L = longrange; – = not reported.

$\mu_{1,1,3}$-bridging ligand. While azide ligands and the Cu(2) ions are 3-connecting nodes in (**185**), Cu(1) ions act as 4-connecting nodes [207]. Compound $[Cu(4\text{-abpt})(N_3)_2]_n \cdot 2nH_2O$ (**186**) [213] displays an interesting 3D framework based on Cu(II)–azide square layers formed by the end-to-end (EE) azido ligands. The square layers are further connected by the wavy chains from the bent 4-abpt ligands to form a 3D network structure.

An unusual 3D-topology and dominant ferromagnetic coupling is observed in complex $[(Cu(N_3)_2)_2Cu(N_3)_2(\text{methylpyrazine})_2]_n$ (**187**) [204] which contains a three and four-connected 3D (4.102)2(42.104)-dmd-net based on tetrahedral and trigonal planar nodes with EO azide coordination. The magnetic interactions in $[(Cu(N_3)_2)_2Cu(N_3)_2(\text{methylpyrazine})_2]_n$ (**187**) are $J_{1,2} = 14.9(6)$ cm^{-1} for the end-on azido interactions along with an additional coupling ($J = -1.7\,cm^{-1}$) through the pyrazine [211]. $[Cu_6(1,2\text{-pn})_4(N_3)_{12}]_n$ (**188**), $\{[Cu_8(en)_4(N_3)_{16}]H_2O\}_n$ (**189**) and $[Cu_6(N\text{-Ipren})_2(N_3)_{12}]_n$ (**190**) [205] are examples of cluster-based 3D coordination polymers. Complexes (**188**) and (**189**) are 3D coordination polymers featuring copper azido clusters and $[Cu(\text{diamine})_2]^{2+}$ units that are linked by the azido bridges. Complex (**190**) is a 3D coordination framework based on the hexanuclear copper(II) clusters $[Cu_6(N_3)_{12}(N\text{-Ipren})_2]$. Complexes (**188**) and (**189**) show ferromagnetic coupling in the copper azido cluster units and antiferromagnetic interaction between neighboring units, while complex (**190**) shows ferromagnetic ordering at 3.2 K.

9. Unique honeycomb layer structure with EO azide bridging

In complex $[Cu(\mu\text{-pymca})N_3]$ (**191**), zigzag pymca-bridged chains are connected by double end-on azido bridges to afford a unique honeycomb layer structure [214]. This is the first report concerning a honeycomb structure in which two bis(chelating) bridges alternate with one double end-on azide bridge within the hexagonal rings. Such a unique structure may be a consequence of the different charge balance requirements for pymca and 2,2′-bipyrimidine ligands. Quantum Monte Carlo methods have been used to analyze the experimental magnetic data of compound (**191**) showing an antiferromagnetic coupling ($J = -34\,cm^{-1}$) through the pymca ligand and a ferromagnetic coupling ($J = 71\,cm^{-1}$) through the azido bridging ligands [214].

Finally the main observations of the studies on copper azido systems covered in the present review are summarized in Table 13 in order to give an overall impression of the progress of research work in this particular field.

10. Conclusion

Though the recent surge of studies on μ-azido complexes afforded many facets of its functions in preparing the mono- or multi-dimensional metal-assembled complexes but in most of the cases the products are serendipitous. In fact the factors which control the coordinating behavior of the azide still remain elusive. It demands the further persuasion of studies on transition-metal azido complexes keeping an eye on using them as prospective advanced magnetic materials. This is a new potential area, more notable observations may come out which will enrich the coordination chemistry as well as will help in getting deeper insight in developing novel properties in the system.

Magneto-structural correlation generally predicts that end-to-end and end-on coordination mode give antiferromagnetic and ferromagnetic coupling between the paramagnetic metal centers, respectively, irrespective of other co-ligands used. In a theoretical study by Kahn and coworkers, the authors stated that '. . .can a $\mu_{1,1}$-azido group be considered as an almost universal ferromagnetic coupler' [37]. Further studies are in demand to rationalize the facts in this regard.

The topology of a metal–azido system is obviously sensitive to the co-ligand. Despite the large number of transition-metal azido complexes reported to date, on the basis of accrued information it seems impossible to predict, *a priori*, about the bridging mode or topology with a specific ligand in a complex in terms of its nuclearity, coordination modes of azide ion, etc. Towards this objective, many studies have been undertaken to obtain deeper insight into this query in particular and understanding the interplay between their structure and magnetic properties as a whole with a given set of ligand and metal ions. Finally, it warrants a more intensive study with fine tuning of stereoelectronic properties of the co-ligands as well as the variation of metal ions along with sophisticated theoretical calculation. This certainly can afford a much more clear vision in designing such assemblies in a more predictable manner with desired properties.

Until now, the exploitation of the azido ligand for the synthesis of novel clusters with new and interesting properties relevant to single-molecule magnet (SMM) research is only in its infancy. To our mind a very eventful and promising future lies ahead. In future more appropriate schemes will have to be designed for the synthesis of such materials that can exhibit novel properties.

Acknowledgments

We are deeply indebted to the University Grants Commission and CSIR, New Delhi for financial assistance to undertake research work in the molecular magnetism field. Assistance received from Department of Chemistry, Jadavpur University under CAS programme (UGC) and FIST programme (DST) is also gratefully acknowledged.

References

[1] J.S. Miller, J.C. Calabrese, H. Rommelman, S.R. Chittipedi, J.H. Zeng, W.M. Reiff, A.J. Epstein, J. Am. Chem. Soc. 109 (1987) 769.
[2] O. Kahn, Y. Pei, M. Verdaguer, J.P. Renard, J. Sletten, J. Am. Chem. Soc. 110 (1988) 782.
[3] J.S. Miller, M. Drillon (Eds.), Molecule Based Materials, VCH, Weinheim, 2001.
[4] O. Kahn, Molecular Magnetism, VCH, Weinheim, 1993.
[5] M. Pilkington, S. Decurtins, in: J.A. McCleverty, T.J. Meyer (Eds.), Comprehensive Coordination Chemistry II. From Biology to Nanotechnology, vol. 7, Elsevier, 2004, p. 177.
[6] M. Verdaguer, A. Bleuzen, V. Marvaud, J. Vaissermann, M. Seuleiman, C. Desplanches, A. Scuiller, C. Train, R. Garde, G. Gelly, C. Lamenech, I. Rosenman, P. Veillet, C. Cartier, F. Villain, Coord. Chem. Rev. 1023 (1999) 190.
[7] M. Ohba, H. Okawa, Coord. Chem. Rev. 198 (2000) 313.
[8] P. Chaudhuri, Coord. Chem. Rev. 243 (2003) 143.
[9] J. Ribas, A. Escuer, M. Monfort, R. Vicente, R. Cortés, L. Lezama, T. Rojo, Coord. Chem. Rev. 193–195 (1999) 1027, and references therein.
[10] S.R. Batten, K.S. Murray, Coord. Chem. Rev. 246 (2003) 103.
[11] R.D. Willet, D. Gatteschi, O. Kahn (Eds.), Magneto-Structural Correlations in Exchange Coupled Systems, NATO ASI Series, Reidel, Dordrecht, 1985.
[12] M.M. Turnbull, T. Sugimoto, L.K. Thompson (Eds.), Molecular Based Magnetic Materials: Theory, Techniques and Applications, ACS Symposium Series, no. 644, ACS, Washington, 1996.
[13] A. Caneschi, D. Gatteschi, L. Pardi, R. Sessoli, in: A.F. Williams (Ed.), Perspectives in Coordination Chemistry, VCH, Weinheim, 1992.
[14] J.L. Manson, A.M. Arif, J.S. Miller, Chem. Commun. (1999) 1479.
[15] O. Kahn, Comments Condens. Mater. Phys. 17 (1994) 39.
[16] J.R. Long, in: P. Yang (Ed.), Chemistry of Nanostructured Materials, Hong Kong, 2003.
[17] L.K. Thompson, S.K. Tandon, Comments Inorg. Chem. 18 (1996) 125, and references therein.
[18] A. Escuer, G. Aromí, Eur. J. Inorg. Chem. (2006) 4721, and references therein.
[19] Y.-F. Zeng, X. Hu, F.-C. Liu, X.-H. Bu, Chem. Soc. Rev. 38 (2009) 469.
[20] S. Saha, D. Mal, S. Koner, A. Bhattacharjee, P. Gütlich, S. Mondal, M. Mukherjee, K.-I. Okamoto, Polyhedron 23 (2004) 1811.
[21] S. Koner, S. Iijima, M. Watanabe, M. Sato, J. Coord. Chem. 56 (2003) 103.
[22] O. Kahn, Adv. Inorg. Chem. 43 (1995) 179.
[23] R. Robson, Aust. J. Chem. 23 (1970) 2217.
[24] M.A.S. Goher, T.C.W. Mak, Inorg. Chim. Acta 99 (1985) 223.

[25] G.S. Papaefstathiou, S.P. Perlepes, A. Escuer, R. Vicente, M. Font-Bardia, X. Solans, Angew. Chem. Int. Ed. 40 (2001) 884.
[26] G.S. Papaefstathiou, A. Escuer, R. Vicente, M. Font-Bardia, X. Solans, S.P. Perlepes, Chem. Commun. (2001) 2414.
[27] M.M. Whittaker, J.W. Whittaker, J. Biophys. 64 (1993) 762.
[28] M.M. Whittaker, V.L. Devito, S.A. Asher, J. Whittaker, J. Biol. Chem. 264 (1989) 7104.
[29] F. Tuczek, E.I. Solomon, Inorg. Chem. 32 (1993) 2550.
[30] E.I. Solomon, U.M. Sundaram, T.E. Machonkin, Chem. Rev. 96 (1996) 2563.
[31] E.I. Solomon, M.J. Baldwin, M.D. Lowery, Chem. Rev. 92 (1992) 521.
[32] V. Mckee, J.V. Dagdigni, M.G. Patch, C.A. Reed, J. Am. Chem. Soc. 106 (1984) 4765.
[33] V. Mckee, J.V. Dagdigni, R. Bau, C.A. Reed, J. Am. Chem. Soc. 103 (1981) 7000.
[34] J. Comarmond, P. Plumeré, J.M. Lehn, I. Agnus, R. Louis, R. Weiss, O. Kahn, I. Morgenstern-Badarau, J. Am. Chem. Soc. 104 (1982) 6330.
[35] M.F. Charlot, O. Kahn, M. Chaillet, C. Larrieu, J. Am. Chem. Soc. 108 (1986) 2574.
[36] M.A. Aebersold, M. Gillon, O. Plantevin, L. Pardi, O. Kahn, P. Bergerat, I.V. Seggern, F. Tuczek, L. Öhrström, A. Grand, E. Leliévre-Berne, J. Am. Chem. Soc. 120 (1998) 5238.
[37] A. Bencini, C.A. Ghilardo, S. Midolini, A. Orlandini, Inorg. Chem. 28 (1989) 1958.
[38] O. Kahn, T. Mallah, J. Gouteron, S. Jeannin, Y. Jeannin, J. Chem. Soc. Dalton Trans. (1989) 1117.
[39] R.G. Parr, W. Yang, Density Functional Theory of Atoms and Molecules, Oxford University Press, New York, 1989.
[40] E. Ruiz, J. Cano, S. Alvarez, P. Alemany, J. Am. Chem. Soc. 120 (1998) 11122.
[41] S. Triki, C.J. Gómez-García, E. Ruiz, J. Sala-Pala, Inorg. Chem. 44 (2005) 5501.
[42] P. Chaudhuri, T. Weyhermüler, E. Bill, K. Weighardt, Inorg. Chim. Acta 252 (1996) 195.
[43] D.M. Daggan, D.N. Hendrickson, Inorg. Chem. 13 (1974) 2929.
[44] C.G. Pierpont, D.N. Hendrickson, D.M. Daggan, F. Wanger, E.K. Barefield, Inorg. Chem. 14 (1975) 604.
[45] E. Coronado, P. Delhaes, D. Gatteschi, J.S. Miller (Eds.), Molecular Magnetism: from Molecular Assemblies to Devices; NATO ASI Series, vol. 321, Kluwer, Dordrecht, 1995.
[46] D.W. Bruce, D. O'Hare (Eds.), Inorganic Materials, Wiley, 1992.
[47] P. Delhaes, M. Drillon (Eds.), Organic and Inorganic Low-Dimensional Materials, NATO ASI Series, vol. 168, Plenum Press, New York, 1987.
[48] D. Gatteschi, O. Kahn, J.S. Miller, F. Palacio (Eds.), Magnetic Molecular Materials, NATO ASI Series, vol. 198, Kluwer, Dordrecht, 1993.
[49] C.J. O'Connor (Ed.), Research Frontiers in Magneto Chemistry, World Scientific, Singapore, 1993.
[50] R. Neumann, M. Dahan, Nature 388 (1997) 353.
[51] M. Fujita, Y.J. Kwon, S. Washizu, K. Ogura, J. Am. Chem. Soc. 116 (1994) 1151.
[52] M. Fujita, J. Wazaki, K. Ogura, Tetrahedron Lett. 32 (1991) 5589.
[53] O.M. Yaghi, G. Li, H. Li, Nature 378 (1995) 703.
[54] C. Adhikary, D. Mal, K.-I. Okamoto, S. Chaudhuri, S. Koner, Polyhedron 25 (2006) 2191.
[55] C.-Y. Wang, J.-Y. Ye, C.-Y. Lv, W.-Z. Lan, J.-B. Zhou, J. Coord. Chem. 13 (2009) 2164.
[56] S.H. Rahaman, H.-K. Fun, B.K. Ghosh, Polyhedron 24 (2005) 3091.
[57] S.P. Foxon, O. Walter, R. Koch, H. Rupp, P. Müller, S. Schindler, Eur. J. Inorg. Chem. (2004) 344.
[58] M.A.S. Goher, M.A.M. Abu-Youssef, F.A. Mautner, Polyhedron 17 (1998) 3305.
[59] P. Manikandan, R. Muthukumaran, K.R. Justin Thomas, B. Varghese, G.V.R. Chandramouli, P.T. Monoharan, Inorg. Chem. 40 (2001) 2378.
[60] Y.-K. Kim, B.-J. Kim, S.K. Kang, S.-N. Choi, Y.-M. Lee, Acta Cryst. Sec. C 59 (2003) 64.
[61] F.A. Mautner, M.A.S. Goher, Polyhedron 15 (1996) 1133.
[62] F.A. Mautner, M.A.S. Goher, Polyhedron 15 (1996) 5.
[63] F.A. Mautner, M.A.S. Goher, Polyhedron 13 (1994) 2141.
[64] M.A.S. Goher, A. Escuer, M.A.M. Abu-Youssef, F.A. Mautner, Polyhedron 17 (1998) 4265.
[65] R. Cortés, L. Lezama, J. Larramendi, I.R. Jose, M. Insausti, J.V. Folgado, G. Madariaga, T. Rojo, J. Chem. Soc. Dalton Trans. 17 (1994) 2573.
[66] F.A. Mautner, F.R. Louka, T. LeGuet, S.S. Massoud, J. Mol. Struct. 919 (2009) 196.
[67] K.R. Gruenwald, A.M. Kirillov, M. Haukka, J. Sanchiz, A.J.L. Pombeiro, Dalton Trans. (2009) 2109.
[68] A. Escuer, M.A.S. Goher, F.A. Mautner, R. Vicente, Inorg. Chem. 39 (2000) 2107.
[69] W.-W. Sun, X.-B. Qian, C.-Y. Tian, E.-Q. Gao, Inorg. Chim. Acta 362 (2009) 2744.
[70] S. Sikorav, I. Bkouche-Waksman, O. Kahn, Inorg. Chem. 23 (1984) 490.
[71] B. Graham, M.T.W. Hearn, P.C. Junk, C.M. Kepert, F.E. Mabbs, B. Moubaraki, K.S. Murray, L. Spiccia, Inorg. Chem. 40 (2001) 1536.
[72] S.S. Tandon, L.K. Thompson, M.E. Manuel, J.N. Bridson, Inorg. Chem. 33 (1994) 5555.
[73] S. Youngme, T. Chotkhun, S. Leelasubcharoen, N. Chaichit, C. Pakawatchai, G.A. van Albada, J. Reedijk, Polyhedron 26 (2007) 725.
[74] J.D. Woodward, R.V. Backov, K.A. Abboud, D. Dai, H.-J. Koo, M.-H. Whangbo, M.W. Meisel, D.R. Talham, Inorg. Chem. 44 (2005) 638.
[75] G.A. van Albada, M.T. Lakin, N. Veldman, A.L. Spek, J. Reedijk, Inorg. Chem. 34 (1995) 4910.
[76] Q.-L. Wang, X.-Q. Jia, D.-Z. Liao, S.-P. Yan, P. Cheng, G.-M. Yang, H.-X. Ren, Z.-H. Jiang, Trans. Met. Chem. 31 (2006) 434.
[77] A.W. Addison, T.N. Rao, J. Reedjik, J. van Rijn, C.G. Verschoor, J. Chem. Soc. Dalton Trans. (1984) 1349.
[78] X. Wang, Z. Li, Y. Xu, L. Li, D. Liao, Z. Jiang, J. Coord. Chem. 6 (2008) 900.
[79] R. Li, B. Moubaraki, K.S. Murray, S. Brooker, Dalton Trans. (2008) 6014.
[80] P. Mukherjee, O. Sengupta, M.G.B. Drew, A. Ghosh, Inorg. Chim. Acta 362 (2009) 3285.
[81] S. Koner, S. Saha, T. Mallah, K.-I. Okamoto, Inorg. Chem. 43 (2004) 840.
[82] M. Zbiri, S. Saha, C. Adhikary, S. Chaudhuri, C. Daul, S. Koner, Inorg. Chim. Acta 359 (2006) 1193.
[83] M.S. Ray, A. Ghosh, R. Bhattacharya, G. Mukhopadhyay, M.G.B. Drew, J. Ribas, Dalton Trans. (2004) 252.
[84] M.S. Ray, A. Ghosh, S. Chaudhuri, M.G.B. Drew, J. Ribas, Eur. J. Inorg. Chem. (2004) 3110.
[85] G. teVelde, F.M. Bickelhaupt, E.J. Baerends, C. Fonseca Guerra, S. van Gisbergen, J.G. Snijders, T. Ziegler, J. Comput. Chem. 22 (2001) 931.
[86] C. Guerra, J. Snijders, G.T.E. Velde, E.J. Baerends, Theor. Chem. Acta 99 (1998) 391.
[87] S.H. Vosko, L. Wilk, M. Nusair, Can. J. Phys. 58 (1980) 1200.
[88] A.D. Becke, J. Chem. Phys. 98 (1993) 5468.
[89] M.A. Watson, N.C. Handy, A.J. Cohen, J. Chem. Phys. 119 (2003) 6475.
[90] E. Ruiz, J. Cano, S. Alvarez, P. Alemany, Int. J. Quantum Chem. 20 (1999) 1391.
[91] J.P. Perdew, J.A. Chevary, S.H. Vosko, K.A. Jackson, M.R. Pederson, D.J. Singh, C. Fiolhais, Phys. Rev. B 46 (1992) 6671.
[92] A.D. Becke, Phys. Rev. A 38 (1988) 3098.
[93] W. Yang, C. Lee, R.G. Parr, Phys. Rev. B 37 (1988) 785.
[94] B.G. Johnson, P.M.W. Gill, J.A. Pople, J. Chem. Phys. 98 (1993) 5612.
[95] T.V. Russo, R.L. Martin, P.J. Hay, J. Chem. Phys. 101 (1994) 7729.
[96] J.P. Perdew, Phys. Rev. B 33 (1986) 8822.
[97] C. Adamo, V. Barone, A. Bencini, F. Totti, I. Ciofini, Inorg. Chem. 38 (1999) 1996.
[98] A. Bencini, F. Totti, Int. J. Quantum Chem. 101 (2005) 819.
[99] E. Ruiz, P. Alemany, S. Alvarez, J. Cano, J. Am. Chem. Soc. 119 (1997) 1303.
[100] E. Ruiz, C. de Graaf, P. Alemany, S. Alvarez, J. Phys. Chem. A 106 (2002) 4938.
[101] L.-L. Ni, Z.-L. You, L. Zhang, C. Wang, K. Li, Trans. Met. Chem. (2009), doi:10.1007/s11243-009-9289-6.
[102] C. Adhikary, D. Mal, R. Sen, A. Bhattacharjee, P. Gütlich, S. Chaudhuri, S. Koner, Polyhedron 26 (2007) 1658.
[103] C. Adhikary, R. Sen, G. Bocelli, A. Cantoni, S. Chaudhuri, S. Koner, J. Coord. Chem. 62 (2009) 3573.
[104] R. Cortés, M.K. Urtiaga, L. Lezama, J.I.R. Larramendi, M.I. Arriortua, T. Rojo, J. Chem. Soc. Dalton Trans. (1993) 3685.
[105] Y.S. You, C.S. Hong, K.M. Kim, Polyhedron 24 (2005) 249.
[106] S. Sarkar, A. Mondal, J. Ribas, M.G.B. Drew, K. Pramanik, K.K. Rajak, Eur. J. Inorg. Chem. (2004) 4633.
[107] A. Escuer, M. Font-Bardia, S.S. Massoud, F.A. Mautner, E. Peñalba, X. Solans, R. Vicente, New J. Chem. 28 (2004) 681.
[108] S.-Q. Bai, E.-Q. Gao, Z. He, C.-J. Fang, C.-H. Yan, New J. Chem. 29 (2005) 935.
[109] S. Saha, S. Koner, J.-P. Tuchagues, A.K. Boudalis, K.-I. Okamoto, S. Banerjee, D. Mal, Inorg. Chem. 44 (2005) 6379.
[110] K. Matsumoto, S. Ooi, K. Nakatsura, W. Mori, S. Suzuki, A. Nakahara, Y. Nakao, J. Chem. Soc. Dalton Trans. (1985) 2095.
[111] J.P. Costés, F. Dahan, J. Ruiz, J.P. Laurent, Inorg. Chim. Acta 239 (1995) 53.
[112] X.-Z. Li, L.-N. Zhu, C.-Q. Li, D.-Z. Liao, Inorg. Chem. Commun. 9 (2006) 1297.
[113] J. Lin, Z. Shen, Y. Song, H.-J. Xu, Y.-Z. Li, X.-Z. You, Inorg. Chim. Acta 358 (2005) 1963.
[114] S. Sen, S. Mitra, D.L. Hughes, G. Rosair, C. Desplanches, Polyhedron 26 (2007) 1740.
[115] Y. Agnus, R. Louis, J.P. Gisselbrecht, R. Weiss, J. Am. Chem. Soc. 106 (1984) 93.
[116] P. Chaudhuri, K. Oder, K. Wieghart, B. Nuber, J. Weiss, Inorg. Chem. 25 (1986) 2818.
[117] A. Escuer, M. Font-Bardia, E. Peñalba, X. Solans, R. Vicente, Inorg. Chim. Acta 298 (2000) 195.
[118] T.R. Felthouse, D.N. Hendrickson, Inorg. Chem. 17 (1978) 444.
[119] S. Sarkar, A. Mondal, J. Ribas, M.G.B. Drew, K. Pramanik, K.K. Rajak, Inorg. Chim. Acta 358 (2005) 641.
[120] I. Bkouche-Waksman, S. Sikorav, O. Kahn, J. Cryst. Spectrosc. Res. 13 (1983) 303.
[121] P.S. Mukherjee, S. Dalai, G. Mostafa, T.-H. Lu, E. Rentschler, N.R. Chaudhuri, New J. Chem. 25 (2001) 1203.
[122] S. Shit, P. Talukder, J. Chakraborty, G.M.S. Pilet, E.I. Fallah, J. Ribas, S. Mitra, Polyhedron 26 (2007) 1357.
[123] L. Li, D. Liao, Z. Jiang, S. Yan, Inorg. Chem. 41 (2002) 1019.
[124] G. Chastanet, B.L. Guennic, C. Aronica, G. Pilet, D. Luneau, M.-L. Bonnet, V. Robert, Inorg. Chim. Acta 361 (2008) 3847.
[125] M.H.W. Lam, Y.Y. Tang, K.M. Fung, X.Z. You, W.T. Wong, Chem. Commun. (1997) 957.
[126] J. Luo, X.-G. Zhon, S. Gao, L.-H. Weng, Z.-H. Shao, C.-M. Zhang, Y.-R. Li, J. Zhang, R.-F. Cai, Polyhedron 23 (2004) 1243.
[127] Y.-B. Jiang, H.-Z. Kou, R.-J. Wang, A.-L. Cui, Eur. J. Inorg. Chem. (2004) 4608.
[128] Y. Song, C. Massera, M. Quesada, A.M.M. Lanfredi, I. Mutikainen, U. Turpeinen, J. Reedijk, Inorg. Chim. Acta 358 (2005) 1171.
[129] T.C. Stamatatos, G.S. Papaefstathiou, L.R. MacGillivray, A. Escuer, R. Vicente, E. Ruiz, S.P. Perlepes, Inorg. Chem. 46 (2007) 8843.
[130] S. Youngme, T. Chotkhun, S. Leelasubcharoen, N. Chaichit, G.A. van Albada, M. Viciano-Chumillas, J. Reedijk, Inorg. Chem. Commun. 10 (2007) 109.
[131] Y.-F. Zeng, J.-P. Zhao, B.-W. Hu, X. Hu, F.-C. Liu, J. Ribas, J. Ribas-Ariño, X.-H. Bu, Chem. Eur. J. 13 (2007) 9924.

[132] J.-C. Liu, D.-G. Fu, J.-Z. Zhuang, C.-Y. Duan, X.-Z. You, J. Chem. Soc. Dalton Trans. 14 (1999) 2337.

[133] C.L. Sheppard, S.S. Tandon, L.K. Thompson, J.N. Bridson, D.O. Miller, M. Handa, F. Lloret, Inorg. Chim. Acta 250 (1996) 227.

[134] S.S. Tandon, L.K. Thompson, D.O. Miller, J. Chem. Soc. Chem. Commun. (1995) 1907.

[135] V. McKee, S.S. Tandon, J. Chem. Soc. Dalton Trans. (1991) 221.

[136] Z.L. You, H.L. Zhu, Z. Anorg, Allg. Chem. 632 (2006) 140.

[137] R. Kurtaran, K.C. Emregul, C. Arici, F. Ercan, V.J. Catalano, O. Atakol, Synth. React. Inorg. Met. Org. Chem. 33 (2003) 281.

[138] S. Koner, S. Saha, K.-I. Okamoto, J.P. Tuchagues, Inorg. Chem. 42 (2003) 4668.

[139] Z.-S. Meng, L. Yun, W.-X. Zhang, C.-G. Hong, R. Herchel, Y.-C. Ou, J.-D. Leng, M. Xia Peng, Z.-J. Lin, M.-L. Tong, Dalton Trans. (2009) 10284.

[140] J.H. Satcher, M.W. Droege, T.J.R. Weakley, R.T. Taylor, Inorg. Chem. 34 (1995) 3317.

[141] J.K. Tang, O.Y. Yan, H.B. Zhou, Y.Z. Li, D.Z. Liao, Z.H. Jiang, S.P. Yan, P. Cheng, Cryst. Growth Des. 5 (2005) 813.

[142] A.M. Madalan, M. Noltemeyer, M. Neculai, H.W. Roesky, M. Schmidtmann, A. Muller, Y. Journaux, M. Andruh, Inorg. Chim. Acta 359 (2006) 459.

[143] M.S. El Fallah, R. Vicente, A. Escuer, F. Badyine, X. Solans, M. Font-Bardia, Inorg. Chim. Acta 361 (2008) 4065.

[144] Y. Song, C. Massera, O. Roubeau, P. Gamez, A.M.M. Lanfredi, J. Reedijk, Inorg. Chem. 43 (2004) 6842.

[145] S.S. Tandon, L.K. Thompson, J.N. Bridson, M. Bubenik, Inorg. Chem. 32 (1993) 4621.

[146] L. Zhang, L.-F. Tang, Z.-H. Wang, M. Du, M. Julve, F. Lloret, J.-T. Wang, Inorg. Chem. 40 (2001) 3619.

[147] P.K. Nanda, G. Aromí, D. Ray, Chem. Commun. (2006) 3181.

[148] A.N. Georgopoulou, C.P. Raptopoulou, V. Psycharis, R. Ballesteros, B. Abarca, A.K. Boudalis, Inorg. Chem. 48 (2009) 3167.

[149] J.D. Woodward, R.V. Backov, K.A. Abboud, D. Dai, H.J. Koo, M.H. Whangbo, M.W. Meisel, D.R. Talham, Inorg. Chem. 44 (2005) 638.

[150] T.C. Stamatatos, J.C. Vlahopoulou, V. Tangoulis, C.P. Raptopoulouc, A. Terzis, G.S. Papaefstathiou, S.P. Perlepes, Polyhedron 28 (2009) 1656.

[151] T.C. Stamatatos, V. Tangoulis, C.P. Raptopoulou, A. Terzis, G.S. Papaefstathiou, S.P. Perlepes, Inorg. Chem. 47 (2008) 7969.

[152] B. Godin, Y.G. Chen, J. Vaissermann, L. Ruhlmann, M. Verdaguer, P. Gouzerh, Angew. Chem. Int. Ed. 44 (2005) 3072.

[153] P. Mialane, A. Dolbecq, J. Marrot, E. Rivière, F. Secheresse, Chem. Eur. J. 11 (2005) 1771.

[154] P. Mialane, C. Duboc, J. Marrot, E. Rivière, A. Dolbecq, F. Sécheresse, Chem. Eur. J. 12 (2006) 1950.

[155] J. Suárez-Varela, I.B. Maimoun, E. Colacio, Dalton Trans. (2004) 3938.

[156] J.M. Domínguez-Vera, J. Suárez-Varela, K. Ben Maimoun, E. Colacio, Eur. J. Inorg. Chem. (2005) 1907.

[157] S.B. Wang, G.M. Yang, R.F. Li, L.C. Li, D.Z. Liao, Inorg. Chem. Commun. 7 (2004) 1082.

[158] T.K. Maji, P.S. Mukherjee, G. Mostafa, T. Mallah, J. Cano-Boquera, N.R. Chaudhuri, Chem. Commun. (2001) 1012.

[159] (a) S. Dalai, P.S. Mukherjee, M.G.B. Drew, T.-H. Lu, N.R. Chaudhuri, Inorg. Chim. Acta 335 (2002) 85;
(b) Y.S. Zhang, K.L. Yao, Z.L. Lu, J. Chem. Phys. 123 (2005) 124308.

[160] P.S. Mukherjee, T.K. Maji, A. Escuer, R. Vicente, J. Ribas, G. Rosair, F.A. Mautner, N.R. Chaudhuri, Eur. J. Inorg. Chem. (2002) 943.

[161] H.-R. Wen, C.-F. Wang, Y. Song, J.-L. Zuo, X.-Z. You, Inorg. Chem. 44 (2005) 9039.

[162] P.S. Dalai, P.S. Mukherjee, T. Mallah, M.G.B. Drew, N.R. Chaudhuri, Inorg. Chim. Acta 5 (2002) 472.

[163] G. de Munno, M.G. Lombardia, P. Paoli, F. Lloret, Inorg. Chim. Acta 282 (1998) 252.

[164] H.-L. Zhu, P. Huang, C.-Y. Duan, L.-M. Zheng, Y.-J. Liu, M.-F. Wu, W.-X. Tang, Trans. Met. Chem. 24 (1999) 380.

[165] Z.-N. Chen, H.-X. Zhang, K.-B. Yu, B.-S. Kang, Chem. Lett. (1998) 275.

[166] Z.-N. Chen, J. Qiu, Z.-K. Wu, D.G. Fu, K.-B. Yu, W.X. Tang, J. Chem. Soc. Dalton Trans. (1994) 1923.

[167] E.-Q. Gao, S.-Q. Bai, C.-F. Wang, Y.-F. Yue, C.-H. Yan, Inorg. Chem. 42 (2003) 8456.

[168] E.-Q. Gao, Y.-F. Yue, S.-Q. Bai, Z. He, C.-H. Yan, Cryst. Growth Des. 5 (2005) 1119.

[169] H.-R. Wen, J.-L. Zuo, W. Liu, Y. Song, X.-Z. You, Inorg. Chim. Acta 358 (2005) 2565.

[170] C.-Y. Wang, J. Coord. Chem. 62 (2009) 2860.

[171] J. Carranza, J. Sletten, F. Lloret, M. Julve, J. Mol. Struct. 890 (2008) 31.

[172] F.A. Mautner, S. Hanna, R. Cortés, L. Lezama, M.G. Barandika, T. Rojo, Inorg. Chem. 38 (1999) 4647.

[173] A. Escuer, R. Vicente, M.S. El Fallah, M.A.S. Goher, F.A. Mautner, Inorg. Chem. 37 (1998) 4466.

[174] P.S. Mukherjee, T.K. Maji, G. Mostafa, T. Mallah, N.R. Chaudhuri, Inorg. Chem. 39 (2000) 5147.

[175] Y. Xie, Q. Liu, H. Jiang, C. Du, X. Xu, M. Yu, Y. Zhu, New J. Chem. 26 (2002) 176.

[176] L. Li, Z. Liu, S.S. Turner, D. Liao, Z. Jiang, S. Yan, New J. Chem. 27 (2003) 752–755.

[177] Y.S. Zhang, K.L. Yao, Z.L. Liu, J. Magn. Magn. Mater. 288 (2005) 331.

[178] H.-Y. Shen, W.-M. Bu, E.-Q. Gao, D.-Z. Liao, Z.-H. Jiang, S.-P. Yan, G.-L. Wang, Inorg. Chem. 39 (2000) 396.

[179] X.-Y. Song, W. Li, L.-C. Li, D.-Z. Liao, Z.-H. Jiang, Inorg. Chem. Commun. 10 (2007) 567.

[180] C. Adhikary, R. Sen, J.-P. Tuchagues, S. Chaudhuri, S. Ianelli, M. Solzi, S. Koner, Inorg. Chim. Acta 362 (2009) 5211.

[181] G. de Munno, M.G. Lombardi, M. Julve, F. Lloret, J. Faus, Inorg. Chim. Acta 282 (1998) 82.

[182] L. Li, Z. Jiang, D. Liao, S. Yan, G. Wang, Q. Zhao, Trans. Met. Chem. 25 (2000) 630.

[183] T.K. Maji, P.S. Mukherjee, S. Koner, G. Mostafa, J.-P. Tuchagues, N.R. Chaudhuri, Inorg. Chim. Acta 314 (2001) 111.

[184] A. Escuer, M. Font-Bardia, E. Peñalba, X. Solans, R. Vicente, Polyhedron 18 (1999) 211.

[185] Q.-F. Yang, Z.-G. Gu, C.-H. Li, J.-Q. Tao, J.-L. Zuo, X.-Z. You, Inorg. Chim. Acta 360 (2007) 2875.

[186] R. Vicente, A. Escuer, J. Ferretjans, H. Stockli-Evans, X. Solans, M. Font-Barida, J. Chem. Soc. Dalton Trans. (1997) 167.

[187] A. Escuer, R. Vicente, F.A. Mautner, M.A.S. Goher, Inorg. Chem. 36 (1997) 1233.

[188] L.K. Thompson, S.S. Tandon, F. Lloret, J. Cano, M. Julve, Inorg. Chem. 36 (1997) 3301.

[189] V. Tangoulis, D. Panagoulis, C.P. Raptopoulou, C. Dendrinou-Samara, Dalton Trans. (2008) 1752.

[190] J. Peng Zhao, B.-W. Hu, E.C. Sañudo, Q. Yang, Y.-F. Zeng, X.-H. Bu, Inorg. Chem. 48 (2009) 2482.

[191] S.S. Tandon, S.D. Bunge, D. Motry, J.S. Costa, G. Aromí, J. Reedijk, L.K. Thompson, Inorg. Chem. 48 (2009) 4873.

[192] B. Woodard, R.D. Willett, S. Haddad, B. Twamley, C.J. Gomez-Garcia, E. Coronado, Inorg. Chem. 43 (2004) 1822.

[193] X. Hu, Y.-F. Zeng, Z. Chen, E.C. Sañudo, F.-C. Liu, J. Ribas, X.-H. Bu, Cryst. Growth Des. 9 (2009) 421.

[194] Y.-Z. Zhang, H.-Y. Wei, F. Pan, Z.-M. Wang, Z.-D. Chen, S. Gao, Angew. Chem. Int. Ed. 44 (2005) 5841.

[195] Ł. Jaremko, A.M. Kirillov, P. Smoleński, A.J.L. Pombeiro, Cryst. Growth Des. 9 (2009) 3006.

[196] Z. Shen, J.-L. Zuo, S. Gao, Y. Song, C.-M. Che, H.-K. Fun, X.-Z. You, Angew. Chem. Int. Ed. 39 (2000) 3633.

[197] S.C. Manna, S. Konar, E. Zangrando, M.G.B. Drew, J. Ribas, N.R. Chaudhuri, Eur. J. Inorg. Chem. (2005) 1751.

[198] E.-Q. Gao, Y.-X. Xu, A.-L. Cheng, M.-Y. He, C.-H. Yan, Inorg. Chem. Commun. 9 (2005) 212.

[199] W. Dong, Y. Ouyang, D.-Z. Liao, S.-P. Yan, P. Cheng, Z.-H. Jiang, Inorg. Chim. Acta 359 (2006) 3363.

[200] G. Lazari, T.C. Stamatatos, C.P. Raptopoulou, V. Psycharis, M. Pissas, S.P. Perlepes, A.K. Boudalis, Dalton Trans. (2009) 3215.

[201] M. Jiang, Y.-T. Li, Z.-Y. Wu, Z.-W. Yin, J. Coord. Chem. 62 (2009) 380.

[202] Y.-T. Yang, F. Luo, Y.-X. Che, J.-M. Zheng, J. Mol. Struct. 888 (2008) 253.

[203] Y.-F. Zeng, X. Hu, J.-P. Zhao, B.-W. Hu, E.C. Sañudo, F.-C. Liu, X.-H. Bu, Chem. Eur. J. 14 (2008) 7127.

[204] M.A.M. Abu-Youssef, A. Escuer, F.A. Mautner, L. Öhrström, Dalton Trans. (2008) 3553.

[205] Z.-G. Gu, Y.-F. Xu, X.-J. Yin, X.-H. Zhou, J.-L. Zuo, X.-Z. You, Dalton Trans. (2008) 5593.

[206] M. Salah El Fallah, R. Vicente, J. Tercero, C. Elpelt, E. Rentschler, X. Solans, M. Font-Bardia, Inorg. Chem. 47 (2008) 6322.

[207] F.-C. Liu, Y.-F. Zeng, J.-P. Zhao, B.-W. Hu, X.-H. Bu, J. Ribas, S.R. Batten, Inorg. Chem. Commun. 10 (2007) 129.

[208] Z.-G. Gu, J.-L. Zuo, X.-Z. You, Dalton Trans. (2007) 4067.

[209] F.-C. Liu, Y.-F. Zeng, J.-P. Zhao, B.-W. Hu, E.C. Sañudo, J. Ribas, X.-H. Bu, Inorg. Chem. 46 (2007) 7698.

[210] J.-R. Li, Q. Yu, E.C. Sajudo, Y. Tao, X.-H. Bu, Chem. Commun. (2007) 2602.

[211] C.-Y. Liao, M. Nayak, H.-H. Wei, S. Mohanta, Polyhedron 27 (2008) 2693.

[212] S.S. Tandon, S.D. Bunge, N. Patel, L.K. Thompson, Inorg. Chem. Commun. 12 (2009) 1077.

[213] J.-J. Liu, X. He, M. Shao, M.-X. Li, J. Mol. Struct. 919 (2009) 189.

[214] J. Suárez-Varela, A.J. Mota, H. Aouryaghal, J. Cano, A. Rodríguez-Diéguez, D. Luneau, E. Colacio, Inorg. Chem. 47 (2008) 8143.